INFORMATION TO USERS

This manuscript has been reproduced from the microfilm master. UMI films the text directly from the original or copy submitted. Thus, some thesis and dissertation copies are in typewriter face, while others may be from any type of computer printer.

The quality of this reproduction is dependent upon the quality of the copy submitted. Broken or indistinct print, colored or poor quality illustrations and photographs, print bleedthrough, substandard margins, and improper alignment can adversely affect reproduction.

In the unlikely event that the author did not send UMI a complete manuscript and there are missing pages, these will be noted. Also, if unauthorized copyright material had to be removed, a note will indicate the deletion.

Oversize materials (e.g., maps, drawings, charts) are reproduced by sectioning the original, beginning at the upper left-hand corner and continuing from left to right in equal sections with small overlaps. Each original is also photographed in one exposure and is included in reduced form at the back of the book.

Photographs included in the original manuscript have been reproduced xerographically in this copy. Higher quality 6" x 9" black and white photographic prints are available for any photographs or illustrations appearing in this copy for an additional charge. Contact UMI directly to order.

UMI

A Bell & Howell Information Company
300 North Zeeb Road, Ann Arbor MI 48106-1346 USA
313/761-4700 800/521-0600

Université d'Ottawa · University of Ottawa

HYDRODENITROGENATION OF PYRIDINE OVER ALUMINA SUPPORTED PLATINUM CATALYST

© USHA GOPALAN

A thesis submitted to the School of Graduate Studies and Research
in partial fulfilment of the requirements for the
degree of
MASTER OF APPLIED SCIENCE
in the Department of Chemical Engineering

April 1998

ABSTRACT

The kinetics of vapour phase hydrodenitrogenation of pyridine over a catalyst containing 0.5% platinum supported in alumina was studied using a fixed-bed catalytic reactor. The effect of process variables such as total reactor pressure, reaction temperature and space time on the conversion of pyridine, organic product distribution, yield of hydrocarbons and selectivity for hydrocarbons was studied.

The effect of pressure is more than that of temperature and space time. When the pressure was doubled, the conversion of pyridine increased by 1.3 to four times and the yield and selectivity for hydrocarbons increased many folds. The reaction is believed to proceed via hydrogenation of pyridine to piperidine followed by the ring rupture of piperidine to pentylamine and finally the formation of pentane and ammonia. Pentyl piperidine was a major intermediate found. At higher pressure, ethyl piperidine and traces of cyclopentane were found to be other products. Dipentylamine was another intermediate found at higher pressure. At low pressure, dipentylamine, ethyl piperidine and cyclopentane were not detected.

Many rate equations were tried to fit the kinetic data of the hydrodenitrogenation of pyridine. A Langmuir-Hinshelwood type rate expression with a pseudo order rate constant fitted the data best. From the Arrhenius plot of the pseudo rate constants using a lumped parameter

theoretical model, the activation energy was estimated to be 19.89 kcal/mol. From the mechanistic model, the ring rupture of piperidine to pentylamine was found to be the rate determining step in the hydrodenitrogenation of pyridine.

SOMMAIRE

La kinétique de l'hydrodenitrogenation du pyridin à l'intérieur d'une phase vapeur, utilisant un catalyste contenant 0.5% de platinum supporté par l'alumine fut étudiée utilisant un réacteur catalytique à lit fixe. L'effet des variations de procédé tel que pression totale du réacteur, température de la réaction et espace-temps de la conversion du pyridin, distribution du produit organique, rendement des hydrocarbures et la selectivité des hydrocarbures furent étudiés.

L'effet de la pression est plus grande que celles de la température et espact-temps. Lorsque la pression fut doublée, la conversion du pyridin augmenta de 1.3 à 4 fois et le rendement et la selectivité des hydrocarbures augmentèrent aussi plusieurs fois. Il est perçu que la réaction procède à partir de la transformation par hydrogenation du pyridin au piperidin suivit d'une rupture de l'anneau du dernier pour y former le pentylamin et finalement la formation du pentane et le l'ammoniac. Un intermédiaire fort important retrouvé fut le pentyl de piperidin. À des pressions plus élevées, l'éthyl de piperidin et des traces de cyclopentane furent en fait d'autres produits. Le dipentylamin était un autre intermédiaire retrouvé à des pressions très élevées. À des pressions plus basses, le dipentylamin, l'éthyl de piperidin et le cyclopentane ne furent detectés. Plusieurs équations de débit furent essayés afin de marier les données kinétiques de l'hydrodenitrogenation du pyridin. Un mécanisme de réaction du type Langmuir-Hinshelwood avec une constante avec régime d'ordre choisi se maria bien avec les données. Du tracé d'Arrhenius, avec constant et régime choisi utilisant un modèle théorique regroupant les paramètres, l'énergie d'activation fut estimée étant 19.89 kcal/mol. En terme

d'un modèle mécanique, la rupture de l'anneau changant le piperidin à du pentylamin fut determinée comme étant l'étape qui détermine le régime dans la transformation par hydrodenitrogenation du pyridin.

ACKNOWLEDEGMENTS

I wish to thank Dr. R. S. Mann for his able guidance, encouragement and support throughout the course of this research. My sincere thanks are due to Dr. V. Hornoff, the Chairman of the Department of Chemical Engineering and Dr. Z. Duvnjak, the former Chairman of the department for the departmental financial support. I thank Dr. G. Neale, Graduate Student Coordinator and Dr. H. Tezel, former Graduate Student Coordinator, for their help and support.

I wish to express my sincere gratitude to Dr. K. C. Khulbe for his invaluable suggestions and guidance. I thank Mr. L. Tremblay, Mr. F. Ziroldo and Mr. G. Nina for their technical assistance and help in maintaining the experimental set-up. I convey my thanks to Mrs. A. M. Lamarche for the help in the ESR analysis.

Last but not the least, I thank all my friends and colleagues in the department and my family for their innumerable help and support.

NOMENCLATURE

The symbols, subscripts, superscripts and abbreviations used in this report are listed below. All the notations are completely defined where they appear first in the text.

a_m	-	area of catalyst particle per unit mass
C_i	-	concentration of i
C_P	-	heat capacity per unit mass at constant pressure
D	-	diffusion coefficient
D_B	-	bulk diffusion coefficient
D_K	-	Knudsen diffusion coefficient
D_{MA}	-	mean diffusion coefficient of A in a multi-component system
F_i	-	molar flow of component i, g-mol/hr
G	-	mass velocity of gas based on total cross section of bed
G_m	-	molar velocity of gas based on total cross section of bed
h_G	-	heat transfer coefficient in gas phase
j_D	-	mass transfer number
j_H	-	heat transfer number
k	-	reaction rate constant
K_i	-	adsorption equilibrium constant of component i
$k`$	-	thermal conductivity

k_{-1}	-	reaction rate constant of reverse reaction
k_1	-	reaction rate constant of forward reaction
$k_{G,i}$	-	mass transfer coefficient in gas phase of component *i*
k_p, k_s	-	reaction rate constants (equation 2.6)
k_{ov}	-	observed rate constant (equation 2.6)
k_P	-	pseudo rate constant (equation 2.4)
M	-	molecular weight
N_{Pr}	-	Prandtl number
$P_{f,i}$	-	pressure factor of component *i*
P_i	-	partial pressure of component *i*
r	-	reaction rate, mol/g-catalyst-hr
R	-	reactant molar ratio
r	-	radius of the pore
$R`$	-	dimensionless factor (equation 2.23)
$R``$	-	gas constant
r_{mA}	-	molal reaction rate of component *A*
S	-	selectivity
S_v	-	volumetric hourly space velocity, hr^{-1}
T	-	temperature, K
W	-	mass of the catalyst, g

W/F - space time, hr-g-catalyst/g-mol pyridine

X_i - mole fraction of component *i* (equations 2.14 - 2.20)

X_{fi} - fractional conversion of component *i*

Y - yield

Subscripts

H - hydrogen

in - conditions at the inlet

NC - nitrogen compound

NH_3 - ammonia

0 - initial conditions

out,e - conditions at the outlet

PIP - piperidine

PYR - pyridine

Superscripts

n - order of the reaction

α - order of reaction (equation 2.13)

β - order of reaction (equation 2.13)

Greek Symbol

ΔH_A	-	molal heat of reaction of component A
Δp_A	-	pressure gradient (equation 2.23)
Δt	-	temperature gradient (equation 2.27)
θ_i	-	fraction of catalyst sites occupied by i
λ	-	mean free path
μ	-	fluid viscosity
$\bar{v}$	-	mean Maxwellian velocity
π	-	total pressure (equation 2.2)
ρ	-	fluid density
ϕ	-	shape factor

Abbreviations

CYPENT	-	Cyclopentane
DIPEN	-	Dipentylamine
ETPIP	-	Ethyl piperidine
HDM	-	Hydrodemetalation
HDN	-	Hydrodenitrogenation
HDO	-	Hydrodeoxygenation
HDS	-	Hydrodesulphurization
NC	-	Nitrogen containing compound

PENAM	-	Pentylamine
PENPIP	-	Pentyl piperidine
PENT	-	Pentane
PIP	-	Piperidine
PYR, pyrid	-	Pyridine

TABLE OF CONTENTS

LIST OF TABLES

LIST OF FIGURES

CHAPTER 1

INTRODUCTION

As the energy demand increases and the availability of petroleum decreases, it will become essential to process the alternate fuels which include liquid fuels derived from coal, oil shale, tar sands and heavier petroleum fractions. These alternate feed stocks and residual petroleum fractions contain higher concentrations of nitrogen compounds than the lighter petroleum crudes. These nitrogen compounds lower the grade of the fuels due to the following reasons:

1. The presence of nitrogen in finished petroleum products contributes to the formation of NO_x upon combustion process.
2. The activity of catalysts used in cracking and other processes such as reforming, isomerization and polymerization is reduced because these catalysts are acidic whereas the nitrogen compounds are basic (Oblad et al., 1951; Jewell and Dart, 1964; Larson, 1967).
3. High nitrogen concentrations are detrimental to both product quality and product stability. For example, the gums, lacquers and precipitates formed during the storage or use of oils and fuels are directly related to the presence of nitrogen compounds (Schwartz et al., 1964; Nixon et al., 1959). In addition, the presence of these compounds, even in trace amounts, leads to poor colour and colour stability of oils (Oswald and Noel, 1961; Kartzmark and Gilbert, 1967).

4. Most of the nitrogen compounds are biologically harmful and are often carcinogenic.

It becomes necessary to remove these nitrogen compounds from the fuels before they can be utilized or processed further. Catalytic hydrodenitrogenation (HDN) is a common process to up-grade these fuels. HDN is a common process in which the nitrogen compounds are removed from the hydrocarbon feed stocks in the presence of hydrogen. It is an integral part of the hydrotreatment process. The primary objective of hydrotreatment is the removal of heteroatoms. Hydrotreatment, hydrocracking and reforming are the major large-scale petroleum refining processes.

Nitrogen in the petroleum stocks is found as heterocyclic compounds and non-heterocyclic compounds. The heterocyclic compounds which are usually resistant to HDN are present in large quantities while the non-heterocyclic compounds which are relatively more reactive are present in small concentrations. From the studies on the nature of the nitrogen-containing compounds in petroleum, it has been shown that the concentration of nitrogen increases with the increasing boiling point of the petroleum fractions (Snyder, 1970). The lighter fractions contain predominantly one or two-ring heterocyclic nitrogen compounds whereas the multi-ring nitrogen-containing compounds are concentrated in the heavier fractions. Figure 1.1 presents some of the complex nitrogen compounds normally found in petroleum stocks. It has been reported that similar types of nitrogen-containing compounds are present in petroleum, coal derived liquids and oil shales (Scheppele et al., 1977; Schultz et al., 1967).

Therefore, the principles of hydrodenitrogenation of petroleum liquids will be applicable to that of coal derived liquids and oil shales. But the synthetic liquids are difficult to hydrotreat due to high nitrogen content (concentrations of nitrogen in synthetic liquids are two to five times higher than those in petroleum), high aromaticity and large molecular size.

The previous HDN kinetic studies have considered single model nitrogen compounds or whole coal derived liquids. The present study is focussed on the hydrodenitrogenation of pyridine, a pure heterocyclic nitrogen compound. Pyridine was chosen as the model compound because a large percentage of the nitrogen-containing compounds present in crude oil are derivatives of pyridine.

The objectives of this work are:

- To study the effect of process variables like temperature (T), pressure (P), space time (W/F) and hydrogen to nitrogen compound molar ratio (R) on the conversion, yield and selectivity of HDN of pyridine
- To establish the reaction networks
- Kinetic modeling of the reaction

YRIDINE

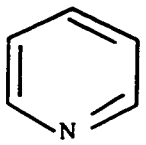

INDOLE

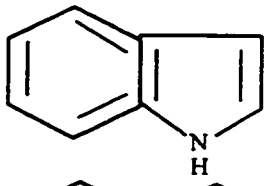

QUINOLINE

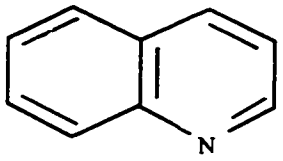

BENZ(A)ACRIDINE

BENZ(C)ACRIDINE

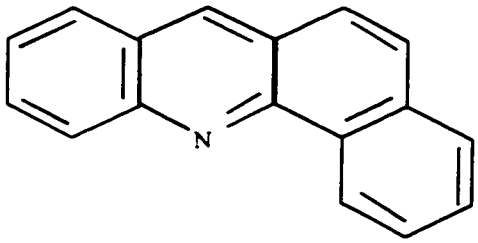

CARBAZOLE

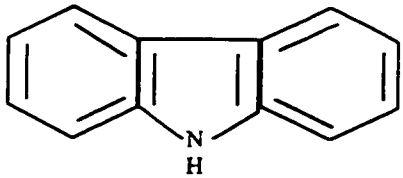

ACRIDINE

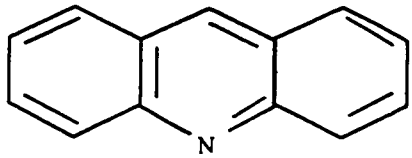

DIBENZACRIDINE

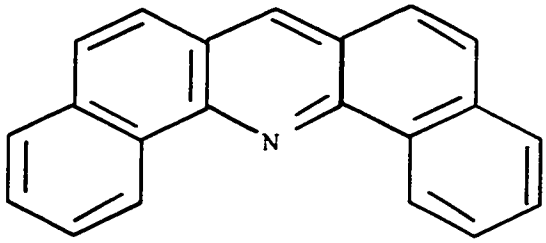

Figure 1.1 Some of the nitrogen-containing compounds found in petroleum coal-derived liquids and oil shales

CHAPTER 2

THEORETICAL ASPECTS

Hydrodenitrogenation is an important hydrotreating process in which hydrogen is added to the oil residuals while nitrogen is removed from them. This chapter gives a general outlook on the work done on the hydrodenitrogenation of pyridine.

2.1 LITERATURE REVIEW

2.1.1 Hydrotreating Processes

Hydrotreating is the catalytic conversion and removal of organic sulphur, nitrogen and oxygen from petroleum crudes at high hydrogen pressures and is accompanied by hydrogenation of unsaturate and cracking of petroleum feed stocks to lower molecular hydrocarbons. The increase in the application of hydrotreating can be ascribed to:

- The ever decreasing availability of light, sweet crudes leading to the increase in fraction of heavy crudes that has to be processed.
- The up-gradation of the feed stocks for the improvement of downstream processing such as catalytic reforming and catalytic cracking.

Hydrotreating involves hydrodesulphurization (HDS), hydrodenitrogenation (HDN), hydrodemetalation (HDM) and hydrodeoxygenation (HDO). These main reactions can be

represented as follows:

Sulphur-containing compound + H_2 → Hydrocarbon + H_2S

Nitrogen-containing compound + H_2 → Hydrocarbon + NH_3

Oxygen-containing compound + H_2 → Hydrocarbon + H_2O

All the above hydrotreating reactions are achieved in the presence of a catalyst and at pressures in the range of 7-14 MPa and temperatures in the range of 573-723 K. An important objective of hydrotreatment is to maximize the amount of sulphur, nitrogen and metal removed while minimizing the rates of hydrogenation and hydrocracking, resulting in the decrease of hydrogen consumption. Removal of oxygenated compound occurs usually in the desulphurization or denitrogenation step (Cusumano et al., 1978).

Hydrotreating, especially HDN, requires significant amount of hydrogen mainly because HDN is believed to proceed via the saturation of the heterocyclic ring followed by ring fracture and subsequent removal of nitrogen as ammonia. In commercial scale, hydrogen is recovered and recycled to the process stream with make-up hydrogen in order to minimize the hydrogen consumption.

2.1.2 Hydrotreating Catalysts

The current commercial hydroprocessing catalysts are transition metal sulphides based on Group VIII and VI metals. These catalysts are prepared by dispersing MoO_3 (typically 12-25 wt.%) and a promoter metal oxide, either CoO or NiO (3-6 wt.%), on γ-Al_2O_3 or SiO_2

modified Al_2O_3 which is followed by sulphiding with a sulphur-bearing stream such as H_2S at high temperatures (Oballa and Shih, 1993). Cobalt and molybdenum ($CoO\text{-}MoO_3/\gamma\text{-}Al_2O_3$ or $Co\text{-}Mo/Al_2O_3$) is most widely used for hydrodesulphurization whereas nickel and molybdenum ($NiO\text{-}MoO_3/\ \gamma\text{-}Al_2O_3$ or $Ni\text{-}Mo/Al_2O_3$) or nickel and tungsten ($NiO\text{-}WO_3/\gamma\text{-}Al_2O_3$ or $Ni\text{-}W/Al_2O_3$) are commonly used for hydrodenitrogenation. Some platinum metal group sulphides have also been reported to have HDN activity comparable with that of Ni-Mo catalysts (Vit and Zdražil, 1989).

2.1.3 Heteroatoms

The fuel feedstocks contain sulphur, nitrogen, oxygen and metal heteroatoms. Crude petroleum contains 0.01-0.3 wt.% nitrogen, 0.1-3 wt.% sulphur, less than 0.5 wt.% oxygen and 20-1000 ppm (by wt.) metals. The percentage of nitrogen in petroleum residuals is more than 0.3% since the nitrogen-containing compounds are concentrated in higher boiling petroleum fractions (Tschamber and DeRuiter, 1966). The nitrogen content in the fuels derived from tar sands and oil shales is even higher. Due to the increasing use of heavy fuels, hydrodenitrogenation becomes an important hydrotreating process.

Nitrogen-containing compounds are generally divided into two categories: six-membered pyridinic ring compound and five-membered pyrrolic ring compound. In the five-membered ring compounds such as pyrroles, indoles and carbazoles, the extra pair of electrons in the nitrogen atom is involved in the π-cloud of the ring and hence not readily available for the

reaction with acids. Therefore, these compounds are regarded as non-basic ($pK_a < 2.0$). In the case of six-membered ring compounds like pyridines, quinolines and acridines, the unshared pair nitrogen electrons is not tied up in the π-cloud and hence available for sharing with acids. Thus, these compounds are bases with $pK_a > 2.0$. Some of the nitrogen-containing compounds in fuels and their pK_a values are given in Table 2.1. The ratio of basic to non-basic compounds in light petroleum is about 1:2 whereas that for synthetic fuels is roughly 2:1. Hence, the concentration of nitrogen in synthetic fuels is higher and are more basic than the light petroleum.

Table 2.1 Nitrogen Containing Compounds in Synthetic Fuels

Nitrogen compounds	pK_a
Pyridine	5.58
Piperidine	11.12
Ethyl piperidine	10.45
Ammonia	9.27
Quinoline	4.90
Acridine	5.58
Aniline	4.63
Pyrrole	0.40
Indole	-3.50
Carbazole	-1.00

2.1.4 Hydrodenitrogenation of Pyridine

This section presents a literature review of the hydrodenitrogenation of pyridine using different catalysts and the different reaction mechanisms that have been proposed.

The literature survey shows that hydrodenitrogenation has received less attention than hydrodesulphurization. The former being a more difficult process than the latter, it requires more severe conditions and higher hydrogen consumption. This large hydrogen consumption can be attributed to the complete saturation of the carbon atoms bound to the nitrogen atom directly or present at the meta position with respect to the nitrogen atom, before the hydrogenolysis of the carbon-nitrogen bond occurs.

Anderson (1846) first isolated and characterized pyridine. Cox (1961) studied the denitrification of pyridine and some of its derivatives. In general, he found that the reaction was first order with respect to pyridine but the apparent first order constant decreased in magnitude with the increase in nitrogen concentration in the feed.

McIlvried (1971) studied the HDN of pyridine and found that the reaction proceeded via a rapid hydrogenation of pyridine to piperidine followed by a slow ring rupture to form n-pentylamine and a rapid denitrification of n-pentylamine to pentane and ammonia. Due to the complexity of the reaction, he also studied the denitrification of piperidine and an amine so that the kinetics of one step could be better understood if the kinetics of the succeeding

steps were known. The catalyst used in his study was presulphided Ni-Co-Mo/Al_2O_3. The data obtained from the denitrification of piperidine fit a Langmuir-Hinshelwood type kinetic model expressed in the following manner:

$$\frac{dP_{PIP}}{d(1/S_v)} = - \frac{0.71\ P_H\ P_{PIP}}{(1 + R)\ (1 + 1.57.P_{PYR_{out}})} * 10^{-4} \qquad (2.1)$$

This rate expression was then used to develop the following kinetic model for pyridine.

$$\frac{dP_{PYR}}{d(1/S_v)} = - \frac{4.55\ \pi\ P_H\ P_{PYR}}{(1 + R)\ (1 + 10.5\ P_{NH_3})} * 10^{-4} \qquad (2.2)$$

where,

P_i - partial pressure of component *i*, psia

R - gas rate, moles hydrogen/mole liquid feed

S_v - volumetric hourly space velocity, hr^{-1}

π - total pressure, psia

subscripts:

PIP - piperidine

PYR - pyridine

NH_3 - ammonia

H - hydrogen

out - conditions at the outlet

Aboul-Gheit et al. (1974) studied the HDN of pyridine in paraffin oil using Co-Mo/Al_2O_3 catalyst in the temperature range of 598-673 K. They concluded:

- Under hydrotreating conditions, pyridine was saturated to piperidine and then the ring was cracked at different positions to produce a mixture of primary and secondary amines.
- As n-pentylamine was present as a major intermediate in most of their experiments, they concluded that a carbon-nitrogen bond rupture should be the principal hydrocracking reaction. At low temperatures, the production of alkyl piperidines was a significant side reaction.
- The initial hydrogen pressure had a decisive influence upon the rate of pyridine HDN and under the conditions employed, the reaction would be complete only at a temperature of 673 K, an initial hydrogen pressure of 1.0133 MPa and a reaction period of 6 hours.

Sonnemans et al. (1973) studied the pyridine HDN at high hydrogen pressures (1.5-7.5 MPa) using Co-Mo/γ-Al_2O_3 and Mo/γ-Al_2O_3 catalysts. The data fit a Langmuir type kinetic model with a first-order reaction in pyridine. The rate equation was given as:

$$r = k \frac{P_{PYR} P_H^n}{P_{PYR_{out}}} \tag{2.3}$$

where:

P_i - partial pressure of component *i*, psia

r - reaction rate

k - reaction rate constant

n - order of the reaction

subscripts:

PYR - pyridine

H - hydrogen

out - conditions at the outlet

They reported that n, the order of the reaction with respect to hydrogen, equaled 1.0 at 523 K and 1.5 at 573-648 K.

Satterfield and Cocchetto (1975) studied the HDN of pyridine and piperidine (the first product formed during the HDN of pyridine) using Ni-Mo/Al_2O_3 and Co-Mo/Al_2O_3 catalysts. Their conclusions were:

- Under their experimental condition, the concentration of piperidine existing in equilibrium with pyridine could be a limiting factor in the overall HDN rate.
- The Ni-Mo/Al_2O_3 catalyst appeared to have greater hydrogenation-dehydrogenation activity than the Co-Mo/Al_2O_3 catalyst but the Co-Mo/Al_2O_3 catalyst appeared to have greater hydrogenolysis activity at 573 K or below.
- For pyridine HDN, as the temperature was increased to 573 K, the equilibrium shifted from piperidine to pyridine, and approximately at 673 K, equilibrium was

established.

Satterfield et al. (1975) studied the interaction between HDN of pyridine and HDS of thiophene over a commercial Ni-Mo/Al_2O_3 catalyst. At low temperatures, thiophene inhibits the reaction by competing with pyridine for the hydrogenation sites on the catalyst which resulted in the retardation of the hydrogenation of pyridine to piperidine and hence the overall reaction rate. At high temperatures, hydrogen sulphide, a HDS reaction product, interacts with the catalyst to improve its hydrogenolysis activity. This increases the rate of piperidine hydrogenolysis activity which is the rate determining step under these conditions and enhances the overall HDN rate. This result was later verified by Satterfield et al. in 1980.

Gupta (1977) studied the vapour phase HDN of pyridine over Co-Mo/Al_2O_3 catalyst. He concluded that:

- the reaction takes place in two steps, hydrogenation of pyridine to piperidine and the subsequent conversion of piperidine to pentane and ammonia via pentylamine, pentyl piperidine and dipentylamine.
- the hydrogenation of pyridine showed zero-order and the reaction rate constant k, varied with temperature and the initial pyridine concentration (C_{P_o}) such that:

$$k = k_P \, C_{P_o}^{n} \tag{2.4}$$

where k_P is the pseudo rate constant dependent only on the temperature and n is the order in

initial pyridine concentration.

Anabtawi et al. (1980), studied the similar reaction using Ni-W/Al_2O_3 and concluded that the reaction proceeded via:

- Saturation of pyridine ring to form piperidine.
- Disproportionation of piperidine to form ammonia and n-pentyl piperidine and formation of n-pentane and n-pentyl piperidine.

The data obtained by them fit the rate equation:

$$r = k_{ov} P_{PYR} P_H \tag{2.5}$$

where k_{ov} could be represented as,

$$k_{ov} = \frac{k_s}{P_{PYR_{out}}} + k_i \tag{2.6}$$

where,

k_i, k_s - reaction rate constants (intercept and slope respectively in a plot of k_{ov} vs $1/P_{PYRo}$), mol/g-catalyst-hr

k_{ov} - observed rate constant for pyridine hydrogenation, mol/g-catalyst-hr

P_i - partial pressures of species i, Pa

r - reaction rate, mol/g-catalyst-hr

The activity and the selectivity in parallel HDN and HDS of carbon supported sulphides of Ru, Rh, Pd, Ir and Pt were studied by Vit and Zdražil (1989). By comparing the behaviour of these sulphides with those of commercial Ni-Mo/Al_2O_3 and Co-Mo/Al_2O_3, they concluded that the carbon-supported sulphides of platinum metals were a better HDS catalysts and much better HDN catalysts than the commercial bimetallic catalysts. The HDN and HDS selectivity of Rh, Ru and Pd catalysts were similar to that of Ni-Mo and Co-Mo systems but the Ir and Pt catalysts were extremely selective for HDN. The exceptional HDN properties of the sulphides of these platinum metals has been attributed to the use of active carbon as the support.

Hillerova et al. (1991) in a study compared the carbon and alumina supported Ni-Mo sulphide catalysts in parallel HDN of pyridine and HDS of thiophene. They concluded that:

- In the absence of pyridine, both Ni-Mo/C and Ni-Mo/Al_2O_3 had similar HDS activities. But in the presence of pyridine, the activity of the carbon supported catalyst was three times higher than the alumina supported one. Evidently, the carbon supported catalysts were much more resistant in HDS to poisoning by nitrogen compounds than the alumina supported samples.
- The HDN activity of both the samples were found to be the same.

In a recent study, Ledoux and Djellouli (1990) compared the HDN activities of Mo/Al_2O_3, Co-Mo/Al_2O_3 and Ni-Mo/Al_2O_3 catalysts under high hydrogen pressure with and without

sulphur in the gas phase. They concluded that all the three catalysts exhibited the same activity without sulphur in the gas phase. In the presence of sulphur, the Ni-Mo catalyst was found to be 2.5 times more active than the other two catalysts. From the analysis of the products, they concluded that Ni-Mo was never totally sulphided and that some metallic nickel atom remained on the surface which could accommodate the undissociated, strongly acidic hydrogen sulphide. This hydrogen sulphide increases the rates of the saturated ring opening and formation of ammonia.

Ajaka et al. (1994) studied the HDN of pyridine over unsulphided and presulphided Mo-zeolite. The data was represented by Langmuir-Hinshelwood model. Their conclusions were:

- The conversion of pyridine over presulphided catalyst was 1.5 times higher than that over unsulphided one whereas the increase in selectivity was about 5 folds.
- The activity of the presulphided catalyst was similar to that of a commercial Ni-Mo/Al_2O_3 catalyst but the conversion was lower.

2.2 HETEROGENEOUS CATALYTIC REACTION

Most heterogeneous catalytic reactions are too complex to be treated by theories like activated-complex theory, collision theory or more general reaction rate theories. Therefore, it is necessary to rely heavily on classical empirical methods (Clark, 1970).

Heterogeneous catalytic reactions consist of at least three single steps: adsorption, surface

reaction and desorption. When there is a single rate-determining step, considerable simplification results. However, only when surface reaction is the rate-limiting step, the overall kinetics are governed by the kinetics of the reaction step. If the desorption of the product is the rate-limiting step, then the overall kinetics as measured in the gas phase do not reflect the surface-reaction rate. Because of the great difficulties in the kinetics of heterogeneous catalytic reactions, the models have been devised to rely heavily on mathematical statistics (Happel and Mezaki, 1969; Kittrell and Mezaki, 1967)

2.2.1 Mechanisms of Heterogeneous Catalytic Reactions

In general, an overall heterogeneous catalytic reaction will involve the following series of steps:

1. Mass transfer of reactants to the external surface of the catalytic particle
2. Diffusion of reactants in the pore
3. Adsorption of reactants
4. Surface reaction
5. Desorption of products
6. Diffusion of products out of the pores
7. Mass transfer of products from the external surface of the catalyst to the surrounding fluid

Mass transfer to and from the external surface of the catalyst (steps 1 and 7) is highly dependent on the fluid flow characteristics of the system. Hence, the rates of these steps

depend on the velocity of the fluid passing over the surface, the particle size and the diffusional characteristics of the molecular species. Mass transfer in and out of the catalyst pores (steps 2 and 6) is dependent on the porous nature of the catalyst, pore shape, average pore size, pore-size distribution and how the pores are interconnected. It is convenient to apply the concept of a rate-limiting step while treating the heterogeneous reactions to calculate the reaction rate which will be that of the slowest step.

2.2.2 Kinetic Models

The kinetic formulations based on the assumption that the rate of reaction between one or more chemisorbed species is the rate-limiting step rather than the rate of adsorption or desorption, bear the name Langmuir-Hinshelwood. The term Langmuir-Rideal or Rideal or Rideal-Eley is applied if the reaction is assumed to be between a chemisorbed species and a molecule reacting with it directly from the fluid phase or from a physically adsorbed layer.

2.2.2.1 Langmuir-Hinshelwood Model

If the reaction takes place between adsorbed species *A* and adsorbed species *B* and if these species are immobile, they must be adsorbed on neighbouring sites for the reaction to take place. If θ_i represents the fraction of available sites on which species *i* is adsorbed, then the probability of reaction taking place is taken to be proportional to the product of all θ_i. For example, consider the following general reaction,

$$A + B \rightleftharpoons C + D$$

The rate of the irreversible reaction is given by

$$r = k_1 \, \theta_A \, \theta_B \tag{2.7}$$

or

$$r = \frac{k_1 \, K_A \, K_B \, P_A \, P_B}{(1 + K_A \, P_A + K_B \, P_B)^2} \tag{2.8}$$

The rate of reversible reaction is given by

$$r = k_1 \, \theta_A \, \theta_B - k_{-1} \, \theta_C \, \theta_D \tag{2.9}$$

or

$$r = \frac{k_1 \, K_A \, K_B \, P_A \, P_B - k_{-1} \, K_C \, K_D \, P_C \, P_D}{(1 + K_A \, P_A + K_B \, P_B + K_C \, P_C + K_D \, P_D)^2} \tag{2.10}$$

where

r	-	reaction rate
k_1	-	reaction rate constant of forward reaction
k_{-1}	-	reaction rate constant of reverse reaction
K	-	adsorption equilibrium constant
θ_i	-	fraction of catalyst sites occupied by component *i*

subscripts

A	-	reactant *A*
B	-	reactant *B*
C	-	product *C*
D	-	product *D*

2.2.2.2 Rideal Model

For this model, reaction is assumed to occur between a chemisorbed radical or atom and a molecule that impacts directly from the gas phase or held in a deep van der Waals layer. To formulate the Rideal mechanism, consider a reaction occurring between adsorbed molecules of *B* and gas-phase molecules of *A*. The rate is given by,

$$r = k_1 \, \theta_S \, P_A \tag{2.11}$$

or

$$r = \frac{k_1 \, P_A \, K_B \, P_B}{1 + K_A \, P_A + K_B \, P_B + K_C \, P_C} \tag{2.12}$$

2.2.2.3 Power Law

The assumption of a uniform catalytic surface is not always true. The nonuniformity of the catalyst surfaces and lack of accurate knowledge of the structure of the chemisorbed species and their concentrations have suggested the use of power rate law instead of Langmuir

model. The general power-law rate expression is,

$$r = k\, P_A^{\alpha}\, P_B^{\beta} \tag{2.13}$$

where

r - reaction rate

k - reaction rate constant

P_i - partial pressure of component i

subscripts

A - reactant A

B - reactant B

superscripts

α - order of reaction with respect to A

β - order of reaction with respect to B

2.3 REACTORS

The two main characteristics adopted to classify the reactors are; (1) the types of phases present and (2) the operating mode of the reactor. The operation of a catalytic reactor is defined by many parameters like, change in mass which defines if the reactor is a batch or a flow reactor, change in temperature which defines if the reactor is isothermal or adiabatic, reactor volume, residence time and space time. The properties of two plug flow reactors, the integral and the differential are discussed in the following sections.

2.3.1 Differential Plug Flow Reactors

On the assumption of plug flow, a small material balance over a differential element of catalyst dW gives,

$$r_A \, dW = F \, dX_A \tag{2.14}$$

where r_A is the reaction rate. From the above equation, it can be seen that if a differential quantity of catalyst is used, then the conversion obtained (dX) would be so small that the compositions of the inlet and outlet streams would be almost identical (Doraiswamy and Sharma, 1984). Under these conditions, the experimental conversion gives the rate directly, corresponding to the partial pressures (average of inlet and outlet values) of the reactants and products in the differential bed.

$$-r_A = \frac{X_{A,\,out} - X_{A,\,in}}{W/F} \tag{2.15}$$

where $X_{A,\,out}$ and $X_{A,\,in}$ represent the inlet and outlet mole fractions of A. The shortcomings of the differential reactor can be overcome by two methods: (1) recycling a large part of the product, or (2) using a stirred reactor (these agitated reactors may be regarded as pseudo differential reactors in that they give rates directly but at integral conversion levels).

2.3.2 Integral Plug Flow Reactors

The integral plug flow reactors are operated at high conversions. The rate of the reaction

changes considerably along the reactor. The main reason for any errors in the integral data is the lack of isothermicity, which is particularly serious in highly exothermic reactions. These errors can be minimized by diluting the catalyst bed with inert solids or by inserting the reactor in a temperature controlled fluidized sand bed.

In a plug flow reactor, the composition of the fluid varies along the reactor, consequently, the material balance for a reaction should be made for a differential element of volume dV. For example, for a reactant A,

$$input = output + disappearance\ by\ reaction + accumulation \tag{2.16}$$

where the accumulation becomes zero.

Input of A, moles/time $= F_A$

output of A, moles/time $= F_A + d F_A$

disappearance of A by reaction in terms of catalyst weight W, moles/time $= (-r_A)\ dW$

Substituting the above in equation (2.16),

$$F_A = (F_A + dF_A) + (-r_A)\ dW \tag{2.17}$$

where

F_A - molar flow rate of A, g-mol A/hr

W - mass of catalyst, g

r_A - net rate of formation of A, g-mol A/hr-g-catalyst

Defining the fractional conversion of A

$$dF_A = d\,(F_{A0}(1 - X_{fA})) = -F_{A0}\,dX_{fA} \tag{2.18}$$

by replacing in equation (2.17),

$$F_{A0}\,dX_{fA} = (-r_A)\,dW \tag{2.19}$$

Equation (2.19) accounts for A in the differential section of catalyst mass dW in the reactor. For the reactor as a whole the above equation is integrated to give,

$$\frac{W}{F_{A0}} = \int_0^{X_{Af}} \frac{dX_{fA}}{-r_A} \tag{2.20}$$

A plot of X_{fA} versus W/F_{A0} can be made and a best curve is fitted to the data by making it pass through the origin. The slope at any X_{fA} is the rate at that point. By evaluating the C_A and plotting it against the rate $-r_A$, the rate constant can be calculated.

The results of this study were derived from a steady-state, plug-flow, integral reactor. The assumptions that were made before deriving the corresponding plug flow rate equation are,

1. There are no thermal gradients in the reactor. This ideal isothermal state was approximated by placing the reactor in a well fluidized, temperature controlled sand bed.
2. Plug-flow exists in the reactor. This can be assumed from the flat velocity profile

which is verified from the small size of the catalyst particles and the presence of a fine porous plate at the inlet of the reactor.

3. No pressure drop across the reactor.

4. No change in the total molar flow rate during the course of reaction. This can be verified by the excess of hydrogen present.

2.4 CATALYSTS

A catalyst is a substance that increases the rate at which a chemical system approaches equilibrium, without being consumed in the process (Bond, 1987). The characteristics that determine the catalytic properties of a catalyst are,

- Catalyst activity which is defined as the ratio of the rate of reaction at any time to the rate of reaction with a fresh catalyst.
- Selectivity which is the rate of formation of desired products to the rate of formation of undesired products.
- Thermal stability, resistance to poisoning and reproducible in its behaviour.
- Resistance to attrition and crushing.
- Hydrodynamic characteristics which is determined by the size, shape and density of the catalyst particle.

In the current study, since the catalyst is used for hydrodenitrogenation purpose, apart from having the above properties, the catalyst should effectively remove nitrogen from the organic

nitrogen compound through carbon-nitrogen bond fission while not getting poisoned by other organic sulphur or metallic impurities and not causing coking.

The question of catalyst reproducibility cannot be separated from the criteria used to measure reproducibility (Rylander, 1967). Catalysts may be compared with respect to the above mentioned properties. The usual and most useful criteria of reproducibility are related to some aspects of performance like the activity or the selectivity. One important factor tending to make catalysts reproducible is constancy in preparation, but this in itself does not provide adequate guarantee because all the catalyst preparations are subject to various subtle and often unknown influences that alter the catalyst quality.

The catalyst used in this study was platinum supported on alumina. The platinum metals (ruthenium, rhodium, palladium, osmium, iridium and platinum) make exceptionally active hydrogenation catalysts (Rylander, 1967).

Platinum metal catalysts are of two types- supported and unsupported. Earlier, platinum catalysts were used in the form of finely divided metal (referred to as blacks) or metal oxides or colloidal catalysts. Platinum metal oxides and blacks were used with compounds difficult to hydrogenate, or when substantial yield losses occur due to the absorption of products by the catalyst support or when strong adsorption on the support poisons the catalyst.

Supported platinum catalysts have a number of advantages over unsupported catalysts. Supported catalysts have greater resistance to poisoning. The support also permits greater efficiency in the use of the metal by increasing the active metal surface and facilitating metal recovery. Platinum metals have been supported on a variety of materials such as carbon, alumina, silica, alkaline earth carbonates and sulphates, zinc, asbestos and silk. Usually carbon or alumina is used as support since either will prove adequate for most reactions.

2.5 MASS AND HEAT TRANSFER

In kinetic studies dealing with fluid reactions on solid catalysts, the interpretation of experimental data is facilitated by operating at high velocities and small particle size. Under these conditions, the temperature and the composition of the fluid in contact with the catalyst surface is nearly the same as in the bulk stream because the resistance to mass and heat transfer from particle to ambient fluid becomes negligible. The temperature and pressure drops pose a significant problem if such high velocities cannot be realized.

In laboratory studies aimed at determining the rate expression for a chemical reaction, these temperature and concentration gradients can be minimized by either using a reactant stream diluted with inerts (to reduce the reaction rate so that the energy evolved is reduced) or by employing high mass velocities.

2.5.1 Mass Transfer

The overall process of a heterogeneous catalytic reaction involves two general diffusional processes namely, (i) mass transfer to and from the external surface of the catalyst and (ii) mass transfer in and out of the catalyst pores (Clark, 1970). Mass transfer to the external surface is controlled in a thin boundary layer, usually less than a millimeter in thickness, next to the surface. The velocity of a fluid passing over the surface of a particle varies rapidly normal to the flow across this boundary layer. At the catalyst surface, the fluid velocity is zero, and rapidly approaches the bulk stream velocity a short distance from the surface. Near the surface, where the fluid velocity is low, little mixing of reactants and products occurs. Mass transfer normal to the surface is by molecular diffusion, and may be taken as proportional to the molecular diffusion coefficient D.

Data on mass transfer from fluid to solid surface are often expressed in terms of the j_D factor as defined by Chilton and Colburn as,

$$j_D = \frac{k_{G,A}\, p_{f,A}}{G_M} \left(\frac{\mu}{\rho\, D}\right)^{2/3} \tag{2.21}$$

where

j_D - mass transfer number

$k_{G,A}$ - mass transfer coefficient of component A in gas phase

$p_{f,A}$ - pressure factor of A

G_M - molar mass velocity of gas based on total cross section of bed

μ - fluid viscosity

ρ - fluid density

D - diffusion coefficient

The molal reaction rate of component A per unit mass of catalyst, r_{mA}, is given by,

$$r_{mA} = k_{G,A}\, a_m\, \phi\, (P_A - P_{A,if}) \tag{2.22}$$

where

a_m - area of particle per unit mass

ϕ - shape factor (assumed to be 0.9 for irregular particles)

P_A - partial pressure of A in bulk fluid

$P_{A,if}$ - partial pressure of A at catalyst surface

Hence the partial pressure drop of component A between the main stream and the catalyst surface may be calculated from equations (2.21) and (2.22) as,

$$\Delta p_A = \frac{r_{mA}}{a_m\, \phi\, k_{G,A}} = R'\, (j_D)^{-1}\, p_{f,A}\, \left(\frac{\mu}{\rho\, D_{MA}}\right)^{2/3} \tag{2.23}$$

where

D_{MA} - mean diffusion coefficient of A in a multi-component system

R' - dimensionless factor

$$= \frac{r_{mA}}{a_m \, \phi \, G_M}$$

The relative magnitudes of the partial pressure can be estimated using the correlation (Yoshida et al., 1962) without requiring the data on viscosities and diffusivities. The result of this estimation are given in Appendix D.

2.5.1.1 Diffusion within the pores

In the complex internal structure of high surface area catalysts, the nature of the individual pores and the porous structure are very important in determining the accessibility of the various regions of the catalyst to the reactants. Pore diffusion in a catalyst occurs by one or more of the following mechanisms (Clark, 1970); Knudsen diffusion, ordinary bulk diffusion, surface diffusion and forced flow. The first two are the most important mechanisms.

Knudsen diffusion

When the mean free path is large in comparison with the pore diameter, the collision between the molecules is less than the collision between a molecule and the wall and hence Knudsen diffusion dominates. This occurs at low gas density or when the pore-diameter is small. The pores are assumed to be straight capillaries. The molecules leave the wall surface randomly independent of the direction in which they hit due to rough pore surface or inelastic

collisions. The amount of gas flowing through the capillary decreases with length.

Based on the kinetic theory of gases, the Kundsen diffusion coefficient is expressed as.

$$D_K = \frac{2}{3} \bar{r} \left(\frac{8\ R''\ T}{\pi\ M}\right)^{1/2} = \frac{2}{3} \bar{r}\ \bar{v} \qquad (2.24)$$

where

$\bar{r}$ - radius of the pore

R'' - gas constant

M - molecular weight of the diffusing component

$\bar{v}$ - mean Maxwellian velocity

The Knudsen flow can be included in a general flow equation by using the Kundsen coefficient.

Bulk diffusion

When the mean free path is much smaller than the pore diameter, a greater number of collisions occur between the molecules compared to the number of collisions with the walls, resulting in bulk diffusion. This occurs at high pressures or with larger pores. The diffusion coefficient is given by,

$$D_B = \frac{1}{2} \bar{v}\ \lambda \qquad (2.25)$$

where

λ - mean free path

$\bar{v}$ - mean Maxwellian velocity

2.5.3 Heat Transfer

If the heat released or absorbed in the catalyst during the course of a fast reaction cannot be removed rapidly enough to keep the catalyst close to the temperature of the bulk fluid, then the nonisothermal effects intrude. In such situations, there are two types of temperature effects that can be encountered such as; within particle Δt and film Δt (the temperature difference between the catalyst and the bulk fluid).

The temperature drop from a catalyst surface to ambient fluid is estimated using a heat transfer factor j_H defined by Chilton and Colburn as,

$$j_H = \frac{h_G}{C_p G} \left(\frac{C_p \mu}{k'}\right)^{2/3} \tag{2.26}$$

where

h_G - heat transfer coefficient in gas phase

C_p - heat capacity per unit mass at constant pressure

G - mass velocity of gas based on total cross section of bed

k' - thermal conductivity

$C_p\mu/k$ - N_{Pr} (Prandtl number)

The temperature difference between the catalyst surface and the bulk stream is given by.

$$\Delta t = \frac{r_{mA}\ \Delta H_A}{a_m\ \Phi\ h_G} \tag{2.27}$$

where

ΔH_A - molal heat of reaction of A

From equations (2.26) and (2.27),

$$\Delta t = \frac{r_{mA}\ \Delta H_A}{a_m\ \Phi\ C_p\ G_M} (j_H)^{-1}\ (N_{Pr})^{2/3} = Q\ (j_H)^{-1}\ (N_{Pr})^{2/3} \tag{2.28}$$

where

G_M - molal mass velocity of gas based on total cross section of bed

$$Q = \frac{r_{mA}\ \Delta H_A}{a_m\ \Phi\ C_p\ G_M}$$

By calculating Q and using the correlation given by Yoshida et al. (1962), Δt can be estimated.

CHAPTER 3

PROPERTIES OF MATERIALS

In this chapter, we will look into the properties of the major reactant, pyridine, used in the research and also some of the possible hydrodenitrogenation products.

3.1 PYRIDINE

All six-membered fully unsaturated heterocycles are formally related to benzene in which one or more of the CH groups of benzene is replaced by a heteroatom. Pyridine is the simplest of such compounds.

3.1.1 Sources and Synthesis

Pyridine was first isolated from bone pyrosylate. Pyridine and its simple alkyl derivatives were produced for a long time from coal tar, in which they occur in large quantities. Coal tar contains about 0.2% of a mixture of pyridine bases. In recent years, this source has been replaced by synthetic processes. For example, pyridine can be produced by the gas-phase reaction of crotonaldehyde, formaldehyde and ammonia over a silica-alumina catalyst. Processes for the manufacture of the alkyl pyridines involve reaction of acetylenes and nitriles over a cobalt catalyst.

Pyridine and its simple derivatives are used as solvents and bases. Among many pyridines

which have been developed as pharmaceuticals are piroxicam (an anti-inflammatory), nifedipine (which is used for the treatment of angina) and isoniazid (used for tuberculosis therapy). 3-Methylpyridine is a commercially important precursor to pyridine-3-carboxylic acid (nicotinic acid), a B group vitamin.

3.1.2 Chemistry

Pyridine is a planar molecule, the ring system being a slightly distorted hexagon because the C-N bonds (1.45Å) are shorter than the C-C bonds (1.48Å). It has a complete cycle of p-orbitals containing six π-electrons so that the electronic structure
is similar to that of benzene (Figure 3.1).

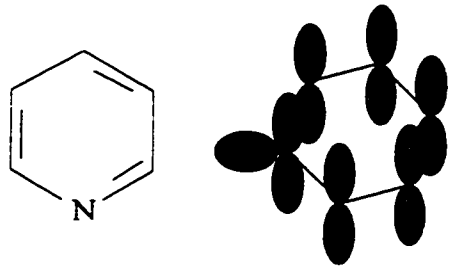

Figure 3.1 Structure of Pyridine

Pyridine can thus be classified as aromatic because it obeys the Hückel rule which based on simple molecular orbital calculations states that planar molecules with a complete and uninterrupted cycle of p-orbitals are stabilized, relative to the acyclic counterparts, when they contain (4n+2) π-electrons where n is zero or an integer. Though pyridine has a benzene-like structure, the nitrogen atom in the ring represents a major perturbation of the benzene

structure. This structure, with a lone pair of electrons in the plane of the ring allows pyridine to have analogous reactions to three model systems (Gilchrist, 1985):

a. Benzene - Substitution reactions and resistance to ring opening.

b. Tertiary amines - Protonation, alkylation and coordination to Lewis acids, occurring at the nitrogen lone pair.

c. Conjugated imines or carbonyl compounds - Susceptibility to attack at the α- and γ-carbon atoms by nucleophiles.

3.2 HYDRODENITROGENATION PRODUCTS

Hydrodenitrogenation of pyridine resulted in many organic products especially at higher temperatures and hydrogen flow rate. Most of the compounds were present in trace amounts and hence were not considered for the analysis. The major compounds that were identified are listed below along with some of their properties.

Table 3.1 Major HDN products of pyridine

Compound	Manufacturer	Boiling point (K)	Density (g/ml)
Cyclopentane	MC/B	323	0.745
Dipentylamine	Aldrich	202.0	0.7771
Ethyl piperidine	Aldrich	130.8	0.8237
Pentane	BDH Inc.	36.1	0.6262
Pentylamine	Eastman	104.4	0.7547
Pentyl piperidine	Prepared in lab	198.2	0.8282
Piperidine	Fisher Scientific	106.0	0.8606
Pyridine	Fisher Scientific	115.1	0.9819

CHAPTER 4

EXPERIMENTAL ASPECTS

The hydrodenitrogenation of pyridine was carried out in a continuous flow, fixed-bed catalytic reactor that was operated in an integral mode under isothermal conditions. The experimental apparatus used in this study was similar to the one used by Gupta (1977), Anabtawi (1980) and Ajaka (1994). A schematic representation of the experimental apparatus is shown in Figure 4.1.

The experimental set-up mainly consisted of three sections namely, the feed section, the reactor section and the sampling and analysis section. These main sections are described in detail in the following paragraphs.

4.1 REACTOR FEED SECTION

The two reactants fed to the reactor were hydrogen and pyridine. Reactant hydrogen was supplied from a high pressure (2500 psig) cylinder equipped with a single-stage regulator (Matheson Gas Products) that was used to maintain the reactor pressure at the desired level. Then the hydrogen stream was passed through the following three different stages of purification : (i) an oxygen trap that contained a highly active metal to convert the oxygen to water, (ii) a moisture trap that contained molecular sieve 13X and, (iii) a hydrocarbon

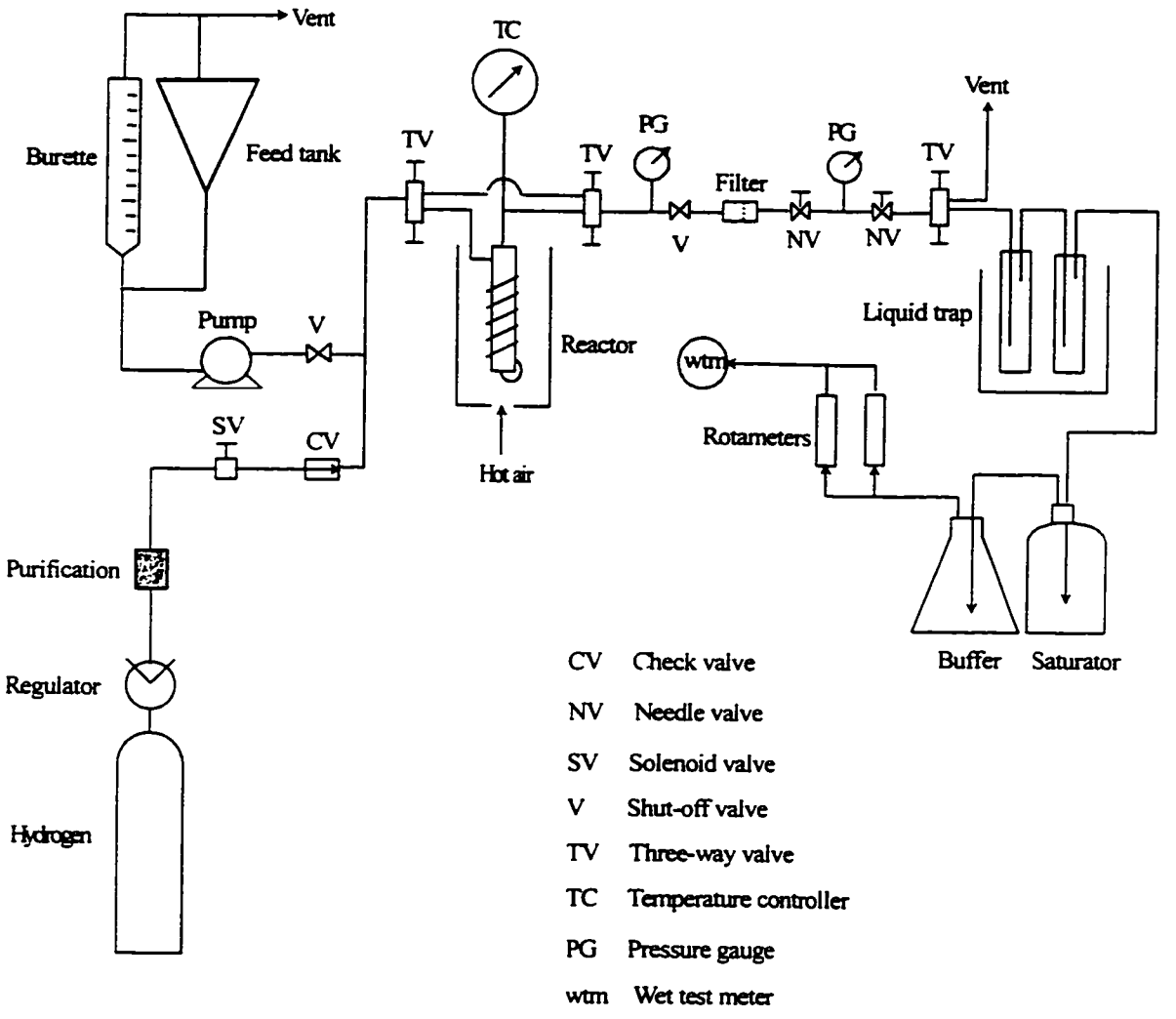

Figure 4.1 The experimental setup used to study the hydrodenitrogenation of pyridine

trap that contained activated carbon. Hydrogen was then passed through a solenoid valve (ASCO, 2200 psi, Ascoelectric Ltd., Canada) and then through a check valve (Nupro, 10 psi) to prevent any back-mixing. The hydrogen stream was finally passed through a preheater before entering the reactor.

A high pressure metering pump (Milton Roy Company, Fl., USA) was used to feed the liquid reactant pyridine to the system. The metering pump was calibrated for different pressures of pyridine. The instantaneous flow rate shown by the pump setting was checked frequently with the cumulative reading shown by the burette reading. Pyridine was pumped through a tee where a damper was attached to reduce the fluctuations caused by the pump and then through a shut-off valve. Finally it was passed through a mixing tee where it was flash vapourized into the preheated hydrogen stream. The preheater was maintained at 503 ± 3 K by wrapping the tubing with a heating tape (GLAS-COL USA). The temperature of the heating tape was controlled by a variable auto transformer (Fisher Scientific Co., USA) and the temperature was monitored by a digital thermometer (Thermo Electric Canada Ltd.). Then the reactants entered the final preheating coil immersed in the fluidized sand bed surrounding the reactor. The purpose of the preheater was to raise the temperature of the reactants to that of the reactor thereby reducing the thermal gradients in the reactor.

4.2 REACTOR SECTION

The reactant stream containing hydrogen and pyridine was connected to a three-way valve

(Autoclave Engineers, 10V-2005). One branch led to the reactor while the other bypassed the reactor to meet again through another three-way valve before entering the liquid trap to condense the organics of the reactor effluent.

The reactor was 316 stainless steel tubing of length 7.25 in. (18.415 cm) and an inner diameter of 0.42 in. (1.067 cm). The catalyst bed was secured from both ends by porous stainless steel plates (40 microns). The catalyst extrudates were crushed to 20/35 mesh size (average diameter of 0.6375 mm).

The reactor and the final preheating coil (1/8 in. outer diameter stainless steel tubing) were immersed in a fluidized sand bed heater. Reaction temperature was measured with an 1/8 in. type-K thermocouple placed in the catalyst bed and connected to a temperature controller (Honeywell). The sand bed was fluidized by hot air. The temperature of the bed was controlled by two temperature controllers (Honeywell). The reactants were heated to the desired temperature in the preheater. The reactor was mounted vertically in the sand bed and the preheated reactants entered through the lower inlet of the reactor. To ensure isothermal operation at steady state, the difference in the temperatures of the sand bed and that of the reaction was kept within 2 to 3 K.

The total pressure of the reactor was measured by a 3500 psig test gauge (Matheson Part No. 63-5633) located after the three-way valve through which the bypassed stream and the

reactor effluent combined. A metering valve (Whitey 316-SS 31RF2) was located after the pressure gauge and was used for the initial adjustment of the flow rate at the beginning of each run and also for shut-off purposes in some instances. The flow rate was further controlled manually with a very fine metering valve (Nupro SS). A 15 micron filter (Nupro Co.) was used to protect this fine metering valve from any blocking of the orifices by the particle in the stream. A 100 psig test gauge (Matheson Part No. 63-5612) located after the valve was used to control the pressure of the exit stream. The temperature of the valves and the tubing from the reactor to the liquid trap was maintained at 533 ± 3 K to prevent any condensation of the products before they reach the liquid trap.

4.3 SAMPLING AND ANALYSIS

The liquid trap to collect the sample was made of two glass test tubes connected in series. The trap was immersed in ice-water to condense the organic liquids in the product stream. A three-way valve was installed before the liquid trap. One line of the valve led to the trap while the other led to the vent. This valve was used for safety reasons, i.e., to avoid the risk of exposure to the fumes while collecting the sample. A fine metering valve was installed just upstream of the three-way valve for finer adjustment of the flow rate of the reactor effluent.

The effluent stream from the liquid trap was passed through a saturator (potassium hydroxide solution) to remove the rest of the organics and some of the ammonia gas. The

remaining stream containing mainly hydrogen and some ammonia was passed through an empty flask that acts as a buffer port and then through a moisture trap. Finally the stream is passed through either one of the rotameters; a Matheson 601 (a maximum hydrogen flow rate of 550 std. cc/min) to monitor low flow rates or a Matheson 602 (a maximum hydrogen flow rate of 2300 std. cc/min) for higher flow rates. The moisture trap located before the rotameters also acts as a filter to guard the rotameter tubes and floats from fouling. To guard against the erroneous rotameter reading caused by the fouling of the tubes and floats, the gas stream was then passed though a wet test meter (GCA, Precision Scientific) before it was vented out. The instantaneous flow rate shown by the rotameter was checked frequently with the cumulative flow rate shown by the wet test mater and a very close agreement between the two readings was observed.

The analysis of the product was done by a gas chromatograph (HP-5730A) equipped with a thermal conductivity detector, a flame ionization detector and temperature programming capability. An integrator (HP-3380A) was used to produce the chromatograms, retention times and peak areas. Quantitative analysis was carried out by injecting liquid samples through the flame ionization detector.

4.3.1 Gas Chromatographic Analysis

The gas chromatographic column was obtained from Chromatographic Specialties Inc. The column was packed with 10% carbowax 20M and 1% KOH on 80-100 mesh chromosorb

P (acid washed). The operating conditions that were found suitable for the separation were; initial column temperature 343 K, initial time 0 min., rate of increase in temperature 8 K/min., final column temperature 473 K, final time 45 min., injector temperature 473 K, detector temperature 523 K and carrier gas (helium) flow rate 10 cc/min.

4.4 CATALYST PREPARATION

The catalyst used was 0.5% platinum supported on alumina (Acros Organic, USA). It was obtained in the form of 1/8 in. diameter extrudate which was then crushed and sieved to 20/35 mesh (average diameter of 0.6375 mm). The surface area of the catalyst and the pore volume were 100 m^2/g and 0.40 cc/g respectively. Pumice stone, a porous igneous rock, usually containing 67 to 75% silica and 10 to 20% alumina of glassy texture, was also crushed and sieved to 20/35 mesh size. 5g of the catalyst was diluted with 3g of pumice and loaded in the reactor. The catalyst was diluted to minimize the errors due to lack of isothermicity which one of the major problems in the integral reactors.

4.5 CALIBRATION

The gas chromatographic column was calibrated qualitatively and quantitatively with several standard solutions of varying concentrations of the reactant and expected products. The plot of the peak area versus the concentration of the corresponding compound was found to be linear in the range of interest. The major products of pyridine HDN and their retention times are listed in the following table. The calibration curves are given in

Appendix A.

Table 4.1 Compounds and their retention times

Compounds	Retention times
Cyclopentane	1.86
Dipentylamine	13.8
Ethyl piperidine	6.31
Pentane	1.41
Pentylamine	6.01
Pentyl piperidine	11.90
Piperidine	6.72
Pyridine	10.01

The rotameters and the feed pump were calibrated next. The rotameters were calibrated by passing hydrogen through them at room temperature (294± 3 K) and atmospheric pressure. The rotameter reading was noted and the corresponding flow rate was measured using a soap-bubble meter for low flow rates or a wet test meter for higher flow rates.

The feed pump was calibrated by measuring the discharge rate at the suction side of the pump for the given pump stroke at an upstream pressure of 3.447 and 6.894 MPa.

4.6 ELECTRON SPIN RESONANCE STUDIES

In this study, Electron Spin Resonance (ESR) was used to analyze the catalyst. Both used and fresh (unused) samples were studied. The fresh sample was obtained by crushing the catalyst pellets and sieving to 20/35 mesh size particles. The spectra were taken under the following two conditions.

1. The catalyst was evacuated and heated to about 573 K for 45 minutes.

2. The catalyst was reduced with hydrogen and heated to about 573 K for 45 minutes.

The used catalyst was taken from the reactor after the reaction and the spectra were taken under the same conditions as those for the fresh sample. The equipment used for the study was B-ER 414/418 Spectrometer from Bruker-Physic AG.

4.7 EXPERIMENTAL CONDITIONS

Experimental data for the HDN of pyridine over Pt (0.5%) on alumina catalyst were obtained using an isothermal plug flow reactor. The effect of various reaction variables on the reaction was studied. For the kinetic studies, the reactant molar ratio (R) was kept constant at 11 g-mol hydrogen/g-mol pyridine (< 5% error). The space time (W/F) was varied from 37 to 247 hr-g-catalyst/g-mol pyridine (< 2% error) and the temperature (T) was varied from 523 ± 2 to 623 ± 2 K. The reaction was studied under a total pressure of 6.894 MPa (1000 psig) and 3.447 MPa (500 psig).

CHAPTER 5

RESULTS AND DISCUSSION

The effect of temperature, pressure and space time on conversion (X), yield (Y) and selectivity (S) was studied. Conversion is defined as the moles of pyridine consumed per moles of pyridine fed. Yield is defined as the ratio of moles of the particular product (hydrocarbons in this case) to the moles of pyridine fed. Selectivity is defined as the ratio of the moles of pure hydrocarbons produced to the moles of nitrogen compound produced. Denitrogenation is defined as the amount of pyridine converted to hydrocarbons.

The catalyst was deactivated till the activity of the catalyst became constant and the runs were carried out in this region. The steady state was realized from the operating conditions as well as the product analysis. Results of a blank run indicated that no reaction took place between pyridine and hydrogen in the absence of the catalyst even upto 673 K. The quantitative analysis was carried using a flame ionization detector. Hence in this study, the product distribution was calculated only on the basis of organic products, i.e., ammonia free basis. The significant products of pyridine HDN as identified by the gas chromatography were pentane, cyclopentane, piperidine, ethyl piperidine, pentyl piperidine, pentylamine, dipentylamine. Some of the experimental runs (chosen randomly) were repeated to confirm the reproducibility of the data. The raw data are given in Appendix B and the runs that were

repeated are also indicated.

5.1 EFFECT OF PROCESS VARIABLES

5.1.1 Effect of Temperature

The effect of temperature on the product distribution of pyridine HDN was investigated in the W/F range of 37 to 247 hr-g-catalyst/g-mol pyridine, temperature range of 523 to 623 K and at the total pressures of 6.894 and 3.447 MPa. The reactant molar ratio was maintained at 11 g-mol hydrogen/g-mol pyridine throughout the experiment.

Figures 5.1 to 5.3 show the effect of temperature on the product distribution at space times of 37, 107 and 247 hr-g-catalyst/g-mol pyridine respectively at a total pressure of 6.894 MPa. As the temperature was increased, alkyl piperidines (pentyl piperidine and ethyl piperidine) were formed with an increase in space time. At 572 K, piperidine reached a maximum for space time of 37 hr-g-catalyst/g-mol pyridine. At higher space times, piperidine reached the maximum at lower temperatures and at a space time of 247 hr-g-catalyst/g-mol pyridine, piperidine decreased linearly with the increase in temperature. The production of pentyl piperidine increased with temperature at lower space times. At higher space times, pentyl piperidine also reached a maximum and then decreased with the increase in temperature. The production of pentylamine and dipentylamine increased with temperature at lower space times. At space times greater than 107 hr-g-catalyst/g-mol pyridine, pentylamine and dipentylamine reached a maximum and then decreased with an

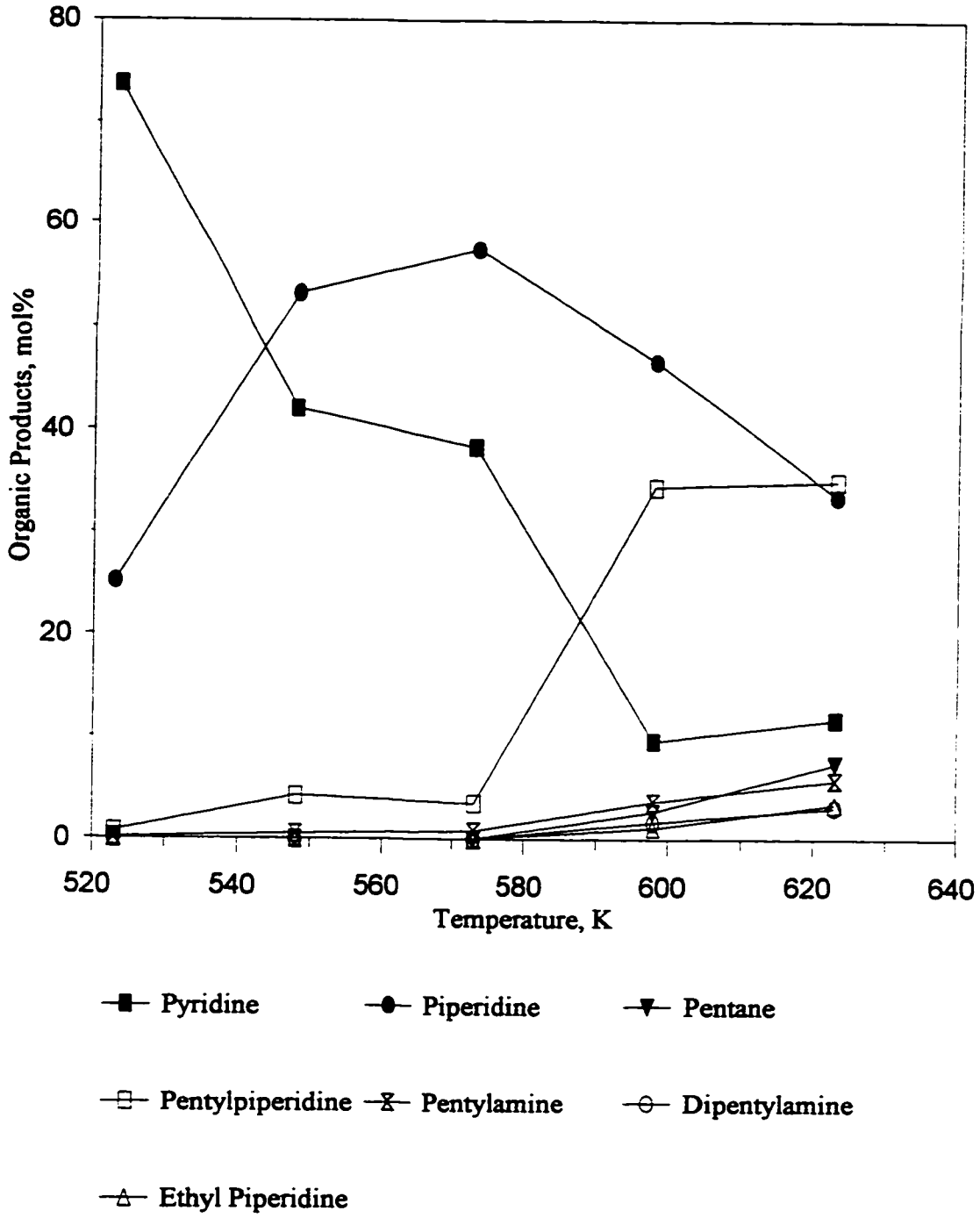

Figure 5.1 Effect of temperature on the organic product distribution at W/F=37 hr-g-catalyst/g-mol pyridine, R=11 g-mol hydrogen/g-mol pyridine, P=6.894 MPa

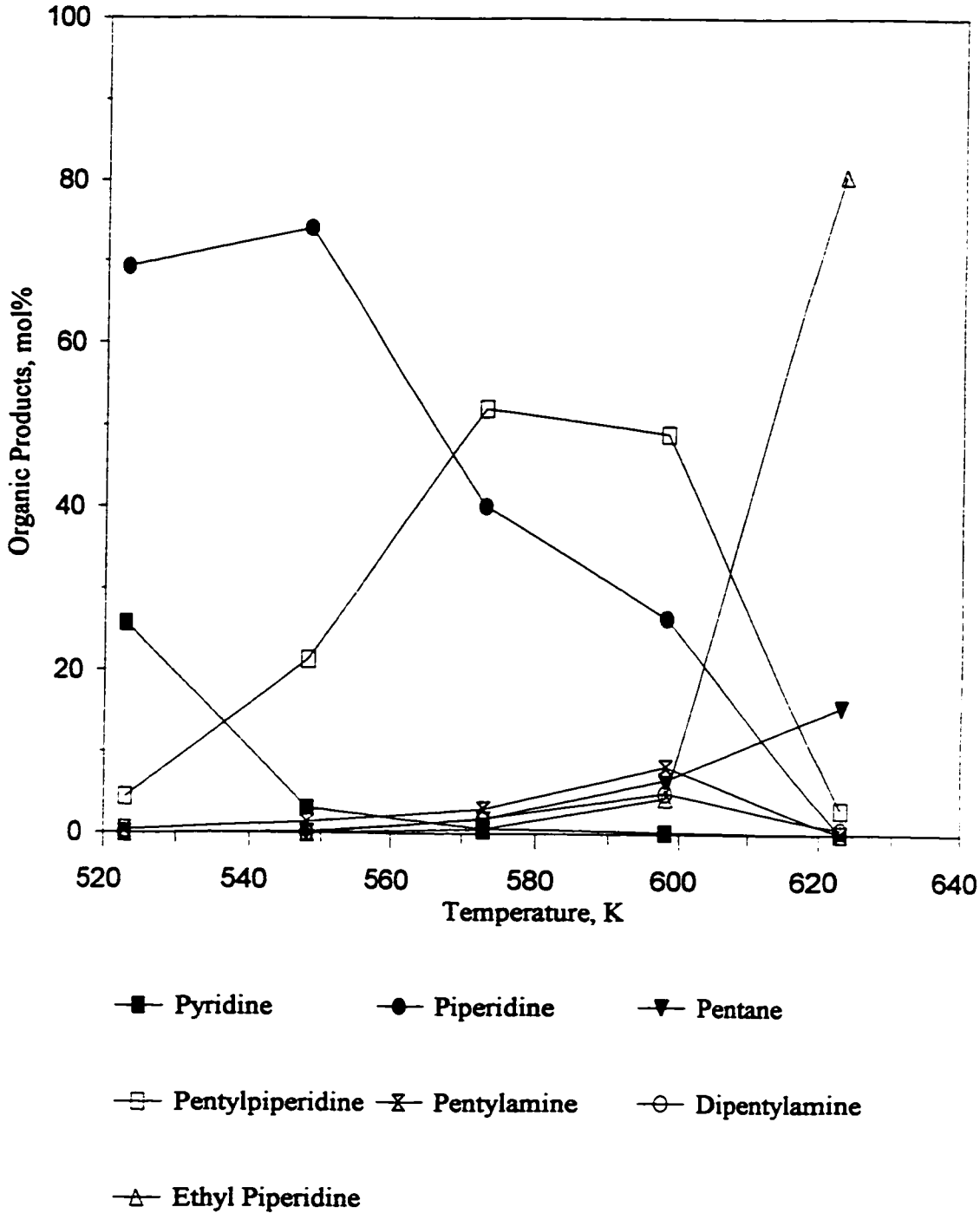

Figure 5.2 Effect of temperature on the organic product distribution at W/F=107 hr-g-catalyst/g-mol pyridine, R=11 g-mol hydrogen/g-mol pyridine, P=6.894 MPa

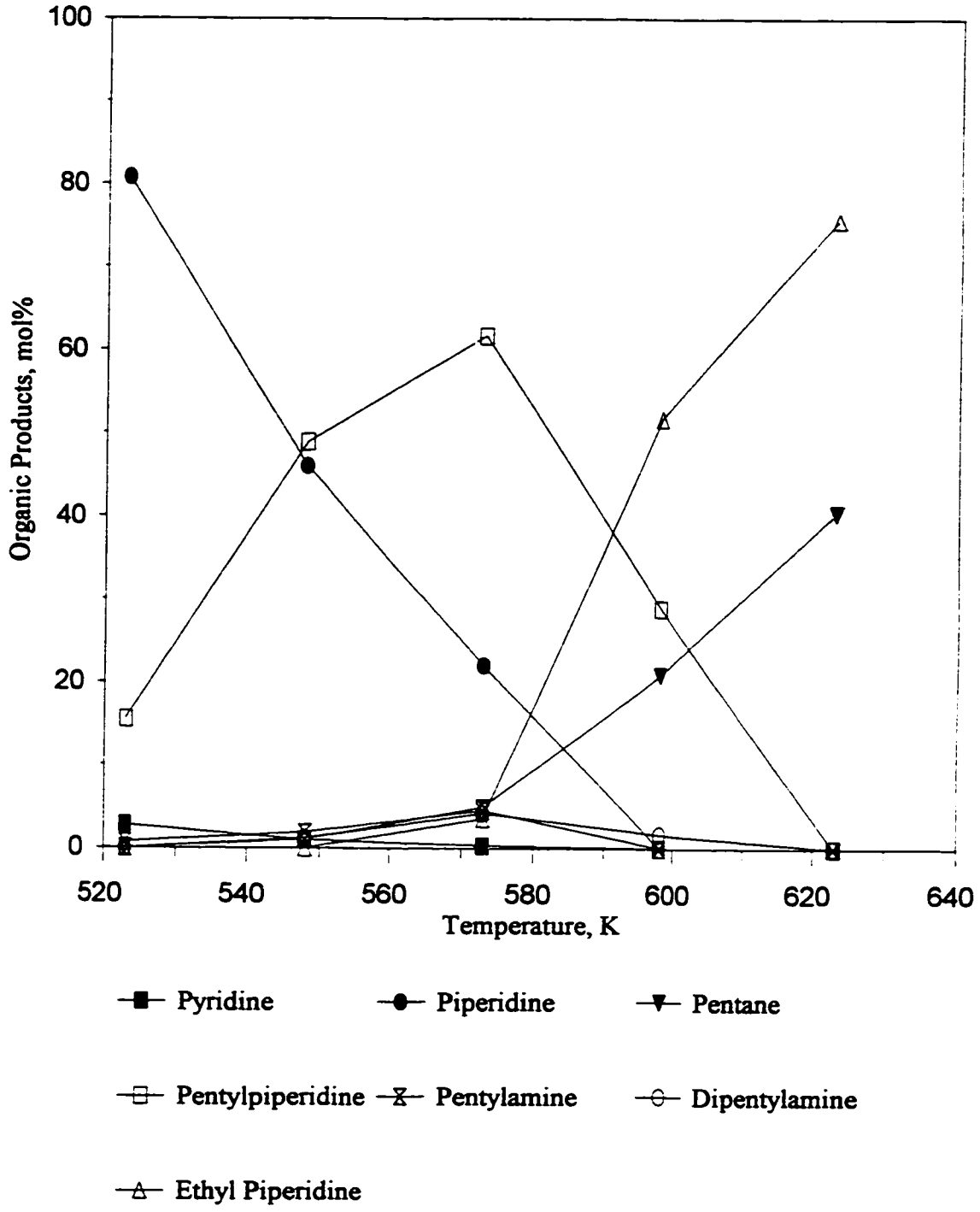

Figure 5.3 Effect of temperature on the organic product distribution at W/F=247 hr-g-catalyst/g-mol pyridine, R=11 g-mol hydrogen/g-mol pyridine, P=6.894 MPa

increase in temperature. The amount of pentane produced increased with temperature and space time. Ethyl piperidine was detected at temperatures greater than 573 K. At higher space times and temperatures above 573 K, the main products detected were ethyl piperidine, pentane, dipentylamine and pentylamine. At 623 K and space time of 247 hr-g-catalyst/g-mol pyridine, traces of cyclopentane were detected. The final products were pentane and ethyl piperidine.

Figures 5.4 to 5.6 show the effect of temperature on the denitrogenation, yield and selectivity respectively. The yield of hydrocarbons increased with temperature and space time. The selectivity for hydrocarbons and denitrogenation of pyridine also increased with temperature and space time. There were other unidentified products which had molecular weights higher than that of dipentylamine. From the gas chromatographic analysis, the amount of these unidentified products were found to be less than 2%.

Figures 5.7 and 5.8 show the effect of temperature on the product distribution at W/F of 88 and 152 hr-g-catalyst/g-mol pyridine at a total pressure of 3.447 MPa. At a space time of 88 hr-g-catalyst/g-mol pyridine, the products detected were piperidine, pentyl piperidine, pentylamine and pentane. Amount of piperine in the product decreased with temperature till 598 K after which there was an increase in the amount of piperidine. Pentyl piperidine and pentylamine reached a maximum at 573 K and then decreased with an increase in temperature. The amount of pentane in the product increased with temperature. Similar

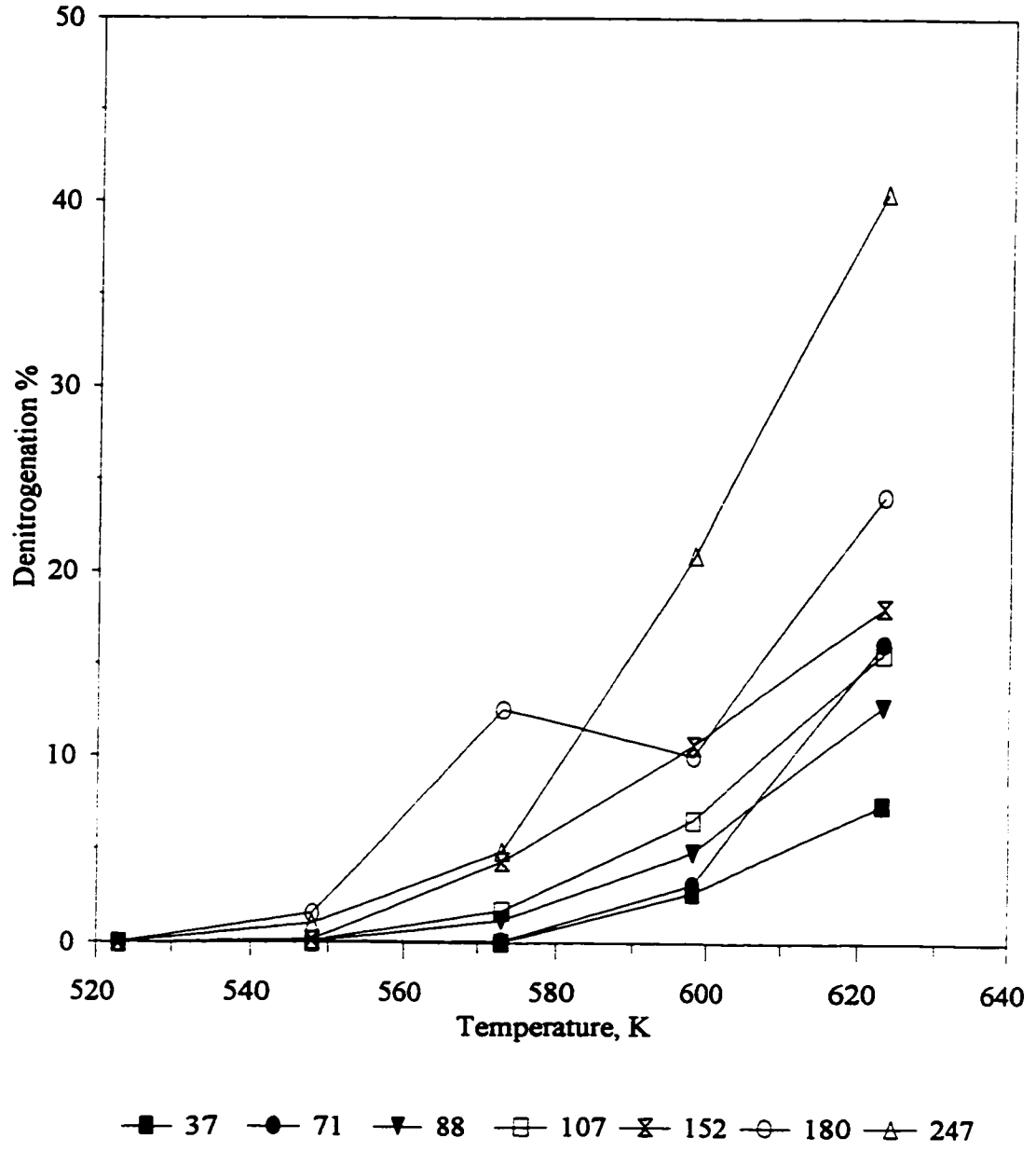

Figure 5.4 Effect of temperature on the denitrogenation of pyridine at different space times, R=11 g-mol hydrogen/g-mol pyridine, P=6.894 MPa

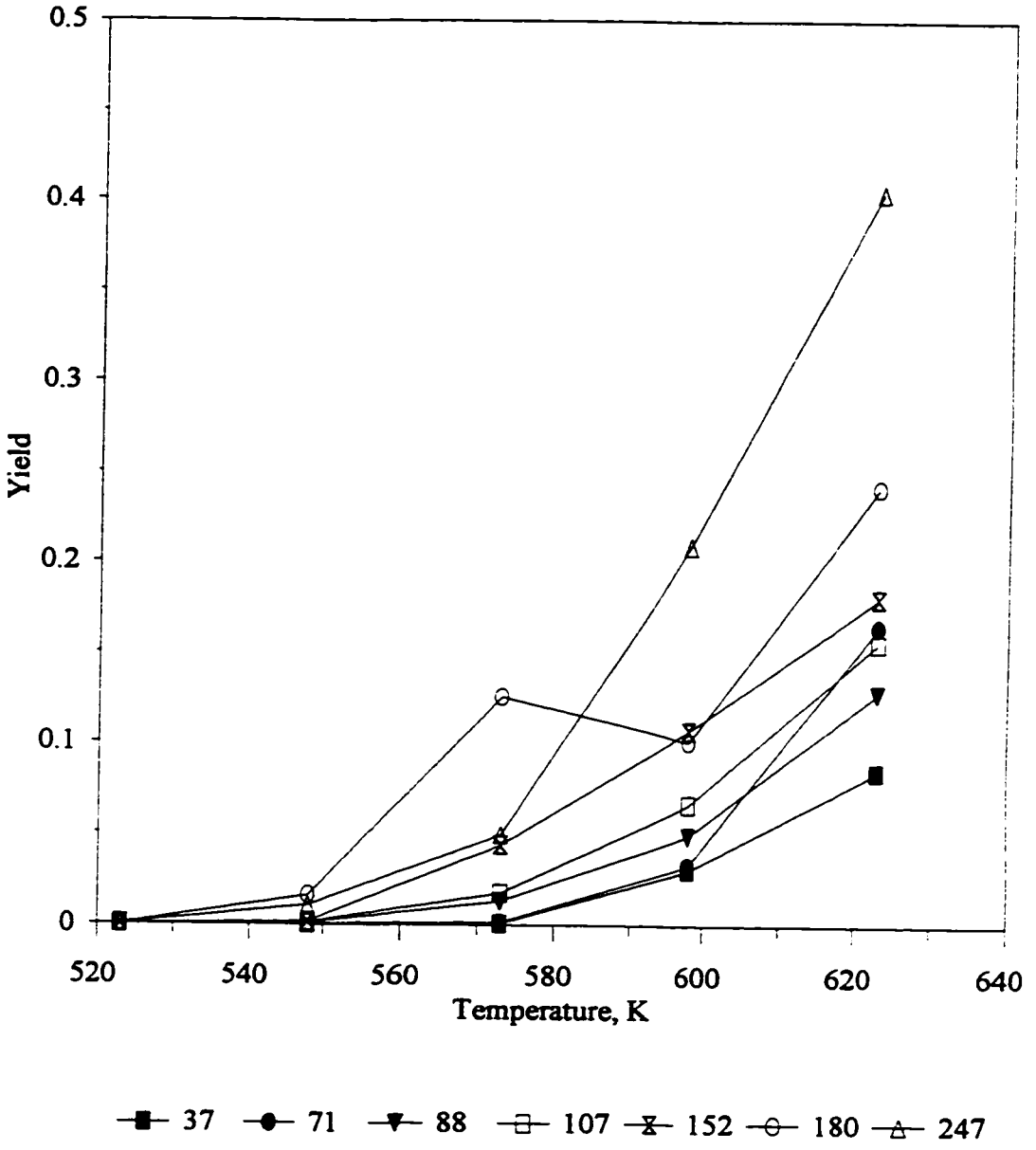

Figure 5.5 Effect of temperature on the yield of hydrocarbons at different space times, R=11 g-mol hydrogen/g-mol pyridine, P=6.894 MPa

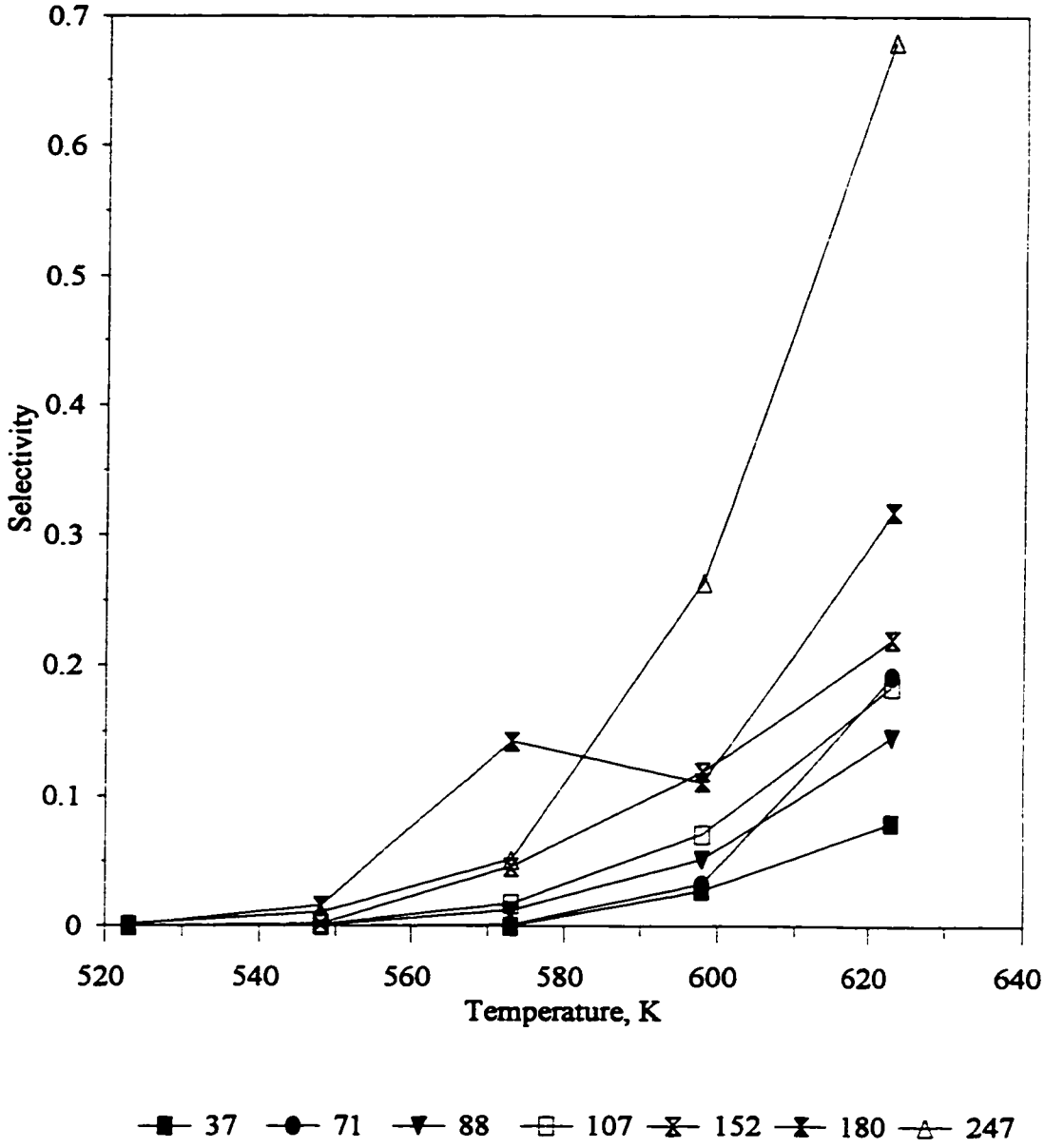

Figure 5.6 Effect of temperature on the selectivity for hydrocarbons at different space times, R=11 g-mol hydrogen/g-mol pyridine, P=6.894 MPa

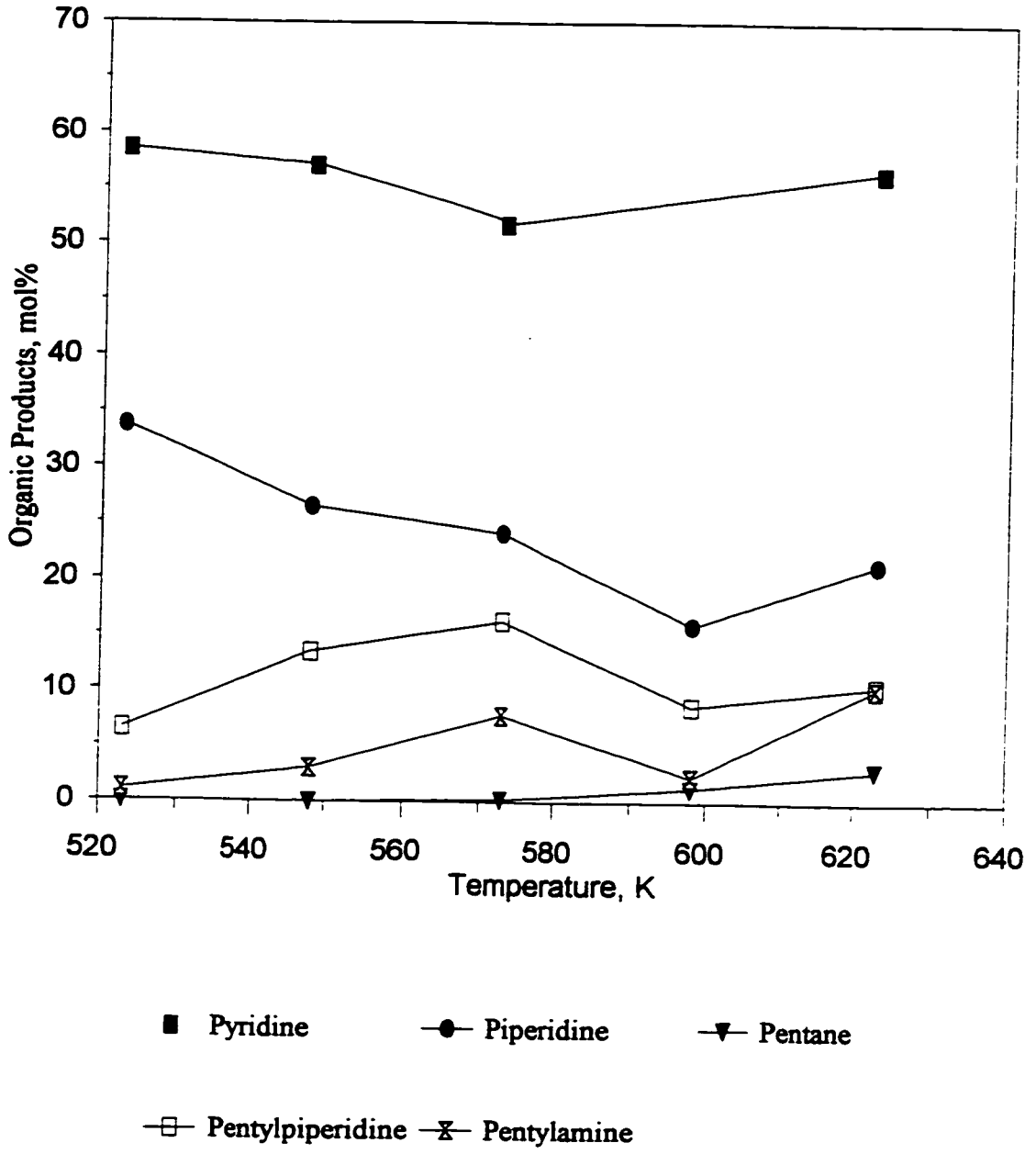

Figure 5.7 Effect of temperature on the organic product distribution at W/F= 88 hr-g-catalyst/g-mol pyridine, R=11 g-mol hydrogen/g-mol pyridine, P=3.447 MPa

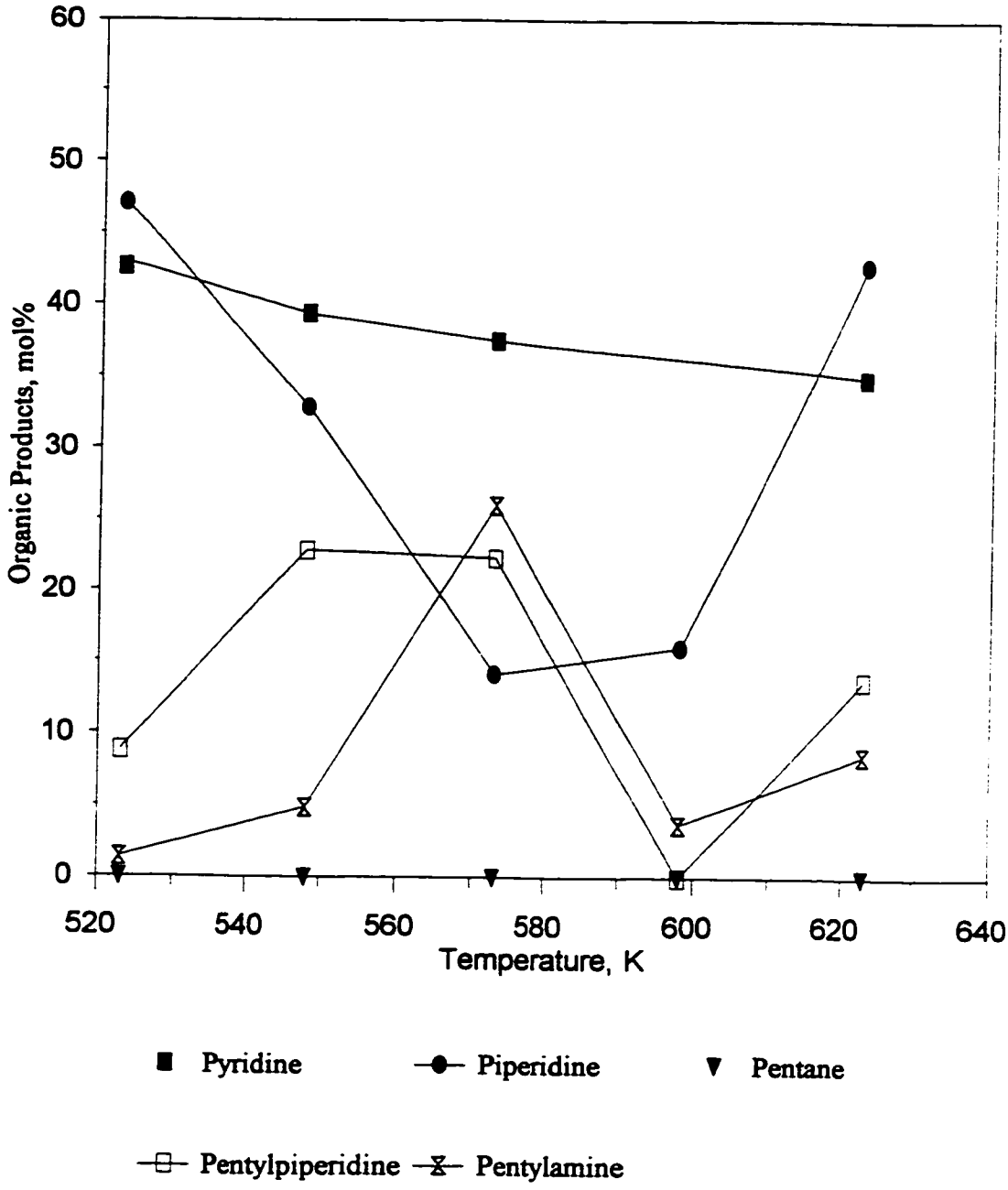

Figure 5.8 Effect of temperature on the organic product distribution at W/F= 152 hr-g-catalyst/g-mol pyridine, R=11 g-mol hydrogen/g-mol pyridine, P=3.447 MPa

trends were observed at higher space times. Traces of cyclopentane was observed at 623 K and higher space times.

Figures 5.9 to 5.11 show the effect of temperature on denitrogenation, yield and selectivity. The yield of hydrocarbons increased with temperature and decreased with space time. At space times above 107 hr-g-catalyst/g-mol pyridine, the yield was very less and varied slightly with an increase in space time. The selectivity for hydrocarbons and denitrogenation of pyridine increased with temperature and decreased with space time. Denitrogenation as well as the selectivity varied only a little at higher space times.

5.1.2 Effect of Space Time (W/F)

The effect of space time on product distribution, conversion, yield and selectivity was studied by varying it between 37 and 247 h g-catalyst/g-mol pyridine and temperatures between 523 and 623 K at the total pressures of 6.894 and 3.447 MPa while keeping the reactant molar ratio constant at 11 g-mol hydrogen/g-mol pyridine.

Figures 5.12 to 5.15 show the effect of space time on product distribution at 523 and 623 K at 6.894 and 3.447 MPa total pressures. At 6.894 MPa., piperidine formed increased with the increase in space time at 523 K and decreased with space time at 623 K. The amount of pentyl piperidine, dipentylamine and pentylamine increased with space time at lower temperatures but started to decrease at higher temperatures. Ethyl piperidine and pentane

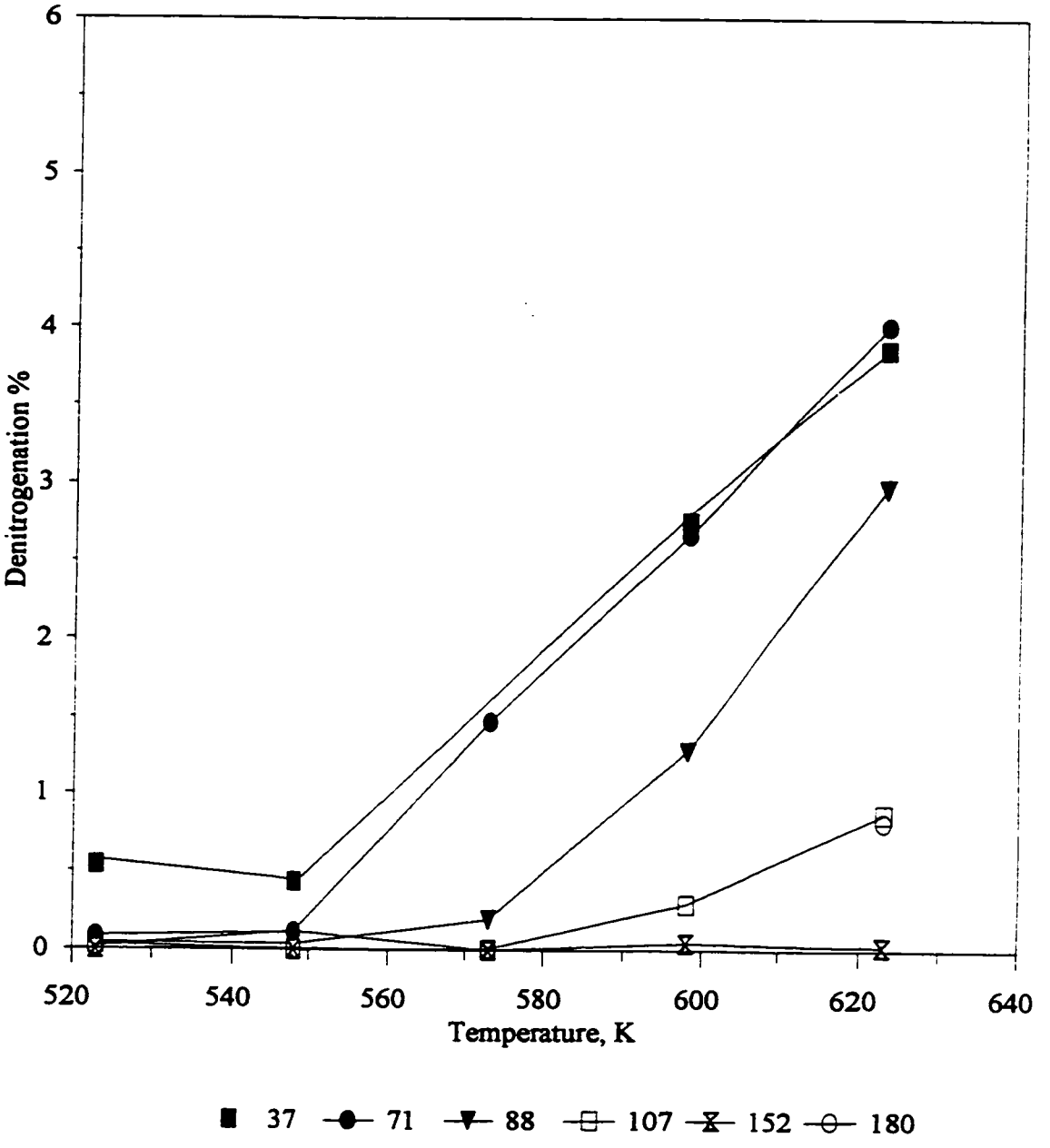

Figure 5.9 Effect of temperature on the denitrogenation of pyridine at different space times R=11 g-mol hydrogen/g-mol pyridine, P=3.447 MPa

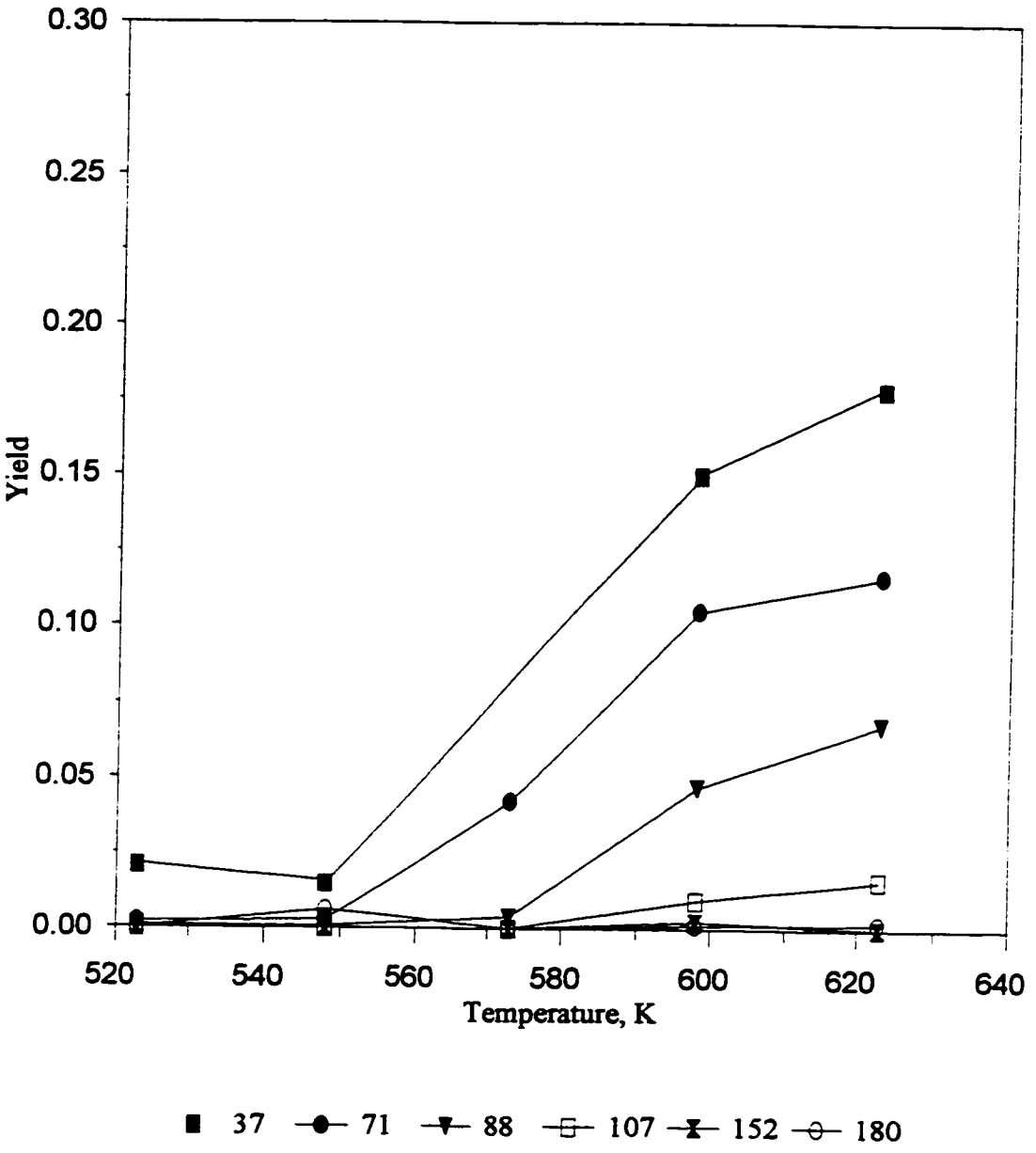

Figure 5.10 Effect of temperature on the yield of hydrocarbons at different space times, R=11 g-mol hydrogen/g-mol pyridine, P=3.447 MPa

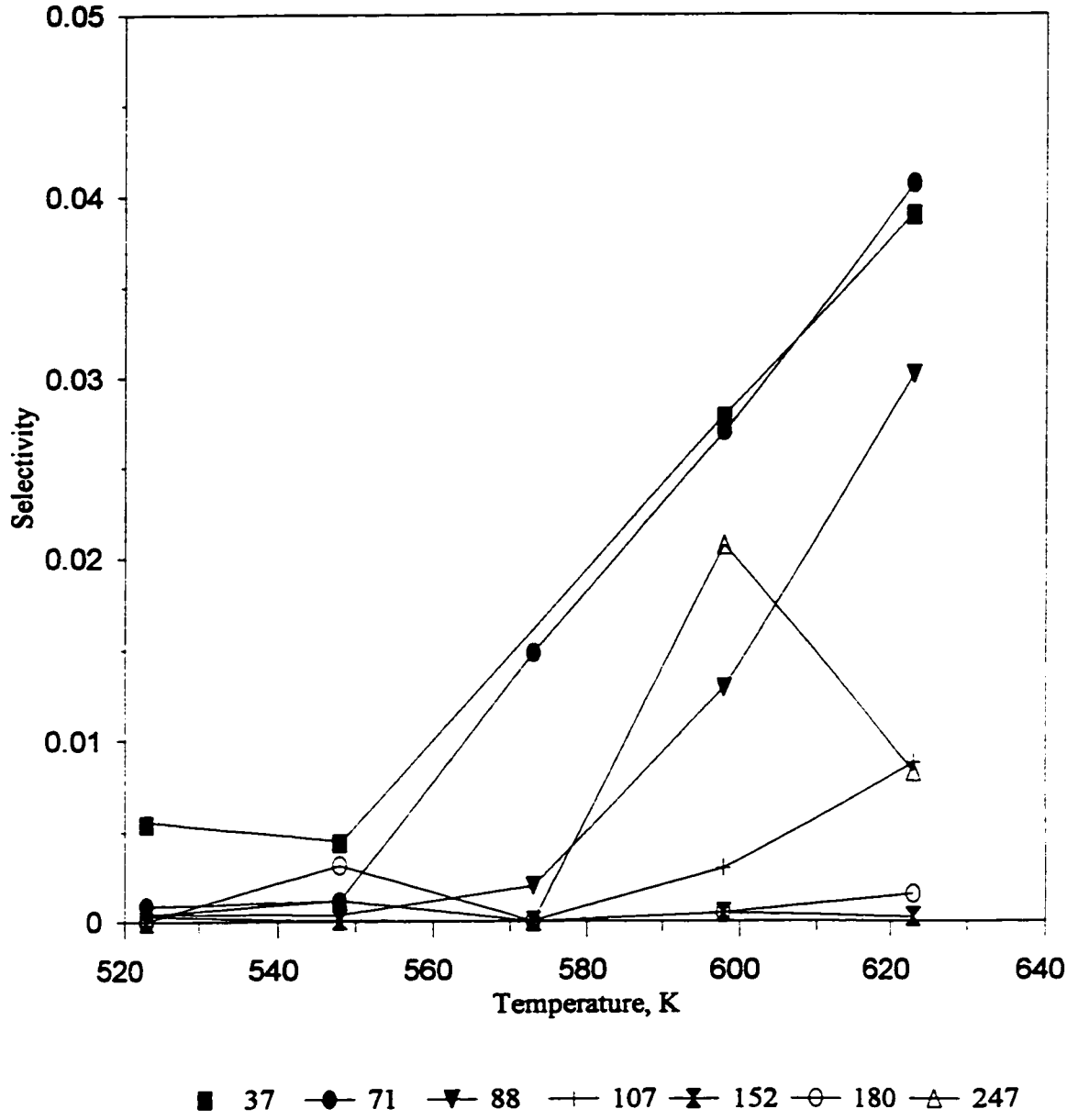

Figure 5.11 Effect of temperature on the selectivity for hydrocarbons at different space times, R=11 g-mol hydrogen/g-mol pyridine, P=3.447 MPa

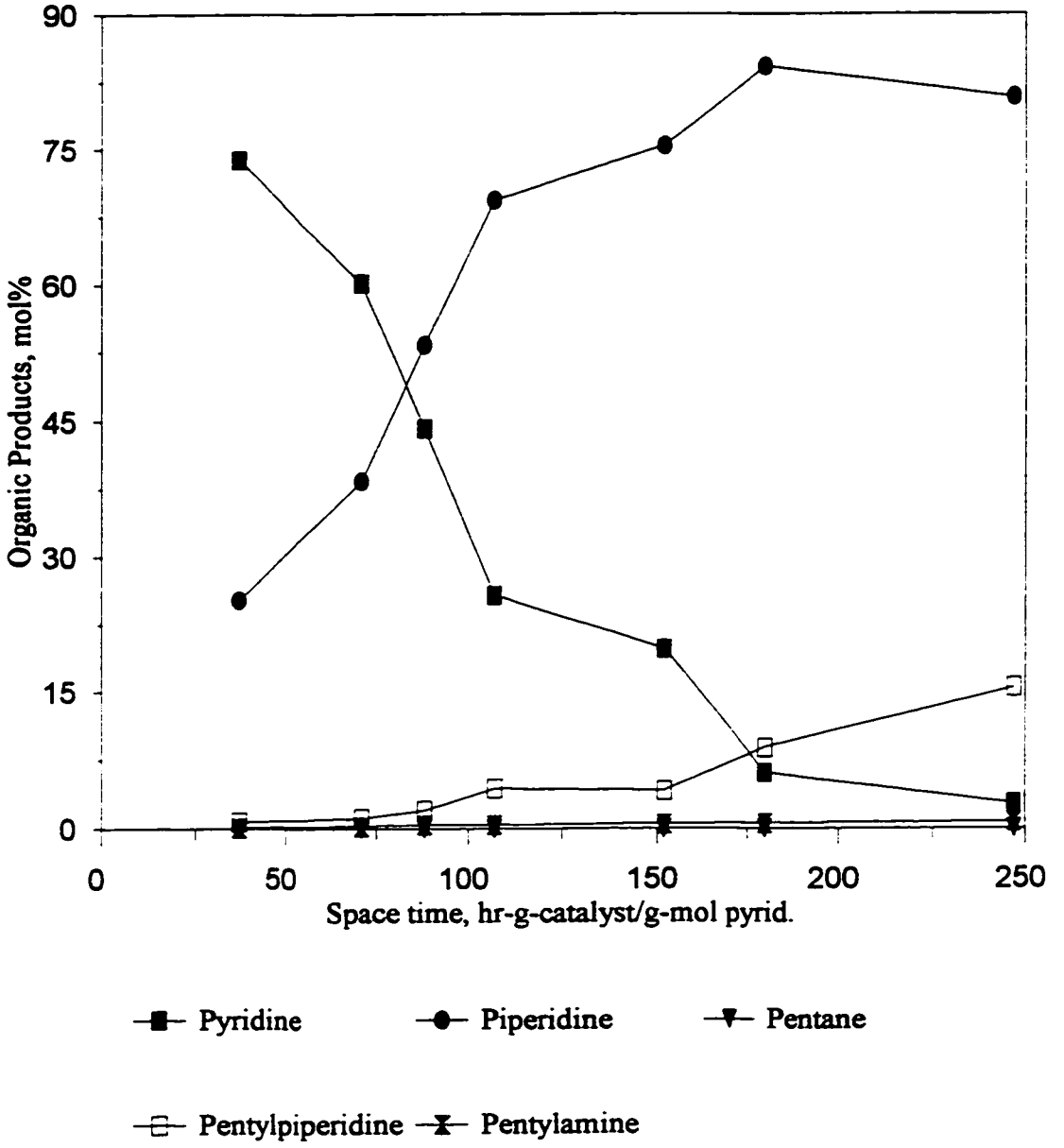

Figure 5.12 Effect of space time on the organic product distribution at T=523 K, R=11 g-mol hydrogen/g-mol pyridine, P=6.894 MPa

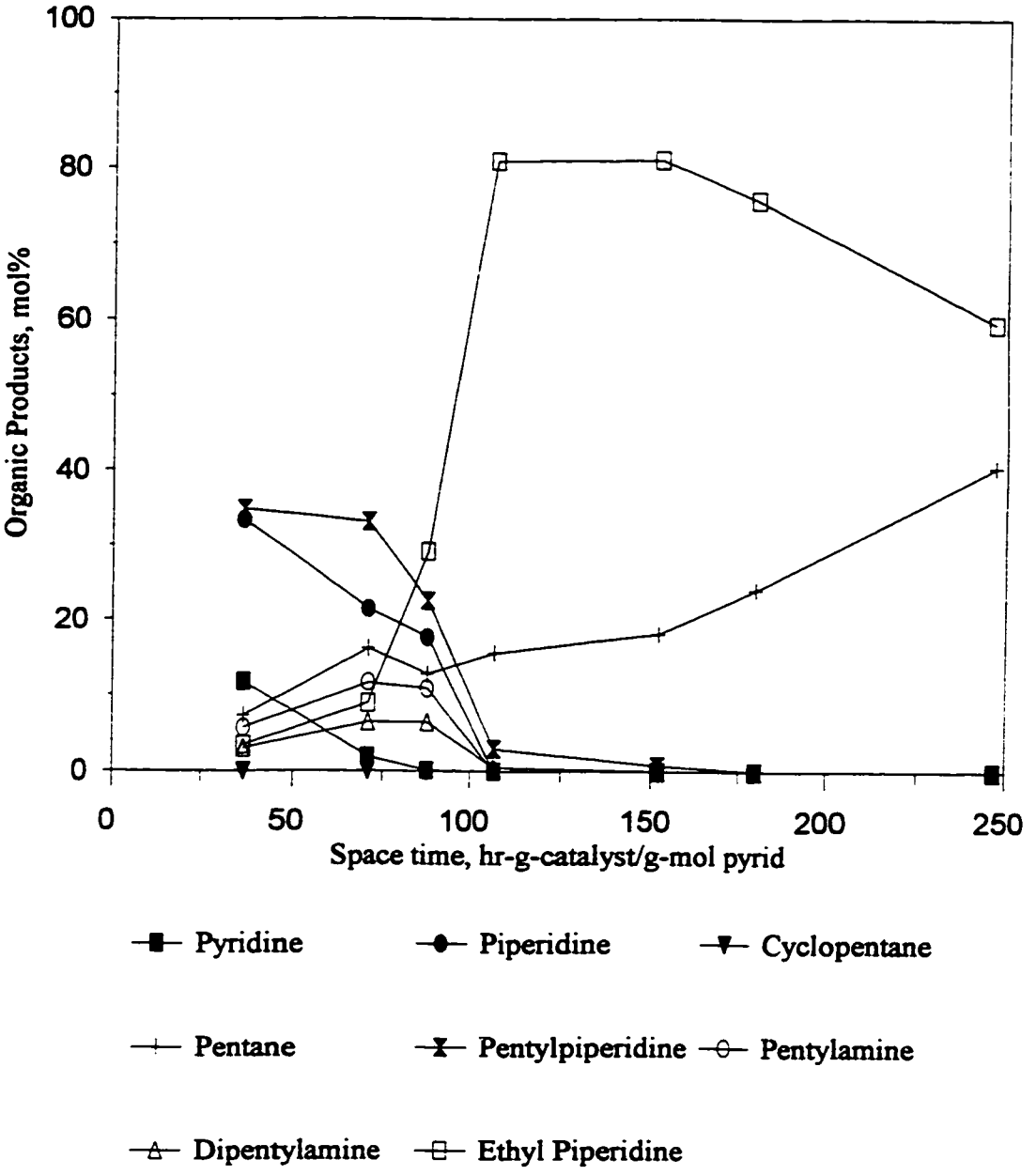

Figure 5.13 Effect of space time on the organic product distribution at T=623 K, R=11 g-mol hydrogen/g-mol pyridine, P=6.894 MPa

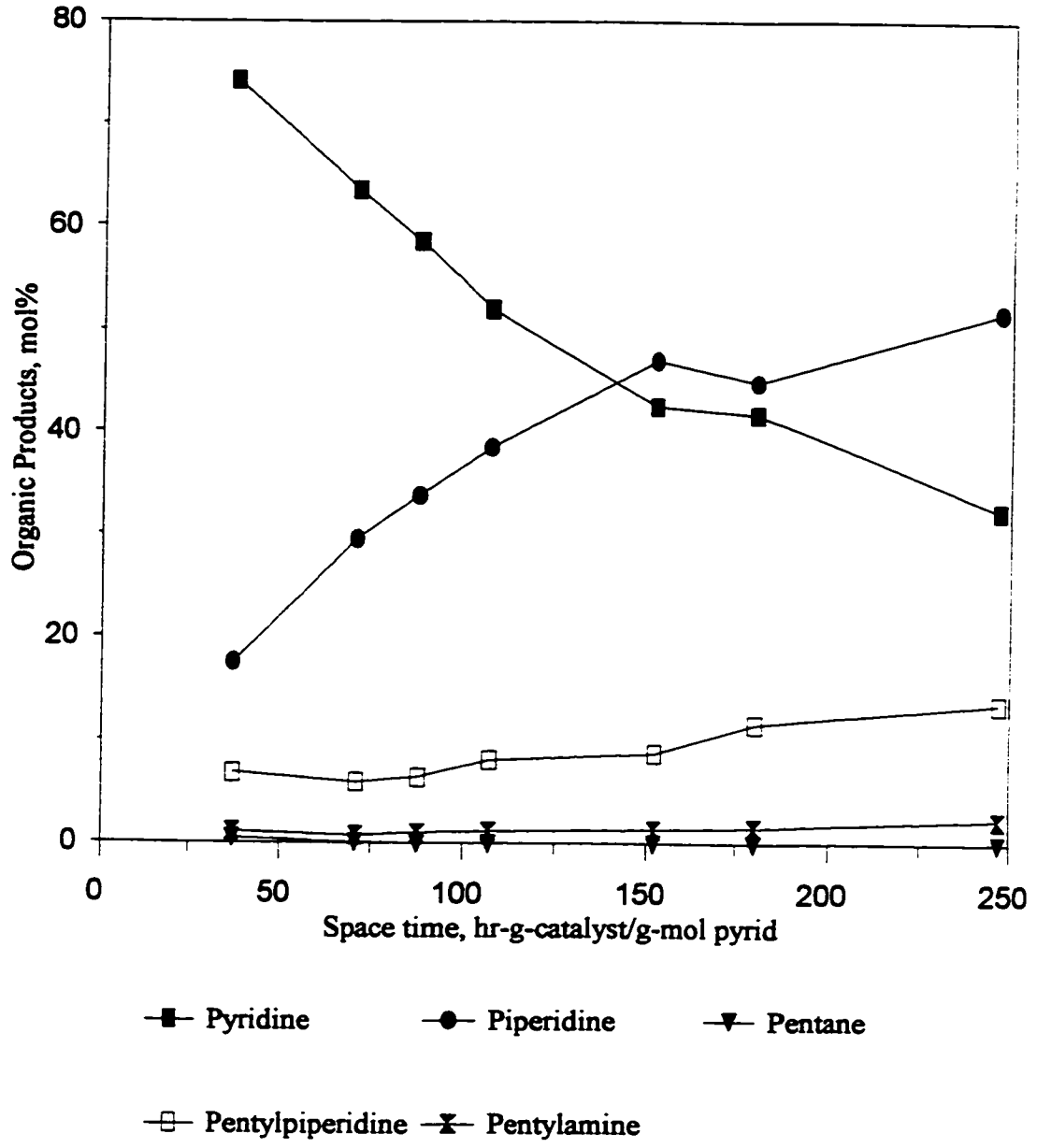

Figure 5.14 Effect of space time on the organic product distribution at T=523 K, R=11 g-mol hydrogen/g-mol pyridine, P=3.447 MPa

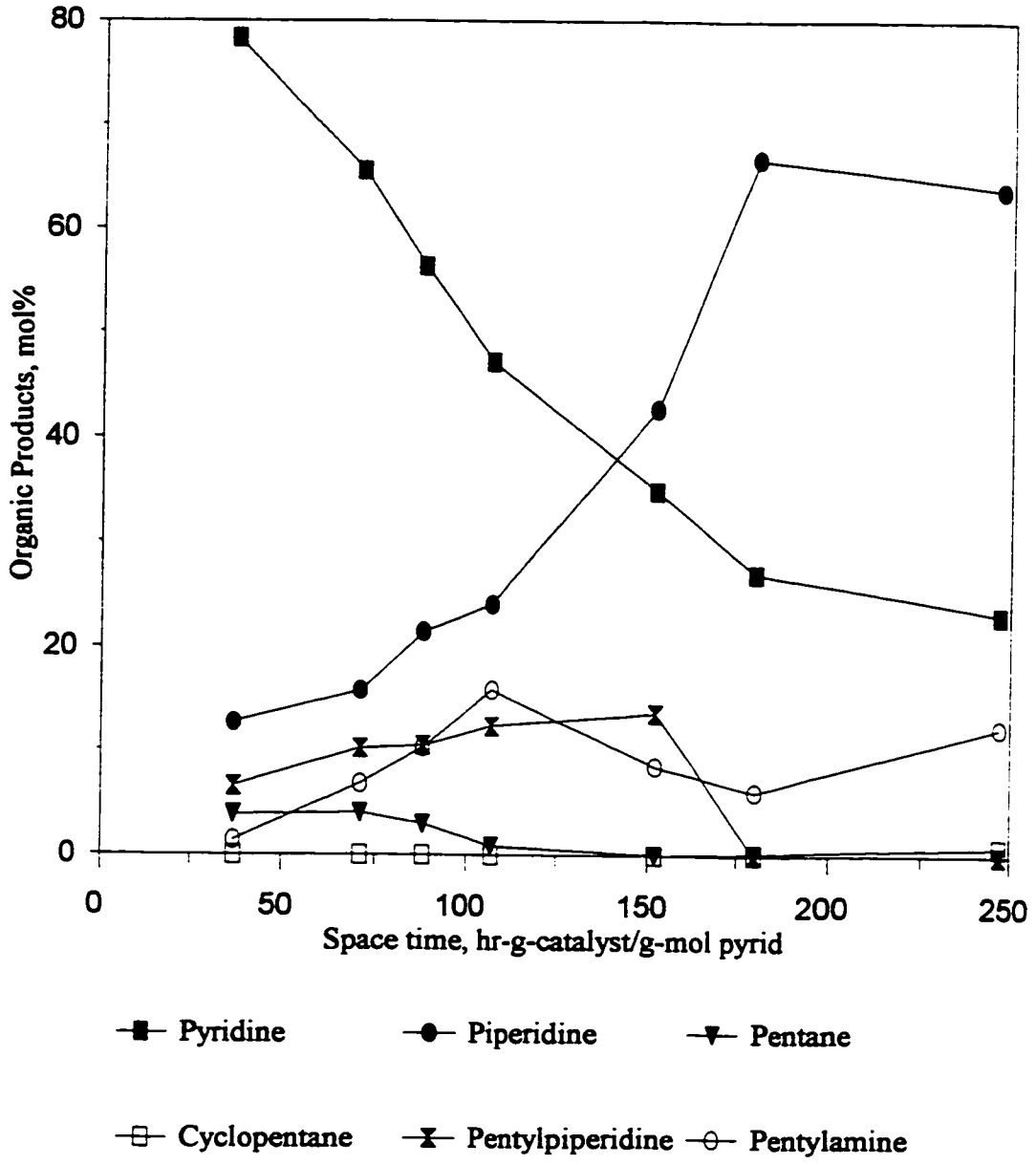

Figure 5.15 Effect of space time on the organic product distribution at T=623 K, R=11 g-mol hydrogen/g-mol pyridine, P=3.447 MPa

increased with an increase in space time and temperature. At 3.447 MPa, piperidine in the product increased constantly with space time at all temperatures. Pentyl piperidine and pentylamine formed increased with space time at lower temperatures but started to decrease with space time at higher temperatures.

Figures 5.16 and 5.17 show the effect of space time on conversion of pyridine at two different pressures. It could be seen from Fig. 5.16 that at 6.894 MPa., more than 97% conversion could be achieved at 597 and 623 K and W/F greater than 180 hr-g-catalyst/g-mol pyridine. At 3.447 MPa, about 75% conversion was achieved at 623 K and W/F of 247 hr-g-catalyst/g-mol pyridine.

5.1.3 Effect of Pressure

The effect of pressure on product distribution, yield, selectivity, denitrogenation and conversion was studied at 6.894 and 3.447 MPa. Figures 5.5, 5.10, 5.16 and 5.17 show the difference between the two pressures with respect to conversion and yield at different temperatures and space times. From the figures could be seen that when the pressure was doubled, the conversion, yield and selectivity had increased. At 6.894 MPa. and higher space times, almost complete conversion was achieved though at 3.447 MPa, the maximum conversion achieved was 77%. As the pressure was doubled, the conversion increased by 1.3-4 times. The yield and selectivity for hydrocarbons also increased considerably with pressure. The increase in selectivity seems to be more than the increase in yield and much

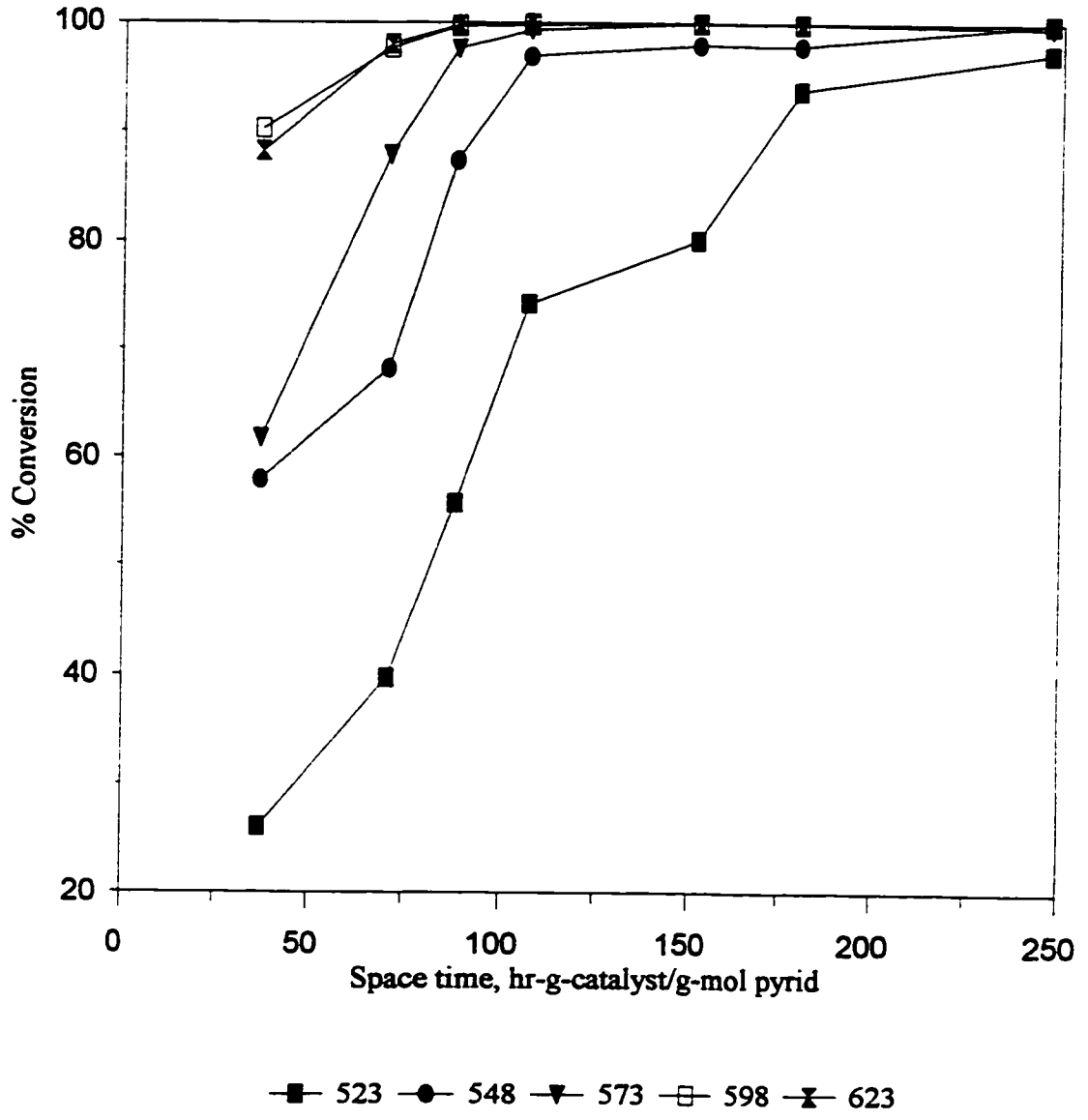

Figure 5.16 Effect of space time on the conversion of pyridine at various temperatures, R=11 g-mol hydrogen/g-mol pyridine and P=6.894 MPa

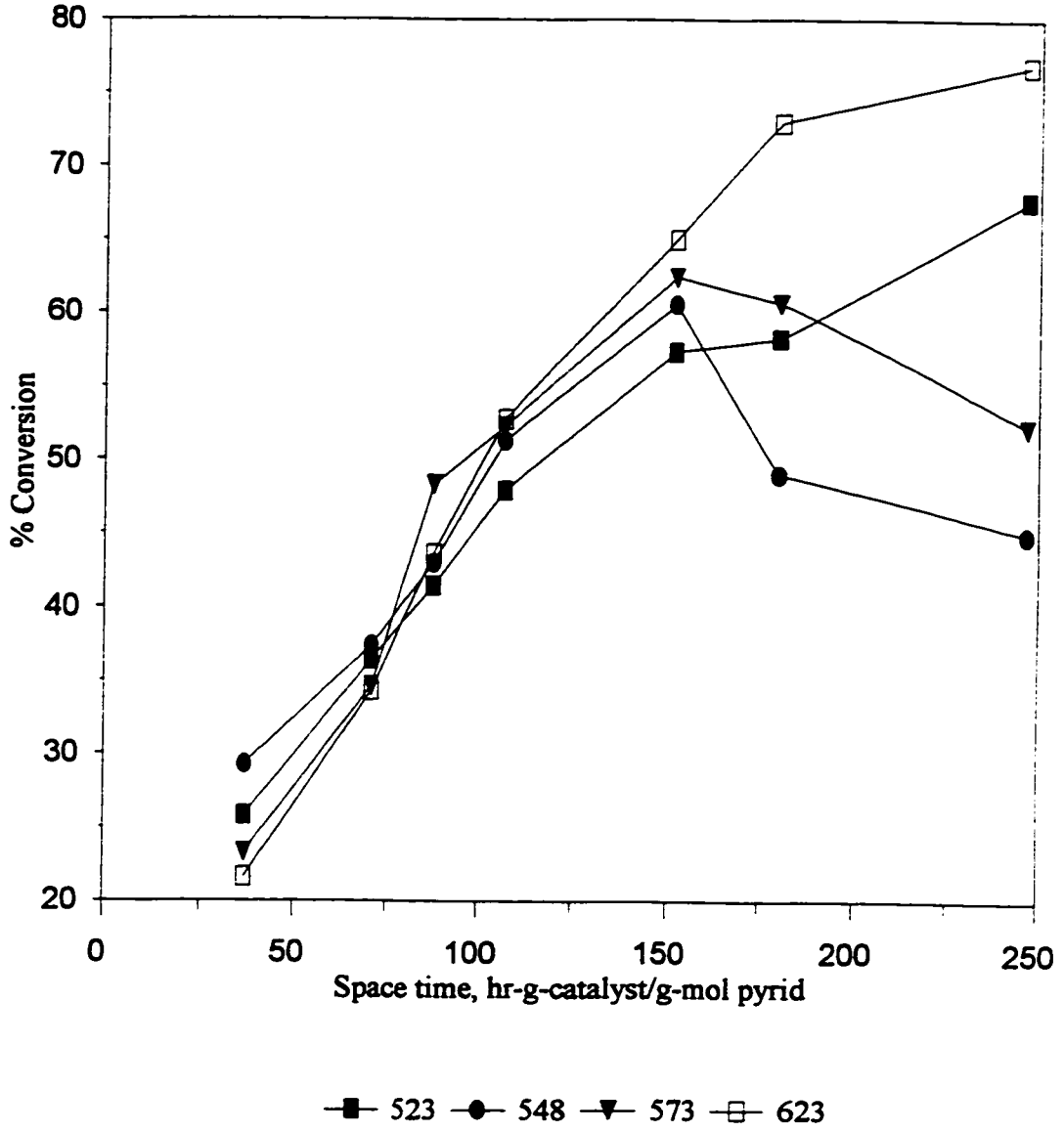

Figure 5.17 Effect of space time on the conversion of pyridine at various temperatures, R=11 g-mol hydrogen/g-mol pyridine and P=3.447 MPa

more than that in conversion. At a space time of 247 hr-g-catalyst/g-mol pyridine, the increase in conversion as the pressure was doubled was only 30% while the percentage increase in yield and selectivity was very high. At higher space times, the reactants will have more access to the catalytic sites than at lower space times. Hence the conversions do not differ much at the two pressures. But, in order for the reactions to proceed until the hydrocarbons are formed, a large amount of hydrogen is required. Hence at higher pressures, the reaction proceeds to completion and the yield and selectivity of hydrocarbons is more and they increased with space time. At lower pressures, as the space time was increased, the conversion increased but the yield and the selectivity did not change considerably indicating that hydrogen pressure was not sufficient enough for the formation of hydrocarbons. The amount of intermediates formed increased with space time.

5.1.4 Effect of Catalyst Support

The effect of catalyst support, alumina, was studied by carrying out the reaction in the presence of γ- alumina (20/35 mesh size) instead of the catalyst. No reaction took place even up to a temperature of about 623 K at both the pressures. This indicates that the support had no effect on the reaction.

5.2 REACTION NETWORK

Many reaction networks have been proposed for the hydrodenitrogenation of pyridine in the literature. There are various factors including catalysts, reaction conditions, method of

analysis, initial concentration of the reactants etc. that affect the results. In this study, based on the products obtained and also considering the reaction mechanisms proposed in the literature, a reaction network has been presented (Figure 5.18). The mechanistic modeling of the reaction has been done using this reaction network.

5.3 KINETIC MODELING

The experimental results can be interpreted and analyzed quantitatively only through

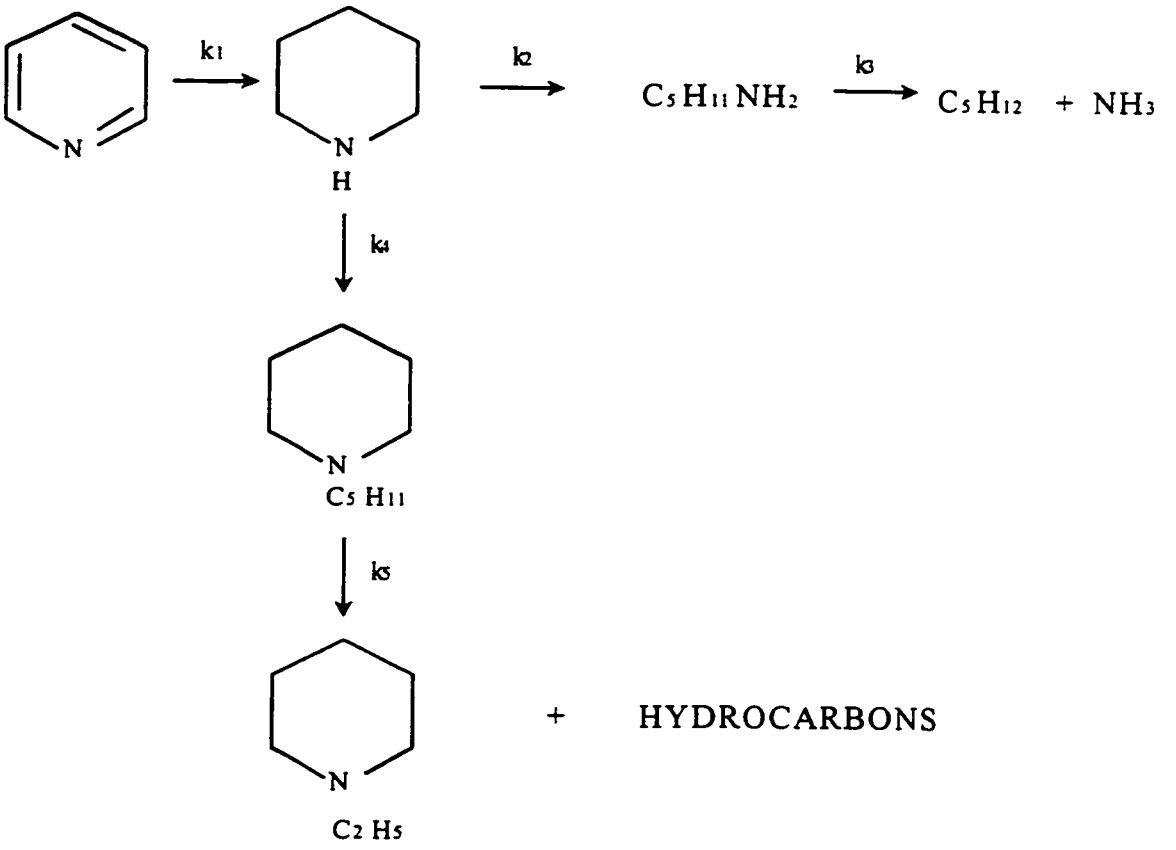

Figure 5.18 The reaction network for the pyridine hydrodenitrogenation using Pt/Al_2O_3 catalyst

mathematical modeling. In this study, two types of models are considered; a lumped model and a mechanistic model. Model 1 is a lumped model in which all the nitrogen compounds are grouped and treated as one reactant. Model 2 is a mechanistic model in which the reactions of each compound are considered separately. The two models resulted in different sets of differential equations. These equations were solved by non-linear least squares methods using Levenberg-Marquardt method and the parameters were estimated. The data fitted to both the models were taken from runs 1 to 35 (6.894 MPa.). The reason for this is explained in the discussions.

5.3.1 Model 1 (Lumped Compounds Model)

The overall HDN reaction is lumped together and given as,

$$NC + 2H_2 \rightarrow HC + NH_3$$

where NC is the reacting nitrogen compound and HC is the hydrocarbon produced. The above equation was studied using a first order kinetic model.

Assuming first order kinetics model, the rate can be expressed as,

$$-r_{NC} = -\frac{dC_{NC}}{dt} = k_1 C_{NC} P_H^{\,n} \qquad (5.1)$$

where

C_{NC} - concentration of nitrogen compound

k_1 - rate constant

P_H - partial pressure of hydrogen

n - order of the reaction with respect to hydrogen

The partial pressure of hydrogen was kept constant during the experiments. Hence the equation (5.1) can be written as,

$$-\frac{dC_{NC}}{dt} = k\ C_{NC} \tag{5.2}$$

where k is the pseudo-first order rate constant. Integrating the above equation will give,

$$\ln(\frac{C_{NC}}{C_{NC_o}}) = -k\ t \tag{5.3}$$

where C_{NC0} is the initial concentration of the nitrogen compound. The plot of ln (C_{NC}/C_{NC0}) versus t results in a straight line with the slope of k.

The Langmuir-Hinshelwood type rate expression for the same reaction is given by,

$$-r_{NC} = \frac{k_1\ K_{NC}\ P_{NC}}{1 + K_{NC}\ P_{NC} + K_{NH_3}\ P_{NH_3}} \tag{5.4}$$

The catalyst surface will be completely covered by the nitrogen compounds at 1 kPa partial pressure and even at high temperatures (Sonnemans et al., 1973). Hence $K_{NC}P_{NC}+K_{NH3}\ P_{NH3}$ >> 1. Since a large excess of hydrogen exists during the reaction, $P_{NH3} = P_{NC0} - P_{NC}$, where

P_{NC_0} is the initial partial pressure of the nitrogen compound. Equation (5.4) can be written as,

$$-r_{NC} = \frac{k_1 P_{NC}}{P_{NC} + (\frac{K_{NH_3}}{K_{NC}})(P_{NC_0} - P_{NC})} \tag{5.5}$$

Substituting the rate expression in the plug-flow reactor equation gives,

$$\frac{W}{F_{NC_0}} = \frac{1}{P_{NC_0}} \int_{P_{NC_0}}^{P_{NC}} \frac{P_{NC} + (K_{NH_3}/K_{NC})(P_{NC_0} - P_{NC})}{k_1 P_{NC}} dP_{NC} \tag{5.6}$$

Integrating the above equation results in,

$$k_1 \frac{W}{F_{NC_0}} = (1 - \frac{K_{NH_3}}{K_{NC}})(\frac{P_{NC_0} - P_{NC}}{P_{NC_0}}) - (\frac{K_{NH_3}}{K_{NC}}) \ln(\frac{P_{NC}}{P_{NC_0}}) \tag{5.7}$$

Substituting X_{NC} for the fractional conversion of the nitrogen compound,

$$k_1 \frac{W}{F_{NC_0}} = (1 - \frac{K_{NH_3}}{K_{NC}}) X_{NC} - (\frac{K_{NH_3}}{K_{NC}}) \ln(1 - X_{NC}) \tag{5.8}$$

The above equation was solved using the Levenberg-Marquardt method.

5.3.2 Model 2 (Mechanistic Model)

This model is based on the reaction network given in Figure 5.22. Each detailed mechanism

of reaction with its controlling factor has its corresponding rate equation that involves many arbitrary constants, the K values. In terms of the space time, most catalytic conversion data can be fitted adequately by relatively simple first- or nth-order rate expressions (Levenspiel). In this study, a simple expression that satisfactorily fitted the data was used instead of complicated rate expressions suggested by theoretical mechanisms. The individual reactions were studied using a pseudo-first order reaction model. The rate expression for each reaction are as follows,

$$- r_{PYR} = - \frac{dC_1}{dt} = k_1 C_1 \tag{5.9}$$

$$- r_{PIP} = - \frac{dC_2}{dt} = - k_1 C_1 + (k_2 + k_4) C_2 \tag{5.10}$$

$$- r_{PEAM} = - \frac{dC_3}{dt} = - k_2 C_2 + k_3 C_3 \tag{5.11}$$

$$- r_{PEPIP} = - \frac{dC_4}{dt} = - k_4 C_2 + k_5 C_4 \tag{5.12}$$

The above equations were integrated numerically and were solved using the non-linear regression method (Marquardt's) and the parameters were estimated.

5.3.3 Discussion of the Results

The kinetics of the HDN of pyridine was studied using Pt/Al_2O_3 catalyst (0.5 wt% Pt). The effects of process variables, the reaction mechanism and the effect of catalyst used were studied. The significant aspects of the results are:

1. The good selectivity of the platinum catalyst for HDN.
2. The effect of process variables.
3. The reaction mechanism proposed based on the experimental data and observations.

Vit and Zdražil (1989) reported that the sulphides of the third-row platinum metals (Ir and Pt) exhibited quite exceptional HDN selectivity. They used carbon supported platinum catalyst (16.2 wt% Pt) for their studies and reported that the active carbon as the support contributed to the exceptional HDN properties of the sulphides of platinum. In this study, the platinum catalyst exhibited very good HDN selectivities even with 0.5 wt% platinum on alumina. The selectivities obtained in this study are much better than the ones reported for the $Ni\text{-}Mo/Al_2O_3$ catalyst (Ajaka, 1992). Complete conversion of pyridine was achieved at temperatures above 573 K at 6.893 MPa total pressure and space times above 107 hr-g-catalyst/g-mol pyridine.

Many reaction mechanisms have been proposed in the literature. McIlvried (1971) suggested the following mechanism for the HDN of pyridine.

Pyridine → Piperidine → n-Pentylamine → n-pentane + ammonia

Presence of any alkyl piperidine intermediates has not been reported because the products were analyzed for only pyridine and total nitrogen. His results showed that only ammonia was strongly adsorbed on the hydrogenation sites and all the nitrogen compounds were equally strongly adsorbed on the denitrification sites or present in too small a concentration to affect the kinetics suggesting a Langmuir-Hinshelwood kinetics. Hence an apparent first order kinetics could be obtained for the complex system. In the present study, the above mechanism could not used because of the presence of alkyl piperidine intermediates.

Aboul-Ghiet et al. (1974) who studied the HDN of pyridine in paraffin oil presented another mechanism as follows:

Pyridine → Piperidine → n-amylamine → pentane + ammonia

Though it has been reported that methyl and ethyl piperidine were formed at lower temperatures, the reaction mechanism did not take into consideration these compounds.

In another study, Hanlon (1987) has proposed a reaction mechanism which involved alkyl transfer of piperidine and n-pentylamine. The reaction scheme proposed was:

Pyridine → Piperidine → n-pentylamine → pentane + ammonia

↑ ↓ + n-pentylamine

n-pentyl piperidine + ammonia

A Langmuir-Hinshelwood kinetic expression has been used in analyzing the data since it was observed that the reactions describing the HDN were complex functions of the initial

reactant partial pressure and also of the strong competitive adsorption characteristics of the nitrogen-containing compounds.

The reaction mechanism proposed in this study was the best to fit the experimental data at higher total pressure. The reaction alkyl piperidine intermediates have been reported in the literature. A part of the reaction network developed by McIlvried (1971) was found to fit the experimental data. At the lower pressure, the mechanism proposed did not provide the best fit because of the absence of ethyl piperidine in the product. Also the product distribution at the lower pressure seemed to vary a little from that at the higher pressure. This indicates that the mechanism could be different at the lower pressure. Satterfield et al. (1980) reported that pyridine conversion was strongly influenced by the total pressure. They also reported the occurrence of a maximum in pyridine conversion at 1.14 MPa. This was attributed to a thermodynamic limitation on the formation of piperidine and also a change in the rate-limiting step. Similar trends (occurrence of a maximum in pyridine conversion) were observed in this study at the lower pressure. In this study, the reaction mechanism discusses the results at the higher pressure alone.

Several models were examined and tested to fit the data obtained in this study. The results obtained from the lumped compounds model and the mechanistic model based on the reaction network proposed are discussed below.

Model 1

This model considers a pseudo-first order reaction for the total nitrogen removal. The experimental data were fitted to equations (5.3) and (5.8) and the best estimate of the rate constant was evaluated by Marquardt's method. The Langmuir-Hinshelwood expression (equation 5.8) fitted the data fairly well. The regression results are given in Appendix C. The values of the rate constant k_1 and the ratio K_{NH}/K_{NC} predicted by this model are given in Table 5.2.

Table 5.2 Values predicted by Model 1

Temperature, K	k_1	K_{NH}/K_{NC}
523	0.00754	0.3046
548	0.0141	0.3751
573	0.0167	0.3143
598	0.0999	2.2625

The Arrhenius plot of ln k_1 versus 1/T was a straight line and the activation energy was found to be 19.89 kcal/g-mol. Sonnemans et al. (1973) reported the rate constants as a function of temperature. The activation energy for the pyridine hydrogenation calculated from their data was 22.45 kcal/g-mol. Ajaka (1991) reported a value of 19.84 kcal/g-mol and Anabtawi (1978) reported a value of 13.69 kcal/g-mol. The value obtained in this study was different from the ones reported. This could be because of the difference in the catalyst used, reaction conditions employed etc. Somewhat different kinetics could result from

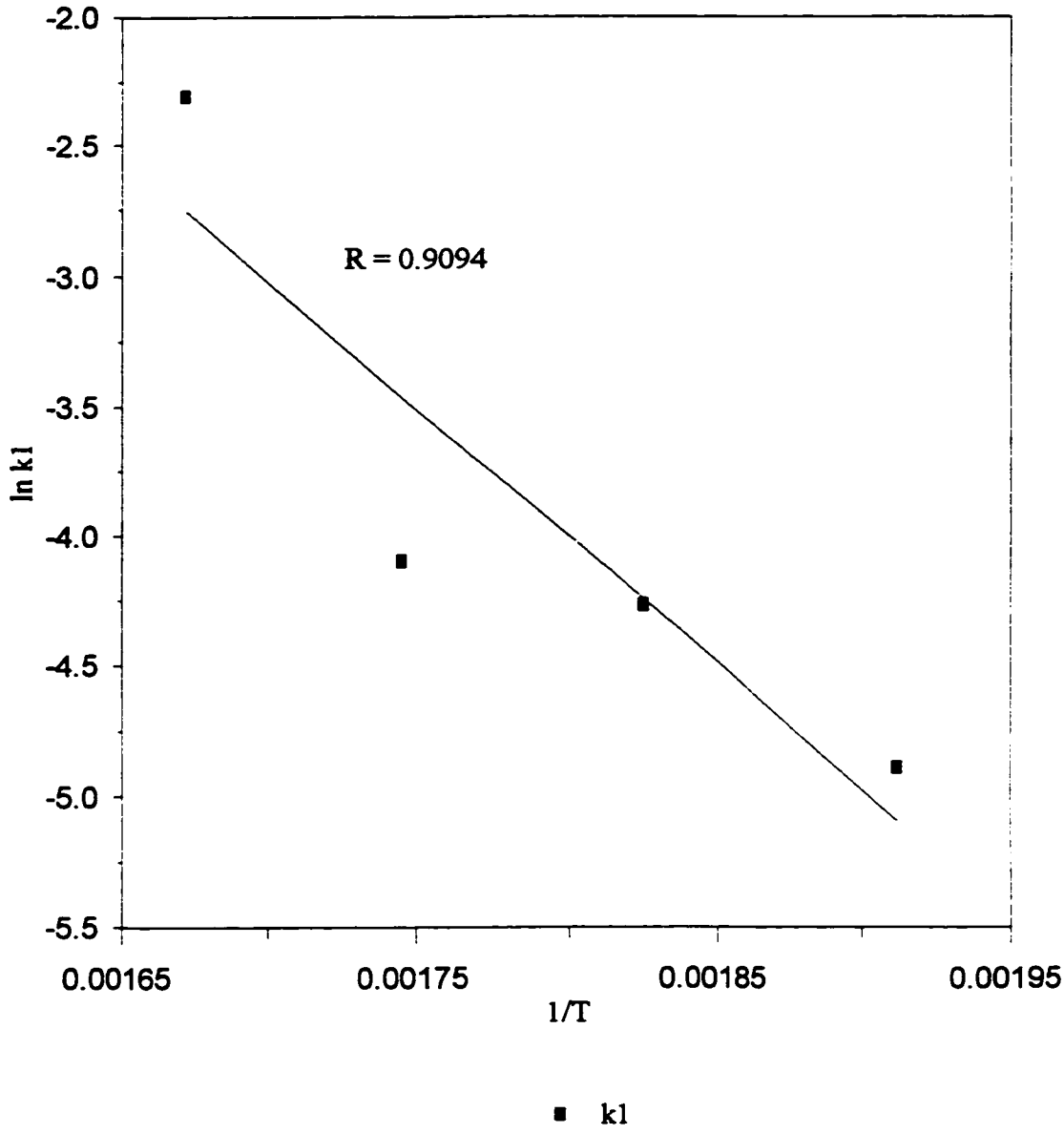

Figure 5.19 Arrhenius plot for the pseudo-first order rate constant for Model 1

different catalysts.

The Arrhenius plot for the pseudo rate constant is given in Figure 5.19. The regression results are given in Appendix C.

Model 2

The rate constants for the different steps (equations 5.9 to 5.12) were estimated for different temperatures. The regression results and the estimated product distribution by the model are given in Figures 5.20 to 5.24. The Arrhenius plots of the pseudo rate constants for the HDN of pyridine are given in Figure 5.25. The average activation energy for the hydrogenation of pyridine to piperidine is 10.46 kcal/g-mol while that for the hydrogenolysis of piperidine to alkyl-piperidines is 19.35 kcal/mol. The average activation energy for the conversion of piperidine to pentylamine is 25.427 kcal/g-mol. The activation energy for the formation of the major intermediate, n-penyl piperidine from piperidine is 19.35 kcal/g-mol. The results indicate that the rate of pyridine hydrodenitrogenation is determined by the rate of ring rupture of piperidine to pentylamine.

5.4 RESULTS OF ESR STUDIES ON THE CATALYST

The interaction between the active component and the support is of great importance to study the catalytic behaviour of a heterogeneous catalyst. Electron spin resonance (ESR) was used to study the effect of support on the platinum species and also the effect of

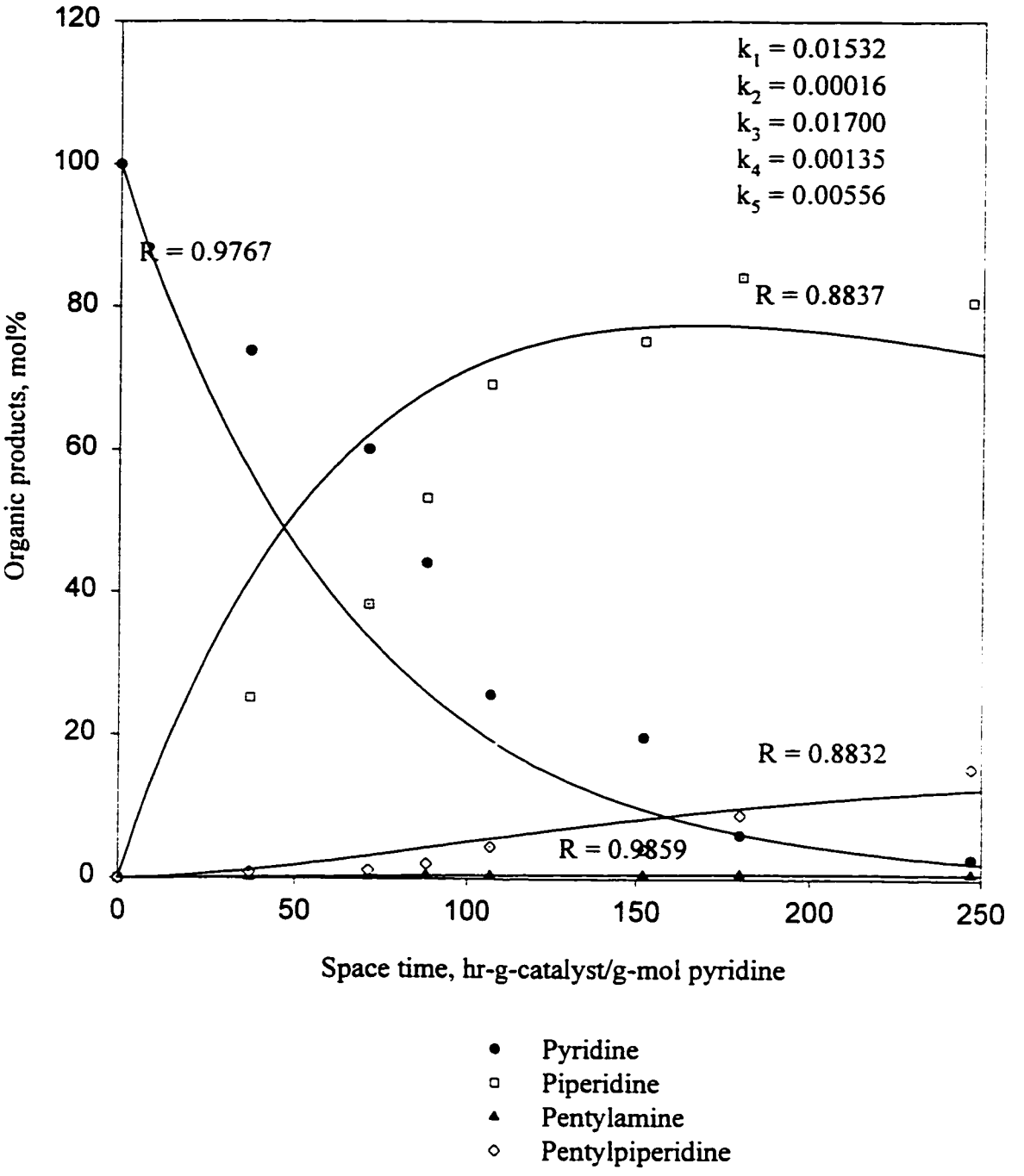

Figure 5.20 Prediction of rate constants for Model 2 at 523 K

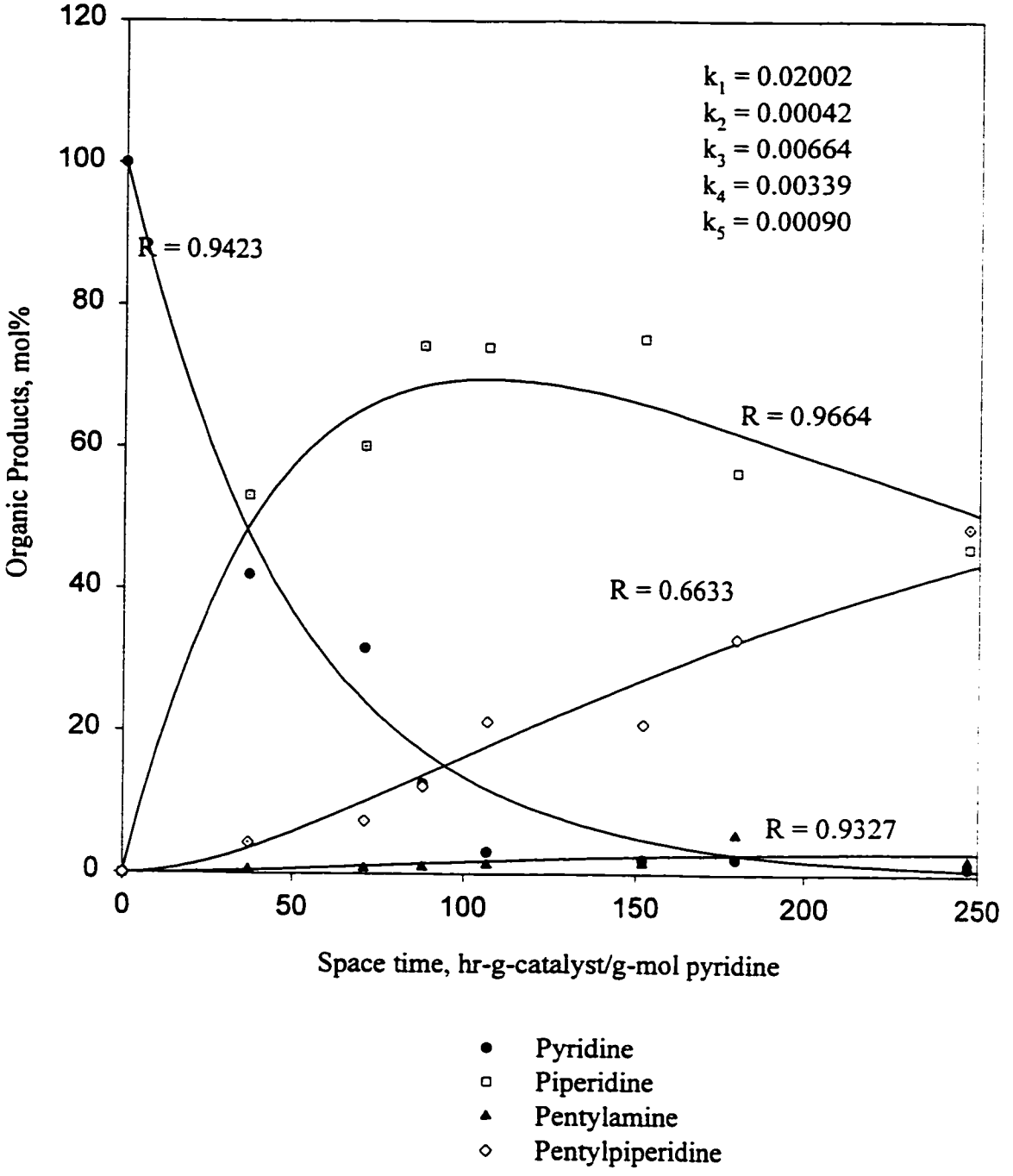

Figure 5.21 Prediction of rate constants for Model 2 at 548 K

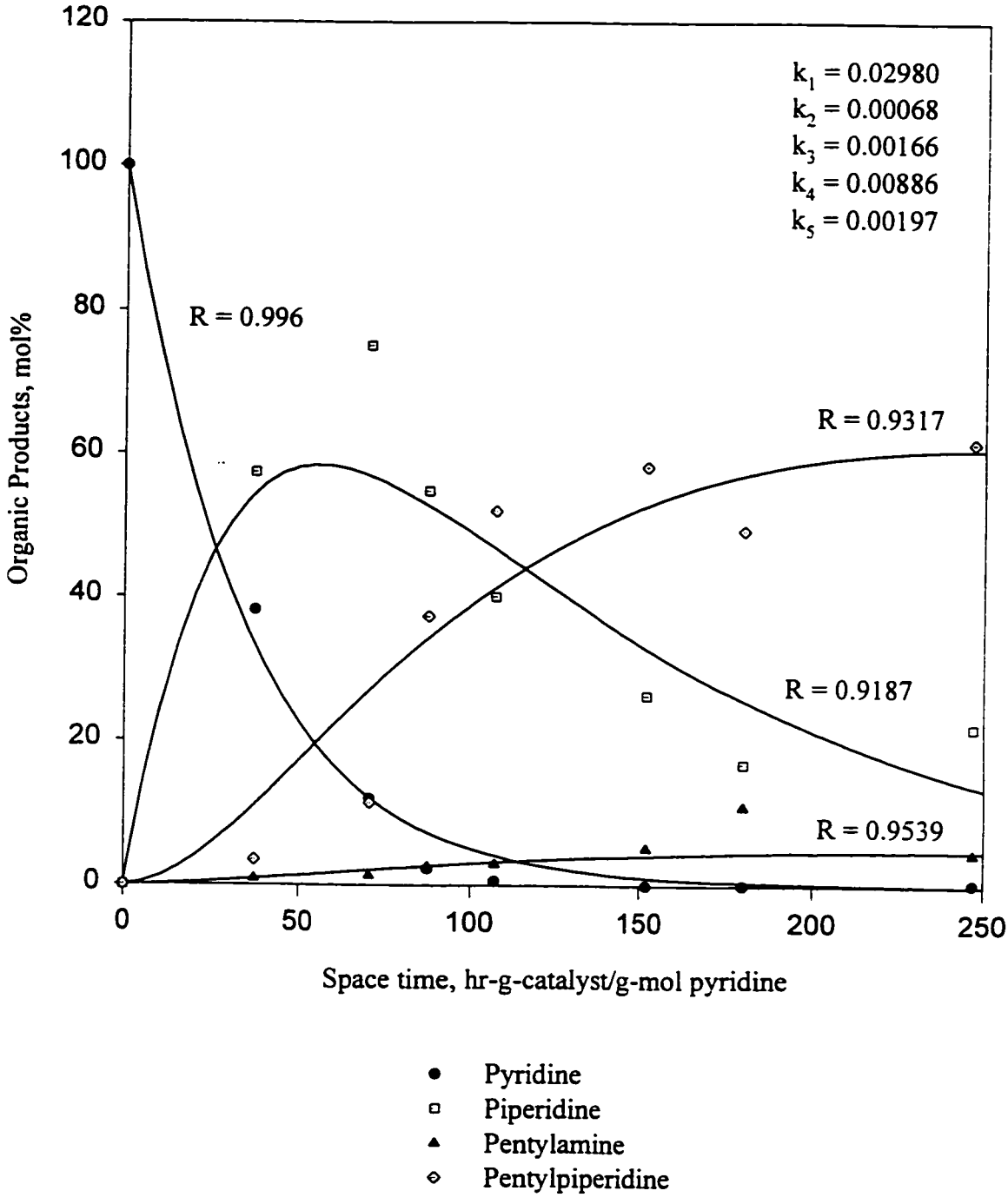

Figure 5.22 Prediction of rate constants for Model 2 at 573 K

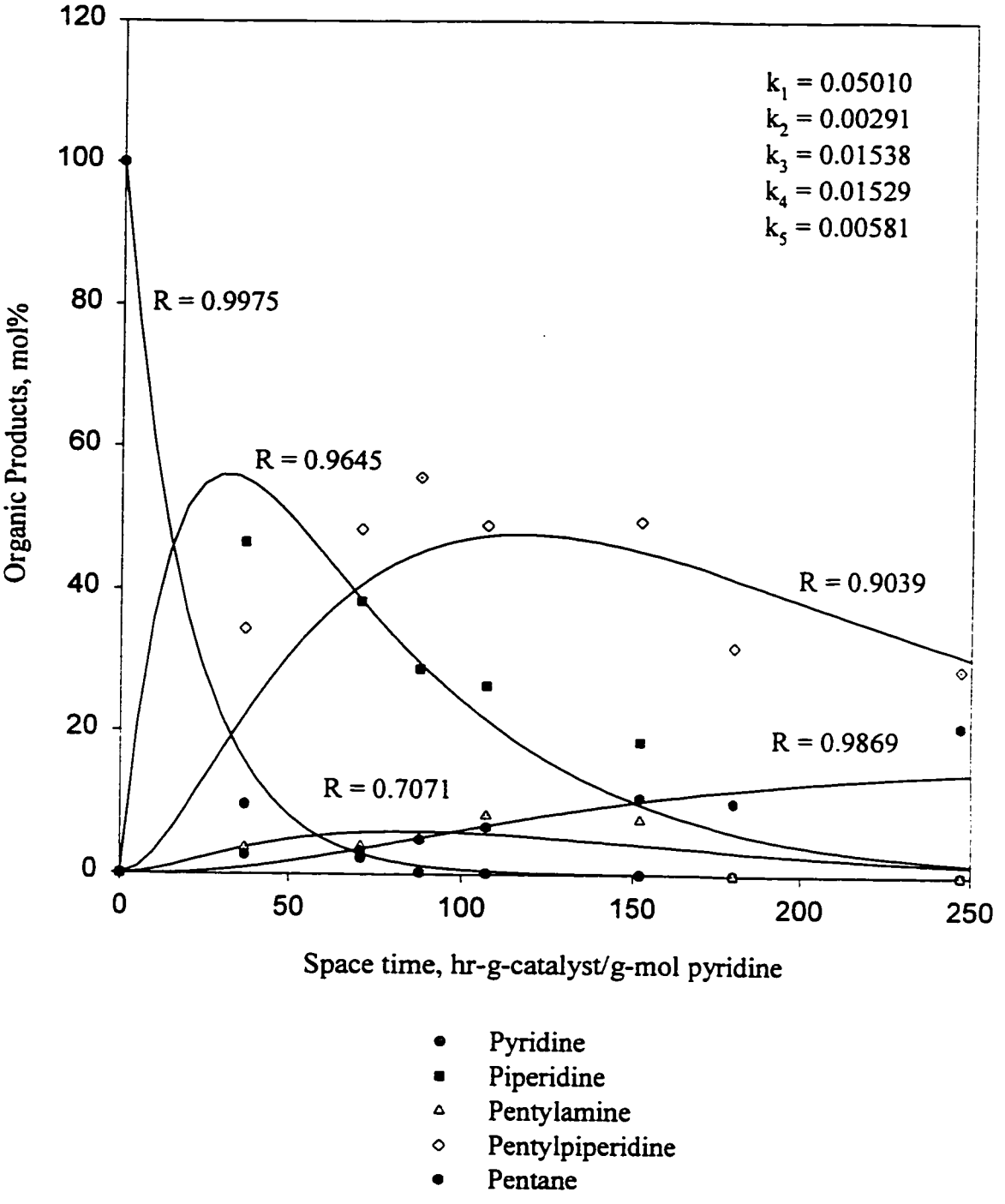

Figure 5.23 Prediction of rate constants for Model 2 at 598 K

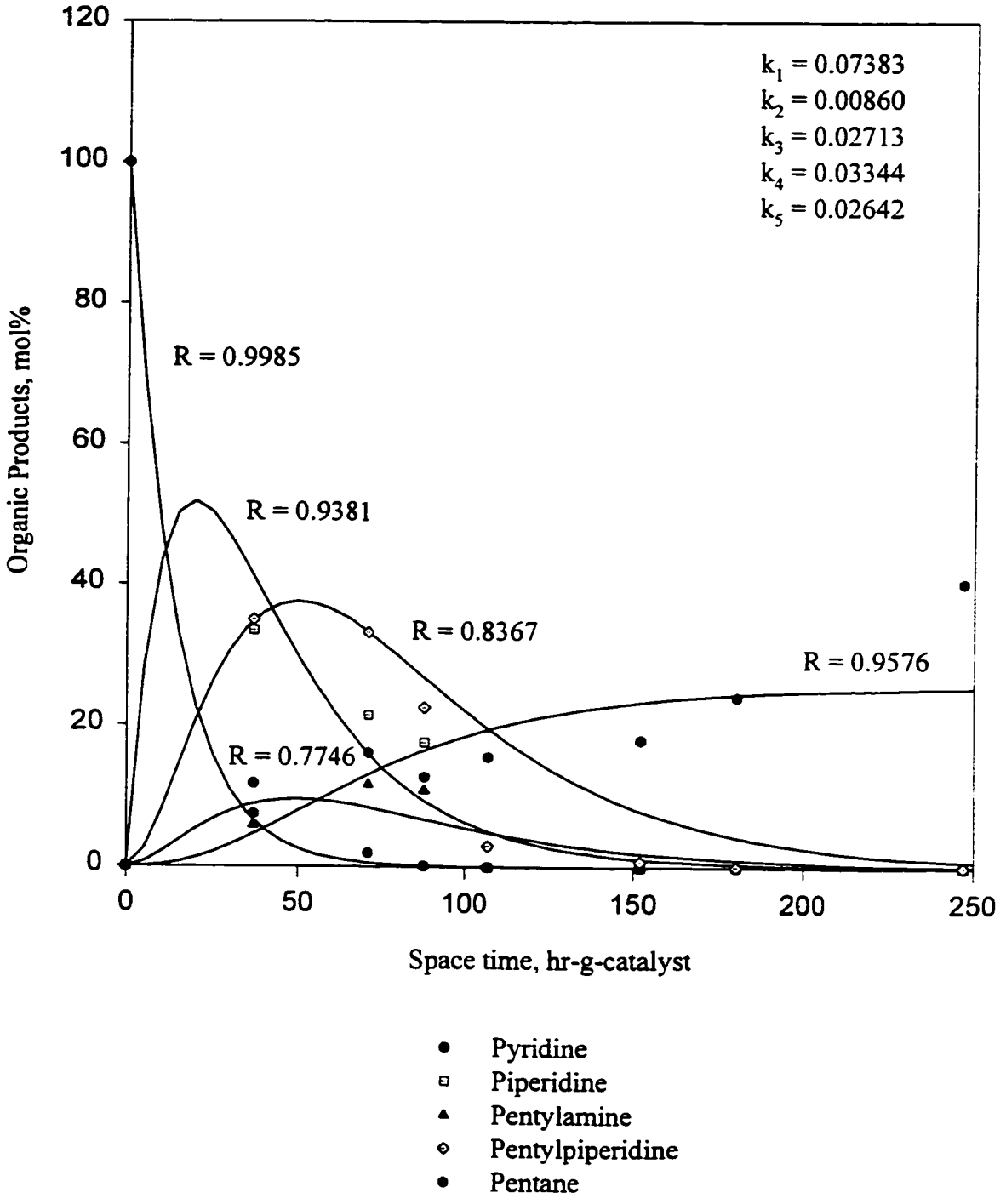

Figure 5.24 Prediction of rate constants for Model 2 at 623 K

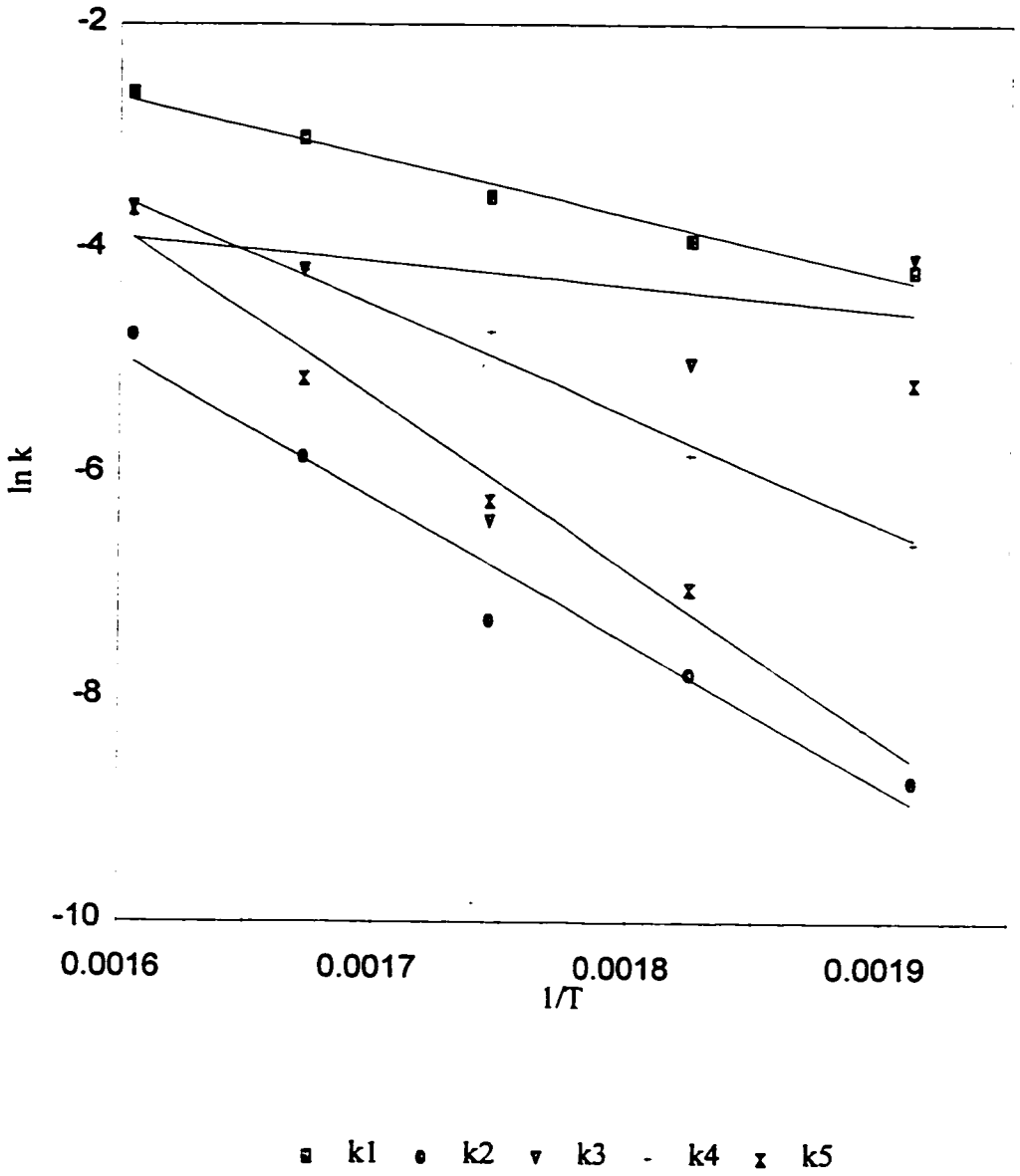

Figure 5.25 Arrhenius plot for the pseudo-first order rate constant for Model 2

reducing the catalyst in the presence of hydrogen.

Hulzinga and Prins (1983) studied the ESR of platinum supported on alumina. By measuring the effect of oxidation and reduction and by analyzing the g values and temperature dependencies, they assigned the two observed ESR signals to Pt^{+} and Pt^{3+} ions. The Pt^{+} was observed after reduction. The other forms of platinum namely, Pt^{4+} and Pt^{2+} are not paramagnetic. Katzer et al. (1979) studied the paramagnetic platinum and oxygen species present in the supported platinum catalyst and reported that the paramagnetic platinum centres, believed to be due to Pt^{3+} were formed when $Pt(NH_3)_4^{2+}/Al_2O_3$ was calcined in O_2. Absorption of O_2 on the Pt/Al_2O_3 catalyst resulted in the formation of two other signals due to O_2^- and results in a corresponding reduction in the platinum signal.

Soria et al. (1996) studied the ESR of the absorption of O_2 and CO_2 on evacuated and heat treated (573 - 673 K) $Pt/CeO_2/Al_2O_3$ catalyst and reported the centres responsible for Pt^{3+} signals. These centres disappeared on adsorption of O_2. In other words, these centres were easily oxidizable which suggested that these centres were located on the surface.

Isotopic ^{195}Pt has a nuclear spin of I = ½, and is 34% abundant. It will give two ESR signals. The other isotope which is 66% abundant and which has a nuclear spin of I = 0 will give a single ESR line. Evacuation at high temperature (623 K) probably causes a partial reduction of the surface by removing O_2 anions according to,

$$O^{2-} - Pt^{4+} - O^{2-} \rightarrow \square Pt^{2+} - O^{2-} + \tfrac{1}{2}O_2$$

In the present study, the ESR signals of both used and unused catalyst samples were studied. The evacuated and heated fresh (unused) sample gives three ESR signals (Figure 5.26). The main signal at g = 2.00 is due to the Pt^{3+}. The other two smaller peaks at g = 2.03 and at g = 1.9581 could be due to Pt^{+}. On heating with hydrogen, the intensity of Pt^{3+} decreased sharply but not to zero level. It could be possible that the signal after reduction could be due to the unaffected Pt^{3+} ions. The other two peaks were not affected as much except for a slight decrease in the intensity.

Figure 5.27 shows the ESR spectra of the used catalyst before and after reduction. The intensity of the Pt^{3+} is higher than that of the unused one. The effect of reducing the catalyst in the presence of hydrogen had the same effect as that of the unused catalyst, i.e., the middle peak decreased sharply while the other two peaks were not affected much. It is possible that Pt^{3+} ions play a role in the catalytic activity of the HDN of pyridine.

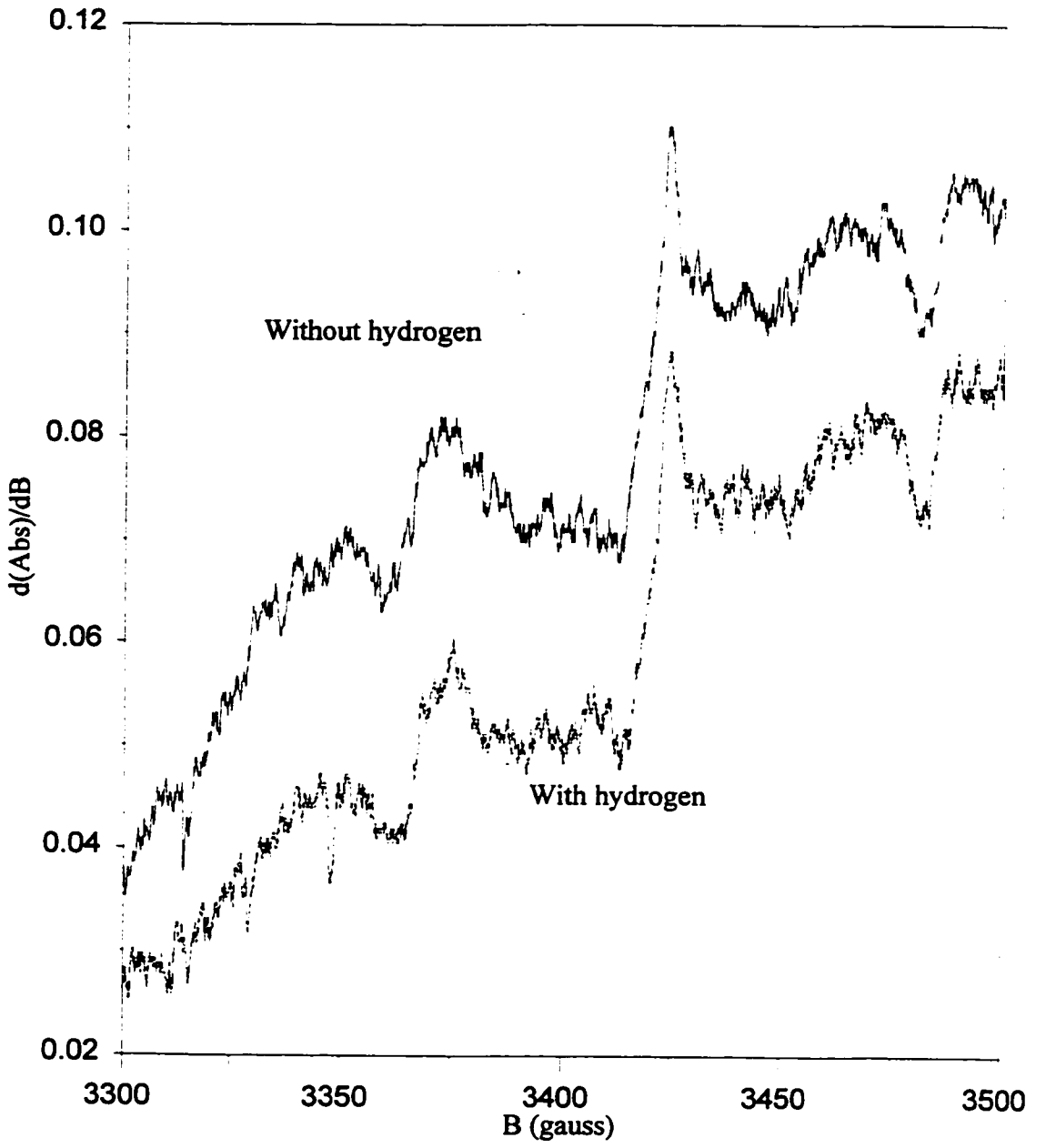

Figure 5.26 ESR spectra of unused catalyst

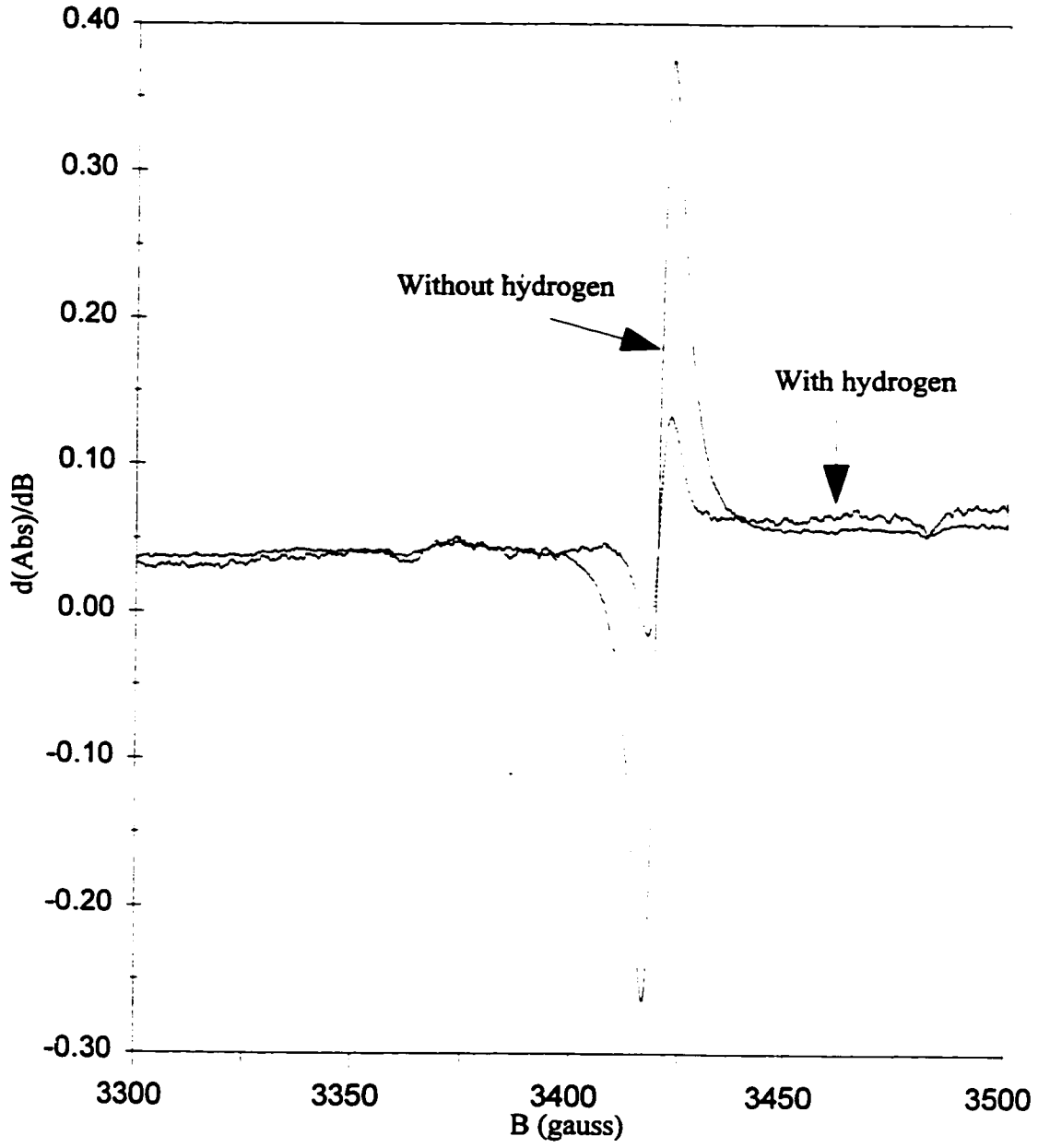

Figure 5.27 ESR spectra of used catalyst

CHAPTER 6

CONCLUSIONS AND RECOMMENDATIONS

Based on the results obtained in the earlier chapter, the following conclusions have been drawn.

- The hydrodenitrogenation of pyridine proceeds via the formation of piperidine, pentylamine, dipentylamine and pentyl piperidine to give pentane and ammonia as final products. Ethyl piperidine was another product detected. Cyclopentane was present in trace amounts. At the lower pressure, both dipentylamine and ethyl piperidine were not detected.
- The conversion of pyridine and the yield and selectivity for hydrocarbons increased considerably when the total reactor pressure was increased. It seems that at the lower pressure, the reaction did not proceed to completion
- A pseudo-first order Langmuir-Hinshelwood type model fitted the data best for the lumped compounds model.
- The reaction network developed in this study along with simple rate equation assuming surface reaction as the rate controlling mechanism best fitted the data and the activation energies thus calculated from the rate constants are comparable to the ones found in the literature.
- Based on Model 2, the pseudo-rate constants and activation energies estimated

suggest that the rate of pyridine hydrodenitrogenation is determined by the rate of hydrogenation of piperidine to n-pentylamine. The hydrogenation of pyridine to piperidine is a fast reaction followed by the slow ring rupture of piperidine to n-pentylamine.

Based on the conclusions, the following recommendations are suggested for future research:

- The HDN of pyridine can be studied at more temperatures in the range of 523 - 623 K so as to evaluate all the kinetic constants more precisely.
- The reaction can be studied at higher temperatures and space times to see if ethyl piperidine (a major product in this study) is further denitrogenated to yield hydrocarbons.
- The HDN of major intermediate products can be studied in order to understand the reaction network better.

LIST OF REFERENCES

Aboul-Gheit, A. K., I. K. Abdou, and A. Mustafa, "Hydrodenitrogenation Studies. Part-1 Pyridine", Egypt. J. Chem., **17**(5), 617-629 (1974).

Ajaka, C. D., R. S. Mann and K. C. Khulbe, "Catalytic Hydrodenitrogenation of Pyridine over presulphided Mo-zeolite", Indian J. Chem.Tech., **1**, 75-80 (1994).

Ajaka, C. D., "Catalytic Hydrodenitrogenation of Pyridine and Quinoline", Ph.D. Thesis, University of Ottawa (1991).

Anabtawi, J. A., R. S. Mann and K. C. Khulbe, "Hydrodenitrogenation of Pyridine over Ni-W/Alumina Catalyst", J. Catal., **63**, 456-462 (1980).

Bond, G. C., "Catalysis by Metals", Academic Press, New York (1962).

Clark, A., "The Theory of Adsorption and Catalysis", Academic Press, New York (1970).

Cox, K. E., Ph.D. Thesis, Montana State College (1961).

Cusumano, J. A., R. A. Dalla Betta and R. B. Levy, "Catalysis in Coal Conversion", Academic Press Inc., New York (1978).

Doraiswamy, L. and M. M. Sharma, "Heterogeneous Reactions - Analysis, Examples and Reactor design", Wiley-Interscience Publications, New York (1984).

Gilchrist, T. L., "Heterocyclic Chemistry", Pitman Publishing Ltd., London, England (1985).

Gupta, R. K., "Hydrodenitrogenation of Pyridine", MASc Thesis, University of Ottawa (1977).

Happel, J. and R. Mezaki, "Identification of Rate Models for Solid Catalyzed Reactions",

Catal. Rev. **3**, 241-270 (1969).

Hillerova, E., Z. Vit and M. Zdražil, "Comparison of Carbon and Alumina Supported Nickel-Molybdenum Sulphide Catalysts in Parallel Hydrodenitrogenation and Hydrodesulphurization", Applied Catalysis, **67**, 231-236 (1991).

Hulzinga, T. and R. Prins, "Electron Spin Resonance Investigations of Platinum Supported on Al_2O_3 and TiO_2", J. Phys. Chem., **87**, 173-176 (1983).

Jewell, D. M. and G. K. Hartung, "Identification of Nitrogen Bases in Heavy Gas Oil; Chromatographic Methods of Separation", J. Chem. Eng. Data., **9**(2), 297-304 (1964).

Kartzmark, R. and J. B. Gilbert, "Hydrotreat Naphthenic Lube Stocks", Hydrocarbon Processing and Petroleum Refiner, **46**(9), 143-148 (1967).

Katzer, J. R., G. C. A. Schuit and J. H. C. VanHooff, "Paramagnetic Platinum and Oxygen Species on Supported Platinum", J. Catal., **59**, 278-292 (1979).

Kittrell, J. R. and R. Mezaki, "Reaction Rate Modeling in Heterogeneous Catalysis", Ind. Eng. Chem., **59**(2), 28-40 (1967).

Larson, O. A., "Kinetic Effects due to Poisons in Hydrocarbon Process", Preprints, Div. Petroleum Chem. ACS, **12**(4), 3 (1967).

Ledoux, M. J. and B. Djellouli, "Comparative Hydrodenitrogenation activity of Molybdenum, Co-Mo and Ni-Mo Alumina-supported Catalysts", Applied Catalysis, **67**, 81-92 (1990).

Levenspiel, O., "Chemical Reaction Engineering", John Wiley & Sons Inc., New York (1972).

McIlvried, H. G., "Kinetics of the Hydrodenitrification of Pyridine", Ind. Eng. Chem. Process Des. Develop., **10**(1), 125-130 (1971).

Nixon, A. C., C. A. Cole and H. B. Minor, "Effect of Composition and Storage on the Properties of Jet Fuels", J. Chem. Eng. Data, **4**, 187-192 (1959).

Oballa, M. C. And S. S. Shih, "Catalytic Hydroprocessing of Petroleum Distillates": Proceedings of the AIChE Spring National Meeting, Houston, Texas, March 28-April 1, 1993, Marcel Dekker Inc., New York (1993).

Oblad, A. G., T. H. Milliken, Jr. and G. A. Mills, "Chemical Characteristics and Structure of Cracking catalysts", Advances in Catalysis III, 199-247 (1951).

Oswald, A. A. and F. Noel, "Role of Pyrroles in Fuel Instability", J. Chem. Eng. Data, **6**, 294-301 (1961).

Rylander, P. N., "Catalytic Hydrogenation over Platinum Metals", Academic Press, New York (1967).

Satterfield, C. N. and J. F. Cocchetto, "Pyridine Hydrodenitrogenation: An Equilibrium Limitation on the Formation of Piperidine Intermediate", AIChE J., **21**(6), 1107-1111 (1975).

Satterfield, C. N., M. Modell and J. F. Mayer, "Interactions between Catalytic Hydrodesulphurization of Thiophene and Hydrodenitrogenation of Pyridine", AIChE J., **21**(6), 1100-1107 (1975).

Satterfield, C. N., M. Modell and J. Wilkens, "Simultaneous Catalytic Hydrodenitrogenation of Pyridine Hydrodesulphurization of Thiophene", Ind. Eng.

Chem. Process. Des. Dev., **19**, 154-160 (1980).

Scheppele, S. E., G. J. Greenwood and P. A. Benson, "Field-Ionization Relative Sensitivities for Analysis of Coal-Derived Liquids Determined as a Function of Ion-Source Temperature and Binary-Mixture Composition", Anal. Chem., **49**(12), 1847-1850 (1977).

Schultz, J. L., R. A. Friedel and A. G. Sharkey Jr., "Mass Spectrometric Analysis of Coal Tar Distillates and Residues", U. S. Bureau of Mines Report Investigations 7000 (1967).

Schwartz, F. G., W. L. Whisman, C. S Allbright and C. C. Ward, "Storage Stability of Gasoline, Fundamentals of Gum Formation, Including a Discussion of Radiotracer Techniques", U.S. Bureau of Mines Bulletin 626 (1964).

Soria, J., A. Martinez-Arias, J. M. Coronado and J. C. Conesa, "Electron Paramagnetic Resonance Spectroscopy study of the adsorption of O_2 and CO on a $Pt/CeO_2/Al_2O_3$ Catalyst", Colloids and Surfaces, A: Physiochemical and Engineering Aspects, **115**, 215-221 (1996).

Vit, Z. and Zdražil, M., "Simultaneous Hydrodenitrogenation of Pyridine and Hydrodesulfurization of Thiophene over Carbon-Supported Platinum Metal Sulfides", J. Catal., **119**, 1-7 (1989).

Yoshida, F., D. Ramaswami and O. A. Hougen, "Temperature and Partial Pressures at the Surface of Catalyst Particles", AIChE J., **8**(1), 5-11 (1962).

APPENDIX A

CALIBRATION CURVES

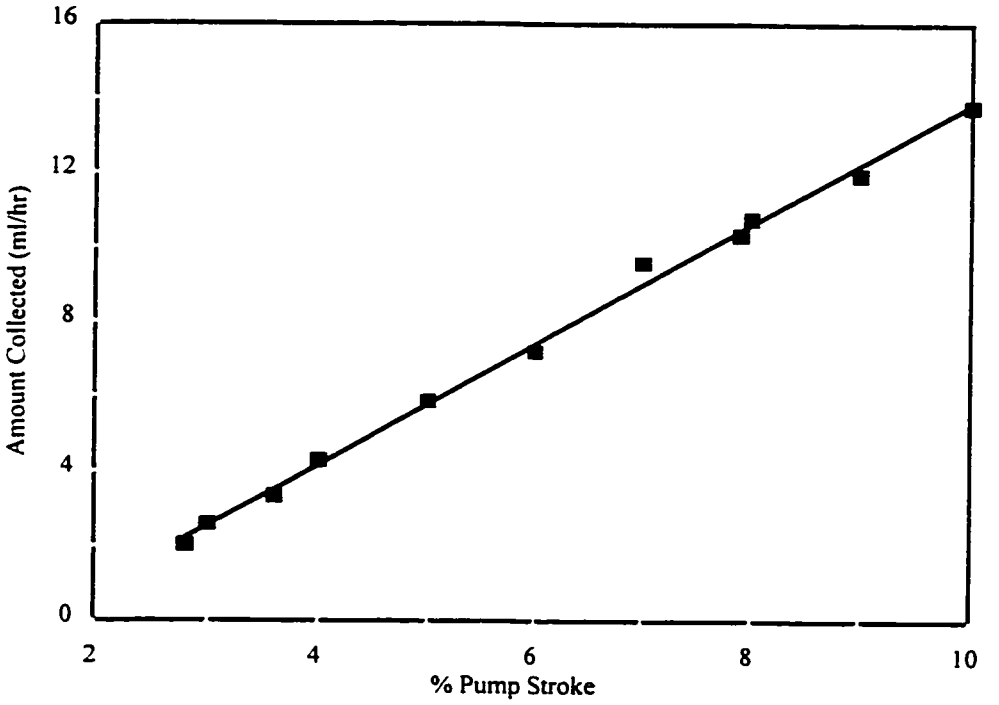

Figure A.1 Feed pump calibration

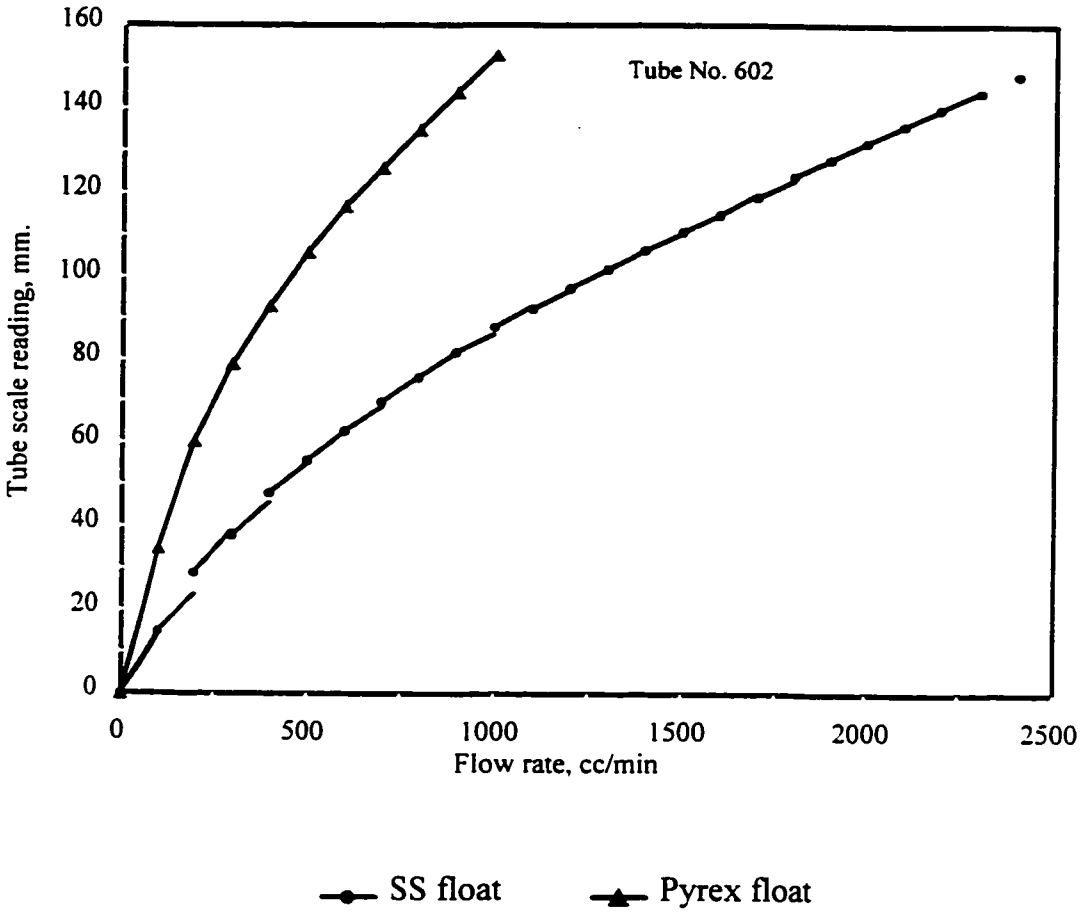

Figure A.2 Rotameter calibration (for hydrogen)

Gas Chromatography

The product analysis was carried out by a gas chromatograph (HP-5730A) and an integrator (HP-3380A) was used to produce the chromatograms. Quantitative analysis was carried out by injecting samples through the flame ionization detector.

The calibration curves for the gas chromatograph are given in Figure A.3. The typical graph produced by the integrator is given in Figure A.4. This is a sample graph that shows the analysis of the HDN products along with their retention times.

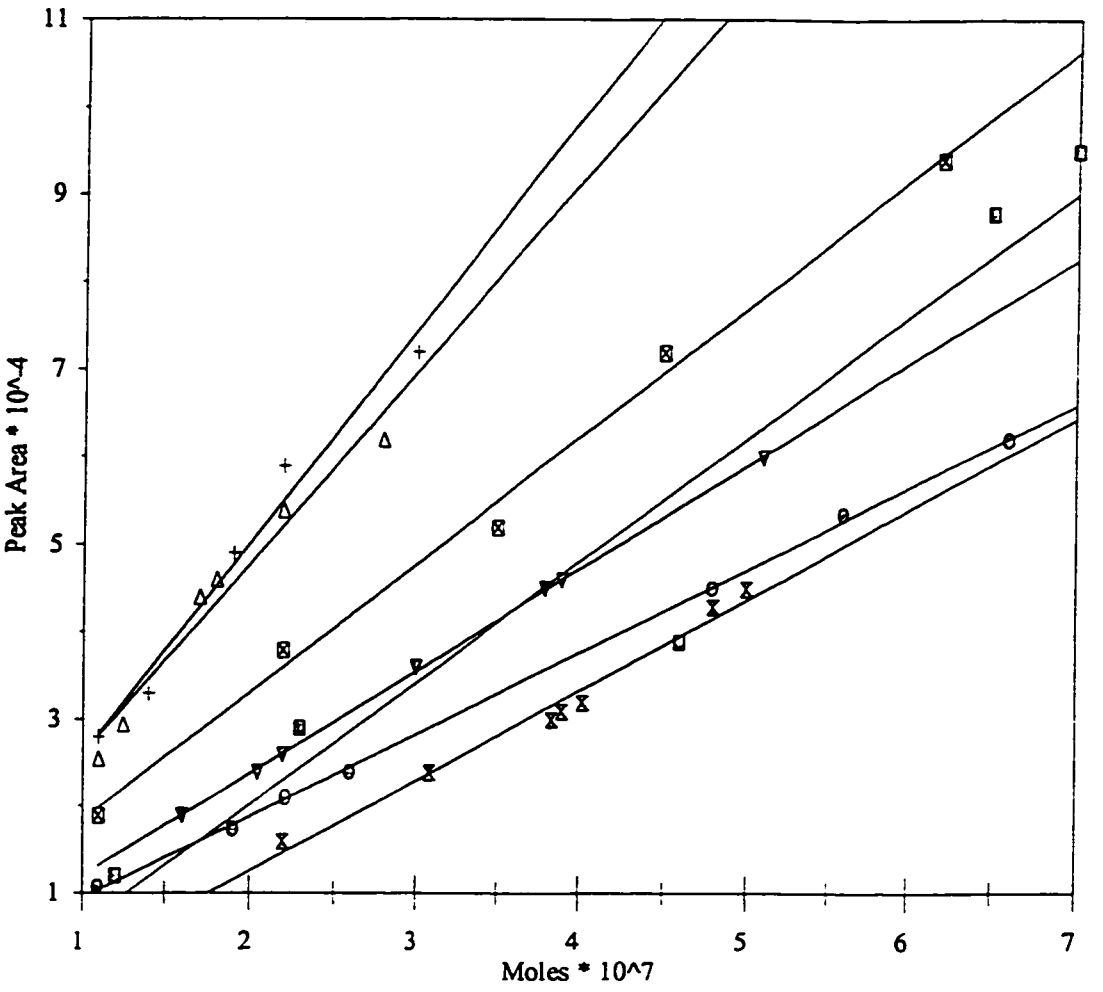

Figure A.3 Gas Chroamtograph calibration

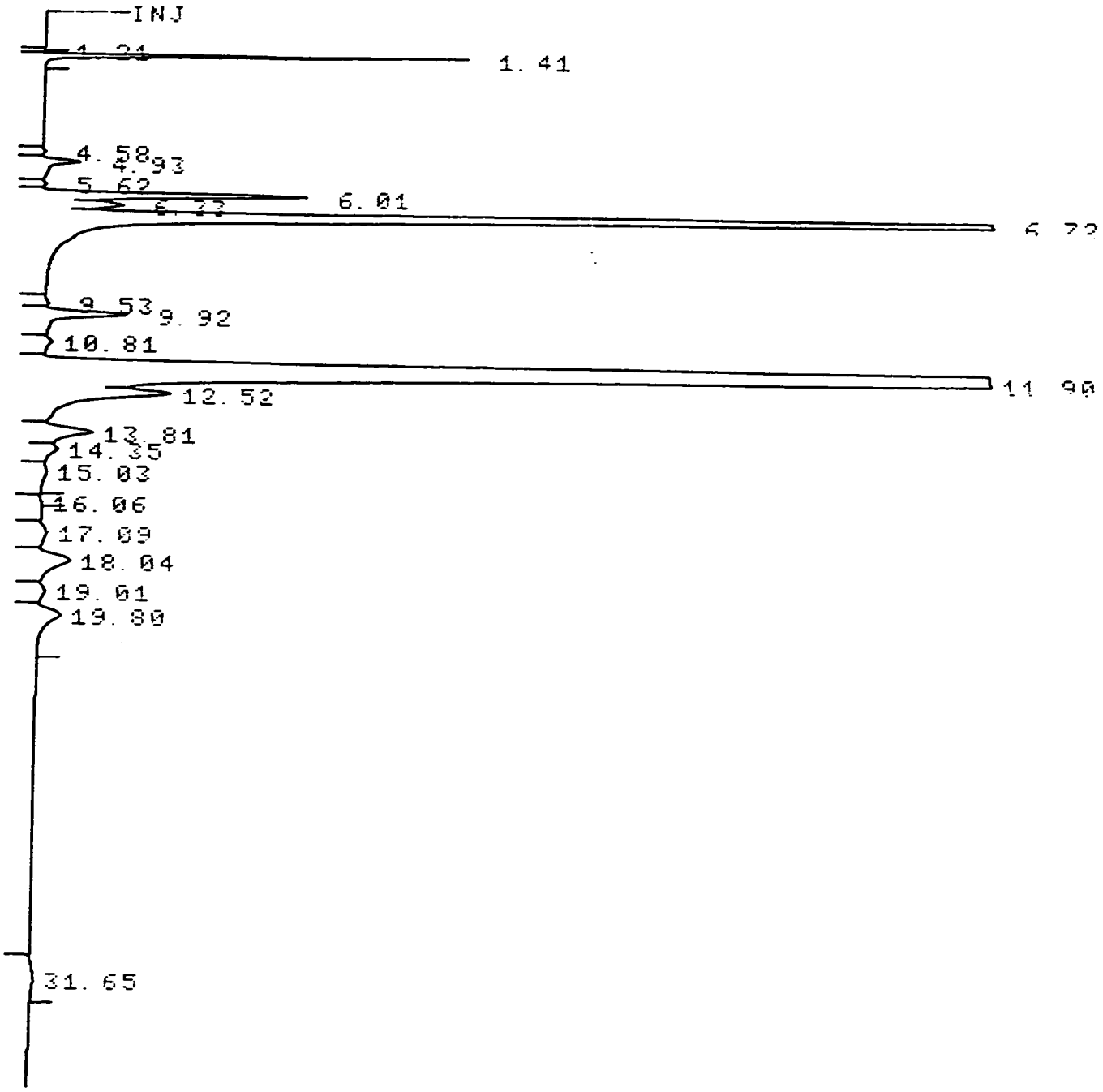

Figure A.4 HDN products

APPENDIX B

EXPERIMENTAL RUNS

Reactant molar ratio (R) = 11 g-mol hydrogen/g-mol pyridine (constant for all runs)

Runs 1 - 7 (The values tabulated are in mol %)

Temperature = 523 K Pressure = 6.894 MPa

Runs	1	2	3	4	5	6	7
W/F	37	71	88	107	152	180	247
PYR	73.84	60.17	44.21	25.78	19.88	6.13	2.78
PIP	25.26	38.39	53.34	69.34	75.41	84.30	80.84
CYPEN	0.00	0.00	0.00	0.00	0.00	0.00	0.00
PENT	0.00	0.00	0.00	0.00	0.01	0.02	0.04
PENPIP	0.77	1.14	2.02	4.43	4.16	8.91	15.59
PENAM	0.14	0.31	0.42	0.45	0.54	0.64	0.76
DIPEN	0.00	0.00	0.00	0.00	0.00	0.00	0.00
ETPIP	0.00	0.00	0.00	0.00	0.00	0.00	0.00

Runs 8 - 14

Temperature = 548 K Pressure = 6.894 MPa

Runs	8	9	10	11	12	13	14
W/F	37	71	88	107	152	180	247
PYR	42.03	31.75	12.59	3.04	2.00	2.11	0.98
PIP	53.15	60.17	74.29	74.14	75.34	56.65	46.02
CYPEN	0.00	0.00	0.00	0.00	0.00	0.00	0.00
PENT	0.02	0.04	0.07	0.14	0.17	1.59	1.06
PENPIP	4.25	7.30	12.13	21.38	21.05	33.20	48.83
PENAM	0.56	0.74	0.91	1.30	1.44	5.44	1.91
DIPEN	0.00	0.00	0.00	0.00	0.00	1.01	1.18
ETPIP	0.00	0.00	0.00	0.00	0.00	0.00	0.00

Runs 15 - 21 (The runs 15 - 21 were repeated and the data given are the averages)

Temperature = 573 K Pressure = 6.894 MPa

Runs	15	16	17	18	19	20	21
W/F	37	71	88	107	152	180	247
PYR	38.22	12.05	2.32	0.61	0.04	0.04	0.36
PIP	57.41	75.03	54.91	40.17	26.43	16.86	22.01
CYPEN	0.00	0.00	0.00	0.00	0.00	0.00	0.00
PENT	0.04	0.12	1.25	1.74	4.40	12.56	4.94

PENPIP	3.50	11.45	37.41	52.15	58.38	49.52	61.71
PENAM	0.83	1.35	2.59	2.97	5.21	10.96	4.55
DIPEN	0.00	0.00	1.23	1.83	3.97	6.46	4.17
ETPIP	0.00	0.00	0.28	0.53	1.56	3.60	2.26

Runs 22 - 28

Temperature = 598 K Pressure = 6.894 MPa

Runs	22	23	24	25	26	27	28
W/F	37	71	88	107	152	180	247
PYR	9.69	2.27	0.32	0.18	0.03	0.01	0.02
PIP	46.61	38.36	28.89	26.50	18.62	0.00	0.00
CYPEN	0.00	0.00	0.00	0.00	0.00	0.00	0.00
PENT	2.72	3.18	4.89	6.64	10.70	10.09	20.96
PENPIP	34.44	48.44	55.73	49.02	49.65	32.12	28.99
PENAM	3.72	3.97	5.02	8.25	7.64	0.00	0.00
DIPEN	1.66	2.49	3.38	4.97	6.07	6.01	1.68
ETPIP	1.16	1.29	1.77	4.45	7.29	51.77	48.35

Runs 29 - 35

Temperature = 623 K Pressure = 6.894 MPa

Runs	29	30	31	32	33	34	35
W/F	37	71	88	107	152	180	247
PYR	11.73	1.92	0.15	0.00	0.00	0.00	0.00
PIP	33.46	21.51	17.69	0.00	0.00	0.00	0.00
CYPEN	0.01	0.01	0.00	0.00	0.00	0.00	0.00
PENT	7.43	16.16	12.78	15.62	18.12	24.18	40.49
PENPIP	34.97	33.20	22.63	2.96	0.81	0.05	0.03
PENAM	5.80	11.68	10.89	0.00	0.00	0.00	0.00
DIPEN	3.13	6.51	6.52	0.56	0.02	0.00	0.00
ETPIP	3.45	8.99	29.33	80.85	81.05	75.76	59.48

Runs 36 - 42 (The runs 36 -42 were repeated and the data given are the averages)

Temperature = 523 K Pressure = 3.447 MPa

Runs	36	37	38	39	40	41	42
W/F	37	71	88	107	152	180	247
PYR	74.15	63.52	58.53	52.04	42.64	41.76	32.28
PIP	17.61	29.60	33.82	38.53	47.13	44.99	51.77
CYPEN	0.00	0.00	0.00	0.00	0.00	0.00	0.00

PENT	0.54	0.09	0.04	0.03	0.00	0.00	0.02
PENPIP	6.94	6.03	6.55	8.17	8.84	11.68	13.63
PENAM	1.16	0.81	1.08	1.23	1.39	1.57	2.31
DIPEN	0.00	0.00	0.00	0.00	0.00	0.00	0.00
ETPIP	0.00	0.00	0.00	0.00	0.00	0.00	0.00

Run 43 - 49

Temperature = 548 K Pressure = 3.447 MPa

Runs	43	44	45	46	47	48	49
W/F	37	71	88	107	152	180	247
PYR	70.68	62.53	56.98	48.64	39.39	50.96	55.05
PIP	18.83	24.29	26.47	29.98	32.89	34.80	30.32
CYPEN	0.00	0.00	0.00	0.00	0.01	0.00	0.00
PENT	0.44	0.11	0.04	0.00	0.00	0.31	0.12
PENPIP	8.82	11.20	13.46	17.68	22.84	10.62	10.89
PENAM	1.54	1.94	3.07	3.70	4.88	3.47	3.70
DIPEN	0.00	0.00	0.00	0.00	0.00	0.00	0.00
ETPIP	0.00	0.00	0.00	0.00	0.00	0.00	0.00

Runs 50 - 56 (The runs 50 - 56 were repeated and the data given are the averages)

Temperature = 573 K Pressure = 3.447 MPa

Runs	50	51	52	53	54	55	56
W/F	37	71	88	107	152	180	247
PYR	76.68	65.31	51.67	47.70	37.54	39.31	47.73
PIP	11.73	18.88	24.17	17.51	14.13	6.99	32.73
CYPEN	0.00	0.00	0.00	0.00	0.00	0.00	0.00
PENT	7.36	1.48	0.20	0.00	0.00	0.00	0.00
PENPIP	7.57	11.51	16.30	19.79	22.29	28.64	19.54
PENAM	2.30	3.79	7.76	15.00	26.03	25.05	
DIPEN	0.00	0.00	0.00	0.00	0.00	0.00	0.00
ETPIP	0.00	0.00	0.00	0.00	0.00	0.00	0.00

Runs 57 - 63

Temperature = 598 K Pressure = 3.447 MPa

Runs	57	58	59	60	61	62	63
W/F	37	71	88	107	152	180	247
PYR	81.58	74.46	72.75	69.26	80.30	65.81	44.45
PIP	10.32	14.81	15.93	18.96	15.97	27.83	21.45

CYPEN	0.00	0.00	0.00	0.00	0.00	0.00	0.00
PENT	2.77	2.68	1.29	0.30	0.05	0.05	2.05
PENPIP	5.35	8.02	8.66	8.73	0.00	0.00	16.09
PENAM	2.24	2.03	2.30	2.95	3.72	6.34	16.88
DIPEN	0.00	0.00	0.00	0.00	0.00	0.00	0.00
ETPIP	0.00	0.00	0.00	0.00	0.00	0.00	0.00

Runs 64 - 70 (The runs 64 - 70 were repeated and the data given are the averages)

Temperature = 623 K Pressure = 3.447 MPa

Runs	64	65	66	67	68	69	70
W/F	37	71	88	107	152	180	247
PYR	78.35	65.64	56.35	47.20	34.94	27.01	23.06
PIP	12.77	15.84	21.48	24.04	42.79	66.76	63.79
CYPEN	0.00	0.00	0.00	0.00	0.00	0.15	0.82
PENT	3.86	4.02	2.98	0.88	0.02	0.00	0.00
PENPIP	6.63	10.29	10.57	12.40	13.72	0.00	0.00
PENAM	1.41	6.85	10.30	15.90	8.53	6.08	12.32
DIPEN	0.00	0.00	0.00	0.00	0.00	0.00	0.00
ETPIP	0.00	0.00	0.00	0.00	0.00	0.00	0.00

APPENDIX C

RESULTS OF REGRESSION

Model 1

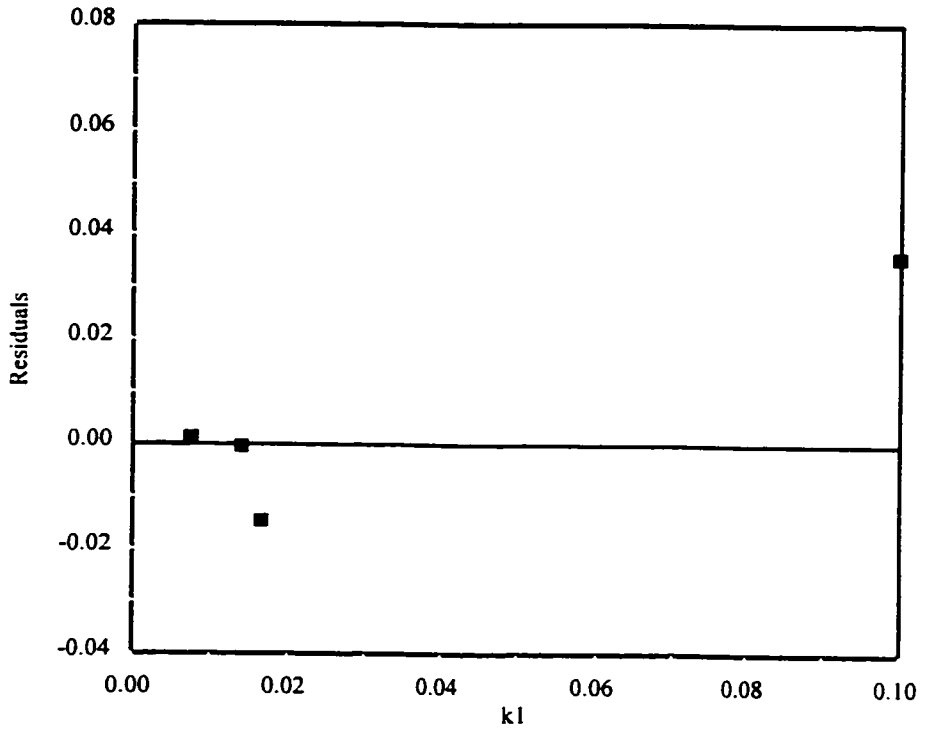

Figure C.1 The residual plot for the estimation of the rate constant in the lumped parameter model

APPENDIX D

MASS TRANSFER EFFECTS

External Diffusion

The pressure drop between the main stream and the catalyst surface are estimated using equation (2.23) and the correlation given by Yoshida et al. From this, the effect of external diffusion can be estimated.

The parameters for estimating the values are as follows (Run 5);

Temperature, T = 623 K

Space time, W/F = 247 hr-g-catalyst/g-mol pyridine

Residence time, R = 11 g-mol hydrogen/g-mol pyridine

Shape factor, ϕ = 0.9 (for irregular particles)

Weight of catalyst, W = 5.00 g

a_m = 1000000 cm^2/g

G_m (pyridine) = Molar mass velocity of pyridine based on total cross section of the bed

$$= \frac{0.0286}{3.14159*(1.067/2)^2}$$

= 0.03199 g-mol/hr-cm^2

r_m (pyridine) = Molar reaction rate of pyridine per unit mass of catalyst

$$= \frac{1 * 0.0286}{5}$$

$= 5.72 * 10^{-3}$ g-mol/hr-g-catalyst

From equation 2.23,

$$R \text{ (dimensionless factor)} = \frac{5.72 * 10^{-3}}{1000000 * 0.9 * 0.03199}$$

$$= 1.9867 * 10^{-7}$$

y_{in} = Mole fraction of pyridine in the feed

= 0.07566

y_{out} = Mole fraction of pyridine in the product

= 0

y_i = Mole fraction of pyridine at the interface

= 0.03783

R/y_i = $5.252 * 10^{-6}$

From the correlation between R/y_i and $\Delta P/P$, the value of $\Delta P/P$ estimated is less than 0.0001. The effects of external diffusion can hence be neglected. Similar calculations for hydrogen gave a R/y_i value of $2.826 * 10^{-6}$ which again gives a $\Delta P/P$ less than 0.0001.

Internal Diffusion

Internal diffusion, which is the transport process inside the catalyst can be either molecular diffusion or pore diffusion.

Two different particle size (20/35 and 35/42) of the catalyst were taken and the conversion of pyridine was studied under similar conditions. At a total pressure of 68.05, temperature

of 548 K and space time of 88, the conversion achieved by using 20/35 mesh size catalyst was about 57.974% while the conversion for 35/42 mesh size catalyst was about 57.263%. The reduction in the particle size did not affect the conversion very much and hence it was concluded that pore diffusion was not controlling the reaction.

The effect of molecular diffusion was studied by changing the feed velocity while keeping the variables constant (Pressure = 68.05 atm., Temperature = 548 K and space time = 71). At a feed velocity of 0.071 g-mol/hr, the conversion was 68.254% while the conversion obtained for a feed velocity of 0.051 was 68.51%. Since the variation in the conversion was insignificant, molecular diffusion was not controlling.

IMAGE EVALUATION TEST TARGET (QA-3)

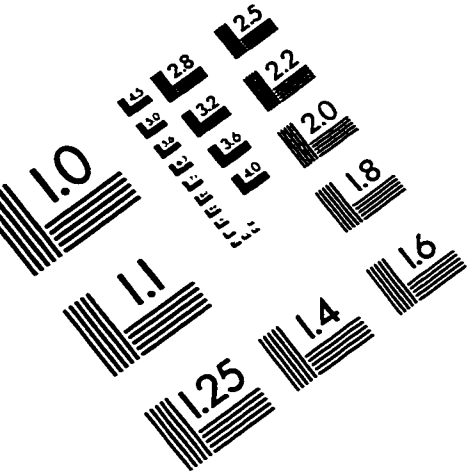

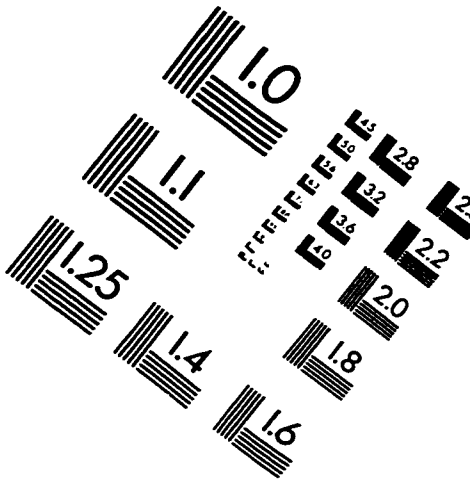

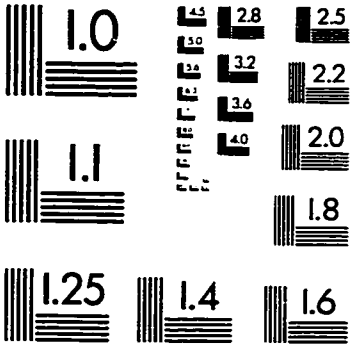

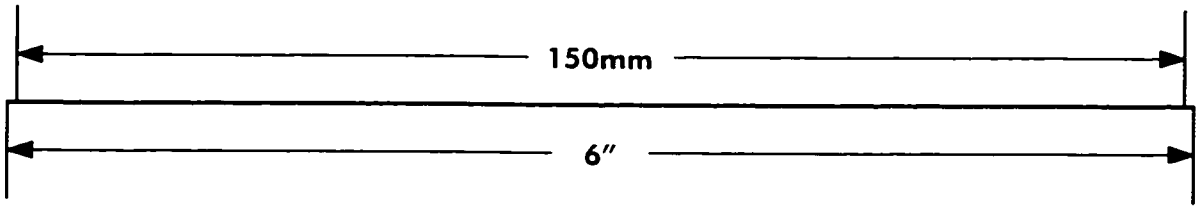

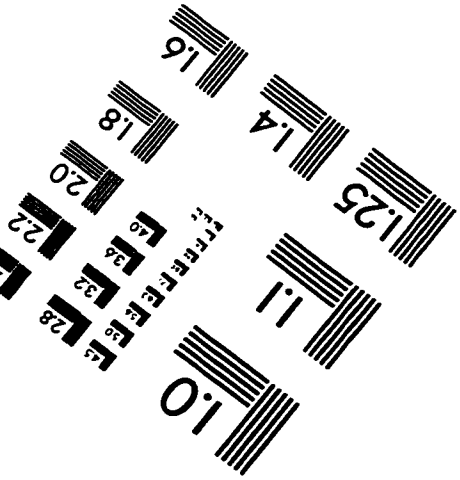

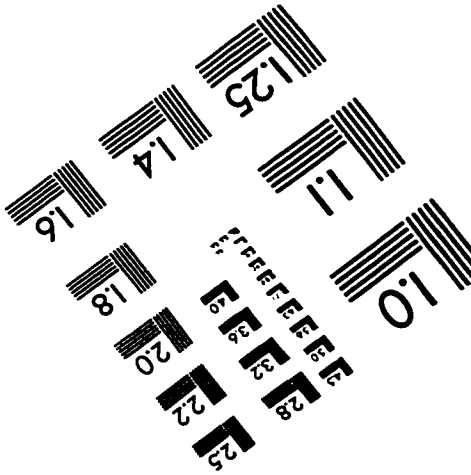

APPLIED IMAGE, Inc
1653 East Main Street
Rochester, NY 14609 USA
Phone: 716/482-0300
Fax: 716/288-5989